Spring 2009

The role of stochastic resonance and physical constraints in the evolution of foraging strategy

Nathan Daniel Dees

Department: Physics

THE ROLE OF STOCHASTIC RESONANCE AND PHYSICAL CONSTRAINTS IN THE EVOLUTION OF FORAGING STRATEGY

by

NATHAN DANIEL DEES

A DISSERTATION

Presented to the Faculties of the Graduate Schools of the

MISSOURI UNIVERSITY OF SCIENCE AND TECHNOLOGY

and

UNIVERSITY OF MISSOURI – ST. LOUIS

In Partial Fulfillment of the Requirements for the Degree

DOCTOR OF PHILOSOPHY

in

PHYSICS

2009

Approved by

Sonya Bahar, Advisor
Ricardo A. Flores
George D. Waddill
Alexey Yamilov
Linda Larson-Prior

ABSTRACT

This work represents a detailed study of the optimization of this process: foraging within a single, finite food patch for a limited amount of time. The work is an example of the computational algorithms of statistical physics being applied to the ecological field of foraging behavior. The analysis begins with an examination of the probability distributions observed in the movement parameters of the zooplankton, *Daphnia*. While foraging, these small aquatic organisms stochastically choose movement parameters with particular levels of variation, or noise, which are similar across several species. Here, related simulations consistently show that these noise levels may be adjusted to maximize foraging efficiency, regardless of the physical constraints imposed in the models. The results are presented as an example of natural stochastic resonance, in which some function of noise (in this case, the variability in parameter choices), when adapted to a biological process (e.g., the gathering of food), can optimize that process. The architect of this optimization is suggested to be natural selection, a hypothesis further explored with a novel evolutionary algorithm which transforms uniform and uncorrelated parameter distributions into "optimal" forms over thousands of generations of competition amongst foraging agents. The results of the algorithm support the implication that the noise levels are evolved quantities, and also reinforce the hypothesis that stochastic resonance may have a role in their evolution. And lastly, the evolutionary algorithm was extended to larger aquatic organisms feeding in patches through the addition of the Reynolds number as a physical constraint. The results of the modified algorithm clearly differentiate between the trajectories predicted for smaller and larger animals, and match very well with the experimental data reported here for both the *Daphnia*, and also for a larger fish species, the paddlefish. Since both organisms filter-feed inside finite patches of food, albeit on different scales, the results clearly show the degree to which the physical constraints imposed upon an animal can dictate the evolution of their behavior.

ACKNOWLEDGMENTS

I would like to thank Dr. Sonya Bahar for being a wonderful and supportive advisor, and for being a friend, and for being 100% dedicated to both roles at all times. I would like to thank my committee for their positive and encouraging approach. I have appreciated much guidance from Dr. Linda Larson-Prior, Dr. Fred Prior, and Dr. David Politte, who have all extended themselves to me both professionally and personally. And I would also like to thank my colleagues in the Center for Neurodynamics, Dr. Jorge Brea and Daisuke Takeshita, who always have the answers to my questions.

I give special thanks to Dr. Frank Moss for allowing me to work with him. It is no wonder that all who know him are truly inspired by him. I thank Dr. Michael Hofmann for the same thing - working with him is purely joyful. And, of course, I give much thanks to my wife, Robin, for her continual sacrifices which have allowed my dreams to be *our* dreams. To her, I owe every opportunity and every reward.

I would like to also acknowledge these funding sources: the Graduate School Doctoral Fellowship, NSF Career Grant No. PHY-0547647, Dr. Sonya Bahar's Startup Funds, and Dr. Frank Moss's Curator's Professor Account.

TABLE OF CONTENTS

LIST OF ILLUSTRATIONS

LIST OF TABLES

1. INTRODUCTION

"It is often said that physicists oversimplify biology. But it must be pointed out that physicists (and engineers) also oversimplify physics."

(Nunez & Srinivasan 2006)

Computational models drawing on the concepts of statistical physics and nonlinear dynamics have now been applied to many fields of research, particularly the biosciences. Biological systems are among the most complex systems in nature; large numbers of variables, abundant nonlinearities, and, in many cases, a less-than-complete understanding of all of the components in their makeup enforce the idea that these systems can be extremely difficult to characterize digitally. Models, on the other hand, are most beneficial when they are simple. Simple models incorporating even a few key details of a complex system may prove to be especially insightful and informative. Such is the motivation here.

1.1. FORAGING THEORY

The work which follows originates from the ecological and biophysical field of foraging theory, warranting a brief introduction to this field. There have been many full-length texts written on the subject, most famously Stephens and Krebs (1986) and Kamil *et al.* (1987), which the reader may refer to for more discussion and detail. Foraging theory, often called *optimal* foraging theory, explores the decisions that animals make when searching for and utilizing food sources. The type of environment which contains the food is usually accounted for, and a typical assumption made by theorists is that, to increase their chances of survival, animals must attempt to maximize their average rate of energy intake. One can never directly ask an animal about its personal approach to gathering food or about the reasons for which it makes specific decisions, but hypotheses about possible answers to these questions are abundant and relevant, and sometimes *testable* through the numerical analysis of computational foraging models and the comparison of these results to experimental observations.

1.2. A BASIC FORAGING MODEL

A basic foraging model is designed to quantitatively explain a specific decision that a forager must make while gathering food. As mentioned above, it is assumed that foragers attempt to maximize their energy intake per unit time. As a result, decisions made by foragers are most often evaluated in terms of the amounts of energy gained and/or lost, and on the advantage or disadvantage that specific decisions may impart.

Basic models run sequentially according to rules imposed on the simulated foragers. These rules are called constraints, and are typically classified as either intrinsic or extrinsic. An intrinsic constraint could represent, for instance, a physical limitation of the forager itself, such as the distance it can travel in a single step. An intrinsic constraint could also be a tolerance level of a fitness-related need, such as a particular diet requirement (Pulliam 1975), or a minimum number of hours of sleep (Rechtschaffen *et al.* 1989). Extrinsic constraints, on the other hand, are rules dictated by the virtual environment in which the animal operates. For example, in a certain environment, there may be an abundance of food, or, alternatively, a lack thereof. In the basic model, foragers are expected to know all of the constraints, and abide by them accordingly.

It is also generally assumed in the basic model that the total time that animals spend foraging is divided between the time spent searching for prey and the time spent pursuing, capturing, and eating this prey. MacArthur and Pianka (1966) called these two time divisions T^S (searching) and T^P (pursuing and capturing). They are also given credit for conceiving of and distinguishing between the two most basic problems studied by foraging theorists: first, whether a forager attacks or ignores a particular item of prey that it has encountered (prey model), and, secondly, how long should a forager remain inside a patch that it has encountered (patch model). Their original quantitative study had the goal of determining the optimal number of prey species types to include in a predator's diet. In other words, they investigated the decision of a forager to hunt a particular number of prey species, and ignore all other possible prey species. The different prey species were assumed to be equally abundant, but differed in the pursuit times, T^P, necessary for capture. The species were then ranked from the lowest to highest pursuit times (easiest-to-capture to hardest-to-capture), and then added to the diet one by one in this order.

In the prey model, by adding more types of prey to the predator's diet, the search time is minimized since the predator will more often run across something eligible to be eaten. However, if the diet is expanded to include too many types of prey, then too much foraging time will be lost attempting to capture and eat the most elusive prey, and the overall energy consumption rate will diminish. In the patch model, the prey is assumed to be contained in localized patches, but still must be pursued and captured within the patch. So, again, increasing the number of prey types in the diet will increase the number of patches eligible to be hunted, and therefore decrease the time spent searching for food (traveling between patches). But, just as in the prey model, as more elusive prey are added to the diet, extra time must be spent (or wasted) pursuing the harder-to-capture prey types.

1.3. THE LAW OF NATURAL SELECTION

Even under the assumption that animals do indeed attempt to maximize energy consumption, MacArthur and Pianka's work does beg some questions, such as, "How would any typical animal know when to limit the number of types of prey species that it decides to pursue?"

An animal's food consumption, and therefore its energy consumption, is important to the animal since its fitness depends upon it. Fitness may be viewed as the "health" of an organism, or, as in evolutionary biology, as the probability that an organism will be able to survive in a particular environment. Organisms with higher fitness levels are able to survive harsher conditions, and those that survive end up being those that reproduce. Each production of offspring passes along this healthy organism's DNA, allowing inheritance of the traits that it possesses, and ensuring that these traits, the traits of a fit organism, will become more common over time. This is the basis of the 150-year-old theory of natural selection.

The question of an animal's management of its prey species is now more easily answered in the context of natural selection, where one may reason that an animal may not necessarily *know* whether or not it is pursuing too many elusive prey items, but if those animals that avoid certain prey have better health, then they will be more likely able to survive in that particular environment. Optimal foraging theorists, therefore, simply

assume that many cycles of this selection of efficient foragers has taken or will take place when they assume that the most optimal foraging strategy will be the one which is the most efficient.

1.4. SUMMARY

MacArthur and Pianka's model does not speculate as to exactly how many types of prey should be present in the diet of a typical forager; rather, they give meaningful predictions about how a particular animal's diet might change if, for instance, environmental conditions altered the availabilities of prey (for a recent example, see Clavero *et al.* 2003). But MacArthur and Pianka also seem very reluctant to rely on the assumptions which led to the conclusions of their own work. For instance, they subjectively mention in their paper that "such 'optimum theories' are hypotheses for testing rather than anything certain," and that, "hopefully, natural selection will often have achieved such optimal allocation of time and energy expenditures." Perhaps they were tentative because their results lacked the support of even a single example of experimental or observational data.

Stephens and Krebs (1986) pointedly wrote that, "Only the behavior and ecology of real animals can determine the ultimate value of foraging models." It is with this very understanding that the following work has been performed. The work is predominately theoretical, but it stands upon direct relationships with recorded observations of real animals, some of which were made during the course of this study. Section 2 introduces a foraging model designed to analyze the decisions made by the real zooplankton *Daphnia* regarding the movement parameters they use to traverse their food patches. Data regarding the decisions that they commonly make – and which provide success – are presented, and the factors which may have rewarded these decisions, such as stochastic resonance, are evaluated. Section 3 discusses the development and use of a novel genetic algorithm to model the evolution of *Daphnia* foraging trajectories through the competition of feeding agents. Winners are chosen in each generation based on their ability to maximize their energy intake, and histograms describing successful movement parameter decisions are passed on from one generation to the next as a form of inheritance. In Section 4, an extrinsic physical constraint is added to the evolution and

feeding models in order to extend their application beyond tiny zooplankton to larger aquatic filter-feeding species, such as the paddlefish. The modified model predicts vastly different optimal trajectories for larger fish, and the results are compared to the observed trajectories of living captive paddlefish. Section 5 offers perspective on the possibility of inherited foraging behavior, and finally, Appendices A (Dees *et al.* 2008a), B (Dees *et al.* 2008b), and C each contain a complete manuscript offering further detail and important results from the material presented in Sections 2, 3, and 4 respectively.

2. *DAPHNIA* PATCH EXPLOITATION

2.1. MOVEMENT PARAMETER DISTRIBUTIONS

Daphnia, commonly called water fleas, are small, bulbous aquatic organisms on the order of 2.5 to 5 mm in length (see Figure 2.1). They move about much differently from fish, which undulate their body and tail. Instead, *Daphnia* are "rowers". They intermittently stroke a set of large second antennae as if the antennae were oars, pushing their bodies forward for a small distance, and then pausing as they bring the antennae forward before stroking again (Pennak 1953). Changing directions is presumably the result of an unevenly-powered stroke between the two antennae, resulting in jagged trajectories with sharp changes in direction, reminiscent of a traditional random walk (Brown 1828, Keiyu *et al.* 1993, Komin *et al.* 2004, Uttieri *et al.* 2004, Schimansky-Geier *et al.* 2005, Haeggqwist *et al.* 2008). To study this motion, researchers have reduced it to precise physical parameters. For example, each stroke resembles a small "hop" which covers a particular distance (a "hop length"), the *pause times* between hops are measured in seconds, and changes in direction can be described as turns through angles ("turning angles").

Figure 2.1. Photograph of a *Daphnia magna*[1]

[1] This photograph was taken by Dr. Lon Wilkens of the UMSL Department of Biology.

2. *DAPHNIA* PATCH EXPLOITATION

2.1. MOVEMENT PARAMETER DISTRIBUTIONS

Daphnia, commonly called water fleas, are small, bulbous aquatic organisms on the order of 2.5 to 5 mm in length (see Figure 2.1). They move about much differently from fish, which undulate their body and tail. Instead, *Daphnia* are "rowers". They intermittently stroke a set of large second antennae as if the antennae were oars, pushing their bodies forward for a small distance, and then pausing as they bring the antennae forward before stroking again (Pennak 1953). Changing directions is presumably the result of an unevenly-powered stroke between the two antennae, resulting in jagged trajectories with sharp changes in direction, reminiscent of a traditional random walk (Brown 1828, Keiyu *et al.* 1993, Komin *et al.* 2004, Uttieri *et al.* 2004, Schimansky-Geier *et al.* 2005, Haeggqwist *et al.* 2008). To study this motion, researchers have reduced it to precise physical parameters. For example, each stroke resembles a small "hop" which covers a particular distance (a "hop length"), the *pause times* between hops are measured in seconds, and changes in direction can be described as turns through angles ("turning angles").

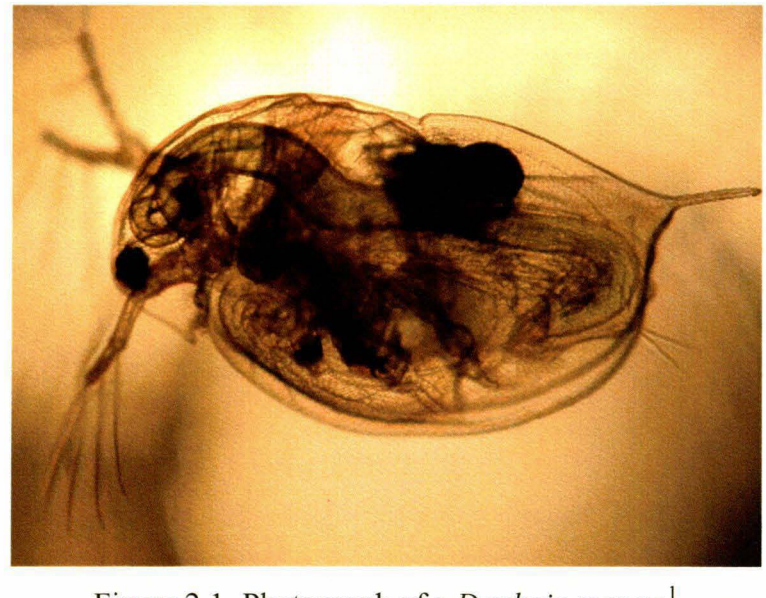

Figure 2.1. Photograph of a *Daphnia magna*[1]

[1] This photograph was taken by Dr. Lon Wilkens of the UMSL Department of Biology.

The swimming trajectories used by *Daphnia* are critical to the fitness of the organisms, mainly because *Daphnia* are filter-feeders. Both large and small filter-feeders collect items of prey by straining the medium that surrounds them as it flows through some specialized cavity in their bodies. Most fish species which are filter-feeders swim with their mouths open, allowing water to flow inside. This water then typically leaves their body through the gills, where appendages called gill rakers separate and secure any food particles that are present. *Daphnia* filter-feed using a slightly different method; they have bristly thoracic legs which flutter inside the outer shell of their underbelly, creating a current of water through this carapace. If the *Daphnia* happens to be located in patches of phytoplankton or algae, particles of these organic substances will be removed from the feeding current by the bristly legs (Pennak 1953).

When *Daphnia* are observed feeding, they are rowing constantly. There are cases in which *Daphnia* react in predictable ways to odors of food (van Gool & Ringelberg 1996) and other stimuli (see Appendix A - Discussion), but in general, their small-scale motion during foraging and otherwise is very stochastic. To analyze a particular individual stroke and try to draw a purposeful conclusion based on its parameters would be essentially impossible. However, over a longer period of time, a full trajectory will be realized, and many hop lengths, turning angles, and pause times may be measured and interpreted statistically. By creating a histogram of these measurements, for example, a *Daphnia's* general preference for particular movement parameters during foraging may be revealed. This is precisely the method by which *Daphnia* were studied at the University of Missouri at Saint Louis and at the Great Lakes WATER Institute in Milwaukee, Wisconsin. Histograms of turning angles for six species of *Daphnia* were reported by Garcia *et al.* (2007), and histograms of hop lengths and pause times for two species of *Daphnia* were reported in Appendix A - Experimental results.

The results of the turning angle data were illuminating and definitive. As mentioned above, six species of *Daphnia* were studied, along with two more groups, the juveniles of *D. magna* and *D. pulex*. All but one species exhibited exponential distributions (histograms) of turning angles. Even more remarkably, the standard deviations, σ, of the distributions were very similar across 8 sets of *Daphnia*, with the average value $\sigma_{ave} = 1.06 \pm 0.5$ radians (Garcia *et al.* 2007). This result includes,

however, a statistical outlier, the value of σ for *D. lumholtzi*. This species of *Daphnia* sometimes has spikes ("spines") protruding directly out of its head, a feature not found in the other species of *Daphnia*. For *D. lumholtzi* (with spines) σ was 2.3 ± 0.4 radians; removing this value from the group average results in σ_{ave} = 0.89 ± 0.2 radians, a much more compact range. Although variations in pause times are somewhat limited by the propensity of the *Daphnia* to sink if it does not stroke, the standard deviations of the pause time distributions, τ, were also very similar across species. τ for *D. pulex* was 0.26 ± 0.04 s, and τ for *D. magna* was 0.35 ± 0.06 s (see Appendix A - Experimental results).

The similarities in the values of σ and τ across different species of *Daphnia* seem to indicate that these animals prefer to have certain levels of variability, jitter, or noise in their choices of movement parameters. (Note that hop lengths are proportional to, and most likely physically constrained by, the size of the animal; *D. magna* are typically about twice as large as *D. pulex*, and have a typical hop length which is 2.37 times longer, according to the results of Appendix A.) This raises two questions: 1) Since the noise levels in the movement parameter distributions are consistent across species, did these noise levels enable the *Daphnia* that utilized them to have "superior" trajectories which resulted in consistently higher rates of food consumption, and therefore higher fitness levels? 2) Did these noise levels provide advantages which allowed certain *Daphnia* to survive at a higher rate and perpetuate their tendencies in parameter choices to future generations of *Daphnia* through natural selection? These questions will be addressed in the text which follows, and in Section 3, respectively.

2.2. THE ROLE OF STOCHASTIC RESONANCE

The theory of Stochastic Resonance (SR) was originally proposed theoretically by Benzi *et al.* (1981), and followed shortly thereafter with observations detailing the theory's possible role in the 100,000 year periodicity of Earth's recurring ice ages (Benzi *et al.* 1982, Nicolis 1982). SR is most simply envisioned as the addition of some function of noise to a signal that is very weak, and therefore outside the range of its intended detector. The signal-to-noise ratio (SNR) for a signal which cannot be detected would obviously be vanishingly small. This situation is demonstrated in Figure 2.2a, where a 0.5 kHz signal is shown oscillating directly below a detection threshold (solid line). Although

quantities of noise present in transmitted signals (or mechanical systems) have been traditionally thought of as somewhat annoying imperfections, the reader will see that when Gaussian noise is added to this signal (Figure 2.2b), there are times when the signal-plus-noise rises above the threshold and can be detected. These detections are symbolized by the pulses shown in Figure 2.2c. Detections occur most often when the original sinusoid is at its peak, and therefore the dominant frequency of the pulses matches the frequency of the original signal (see the peak in the power spectrum at 0.5 kHz in Figure 2.2d). Measuring the SNR of the new, noisy signal will give a much better result than measuring it using the original clean – but subthreshold – signal. In this manner, noise has improved the usefulness of the otherwise undetectable signal.

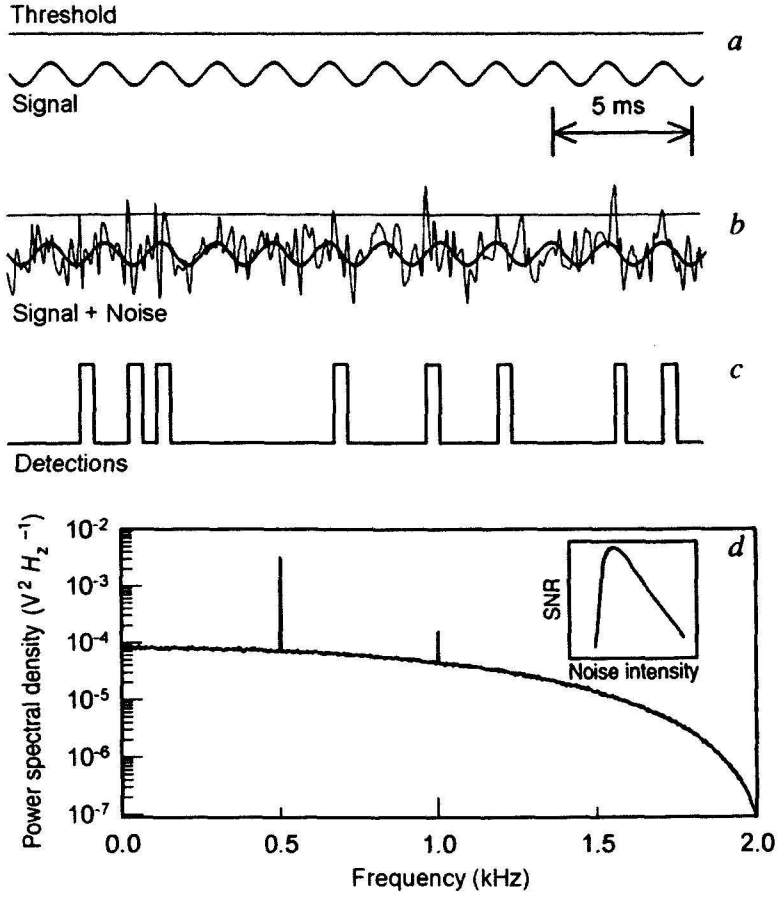

Figure 2.2. Illustration of Stochastic Resonance[2]

[2] Adapted by permission from Macmillan Publishers Ltd: Nature, Weisenfeld & Moss, copyright 1995.

Note in Figure 2.2 that if the noise added to the original signal had a very small amplitude, then the signal-plus-noise might still never rise above the detection threshold. And, alternatively, if the intensity of the added noise were too high, then detections will be made quite often at places other than the peaks in the original signal, thus diminishing the SNR through over-detection. There is obviously an intermediate noise intensity which provides the best possible SNR, and this is illustrated by the plot of SNR versus noise intensity in the inset of Figure 2.2d. The noise intensity which causes a peak in the SNR is the level of noise which optimizes the detection process for this system.

SR has now been identified in a wide range of physical systems (Gammaitoni *et al.* 1998), including many biological adaptations (Moss *et al.* 2004). Studies of animal sensory systems alone, for instance, have determined that specific levels of external noise can optimize the motion-detecting abilities of crayfish (Douglass *et al.* 1993), the sensitivity of the cochlea in leopard frogs (Jaramillo & Wiesenfeld 1998), and the range at which the electrosensitive rostrum of the paddlefish can detect the electric fields generated by its favorite prey, the *Daphnia* (Russell *et al.* 1999). In a similar way, it is legitimate to ponder the hypothesis that specific levels of noise in the choices of movement parameters by *Daphnia* might be advantageous during foraging, possibly optimizing the amount of food that the organisms gather.

2.3. *DAPHNIA* FORAGING MODEL

To test this hypothesis, a computational model of simulated foraging agents was developed in Garcia *et al.* (2007), and then redesigned and further explored in Appendix A. The complete details of the model are discussed in the Simulation methods section of Appendix A, but a brief description is presented here. Since *Daphnia* feed in patch-like accumulations of phytoplankton and photosynthetic algae (Lampert 1989; Franks & Jaffe 2001), the concept of the foraging model originates from the patch model introduced in Section 1.2 above. These patches of phytoplankton and algae form during the daytime hours at the surface of the water while *Daphnia* remain lower in the water column. At night, however, *Daphnia* rise to the surface in a process called *diel vertical migration* (Ringelberg 1993) and traverse these patches, feeding through the night. So, the extrinsic constraints in the model are that *Daphnia* feed on patchy food typically residing at the

surface of the water, and they do this mostly at night. Thus, in the model, the motion of the agents is realized in two dimensions, the agents feed for fixed lengths of time (or, equivalently, over fixed trajectory lengths), and the feeding area consists of a circular grid of uniformly distributed food particles, symbolizing a round patch.

The movement parameters used by real *Daphnia*, as discussed above, form the basis for defining the modeled agents' trajectories, as they represent the internal constraints of the modeled agents' movements. Turning angles, hop lengths, and pause times are chosen at random for each "hop" executed by the foraging agents from representative distributions. These distributions are inspired by data collected from the real animals (Garcia *et al.* 2007; Appendix A – Experimental results). They have pre-defined shapes and therefore precise levels of noise, leading to specific levels of variability in the random choices of movement parameters made by the foraging agents.

For each trial, ten modeled agents begin to forage simultaneously in the food patch, and each agent "consumes" every piece of food that it crosses during the completion of its trajectory. (During each hop, an agent crosses many, many food particles – the scale of the grid is much smaller than the length of a hop in all cases.) After the time has expired, or after the full length of the trajectory has been reached, for all agents, the total amount of food gathered from the patch is tabulated. This amount is plotted on a graph against the noise level of the turning angle or hop length distribution in question. After many noise levels for a particular parameter distribution have been tested in this manner, the result is a complete curve of food gathered versus noise level, such as the example shown in Figure 2.3. If there is a specific noise level that provided the greatest advantage to the foraging agents during the trials of the model, then there should be a peak in the amount of food gathered at this noise level on the plot, such as the one seen in Figure 2.3. This noise level is therefore the "preferred" noise level, and the trajectories realized using parameters picked from distributions defined by this noise level might offer fitness advantages to those organisms using them.

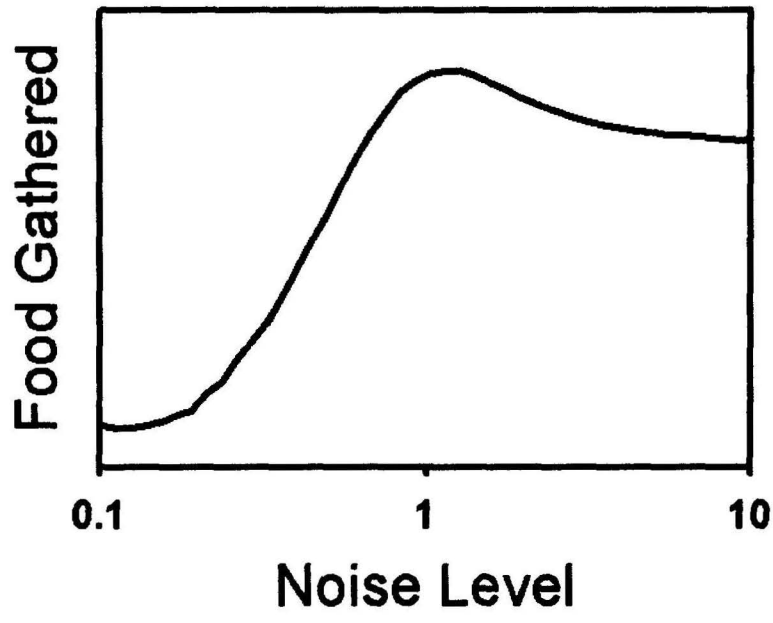

Figure 2.3. Food Gathered vs. Noise Level

There are just a few aspects of the *Daphnia* foraging model which are more complex than the rules of the basic foraging model introduced in Section 1.2. For instance, as the foraging agents feed, the food particles "consumed" are removed from the food patch and no longer available to be eaten by that or any other agent. This invokes an extrinsic constraint known as destructive foraging (Viswanathan *et al.* 1999). In destructive foraging, food sources are destroyed once they are used; in non-destructive foraging, the food sources replenish immediately or over some period of time after they are exploited. Also, in the *Daphnia* foraging model, the time allotted for foraging is not divided between the activities of searching for prey and then pursuing and capturing prey. The experimental data that this theoretical research relies on assumes that *Daphnia* have already found the patch; therefore, it is their motion within a single food patch that is of interest. Likewise, the *Daphnia* foraging model does not analyze how much time a forager should spend inside this patch. The feeding time is fixed here at a level more appropriate for traversing a single patch. The non-trivial complexities of a model containing many patches for *Daphnia* to search between are discussed further in Section 3.2.

2.4. RESULTS

The results of this study (Appendix A) are very simple and very robust. Through the use of two feeding protocols (feeding during the hops, as described above, and feeding during the pause times, as described in Appendix A – Simulation methods), and through the use of several foraging time allotments, many adjustments to turning angle and hop length noise levels, and even several fixed hop length values, in every case, and for every combination of constraints, the resultant curves of food gathered versus noise level always featured a peak at some optimum level of noise in the turning angle or hop length distributions. In reference to question (1) posed above, these peaks lend support to the hypothesis that there may indeed be optimum amounts of variation in foragers' choices of movement parameters which maximize their ability to gather food within a patch. The following section will discuss the possible implications of this finding – and whether or not the noise levels observed in *Daphnia* today might have been selected naturally.

3. EVOLUTION OF PREFERRED NOISE LEVELS

3.1. NATURAL SELECTION OF FAVORABLE NOISE

As discussed above, SR offers a means by which a system may exploit some variety of noise for use as an optimization tool. After its discovery, SR began to be frequently observed, but was rarely purposefully employed. In 1996, the breakthrough experiments of Morse and Evans showed that the addition of certain levels of noise to electrical representations of vowel sounds increased the decipherability of these sounds based on responses obtained from the experimental stimulation of investigational cochlear implant devices using the dissected sciatic nerves of toads (*Xenopus laevis*). These sciatic nerves served as significant biological (not computational!) models of nerves in the human auditory system since the two types are very similar genetically. This simple utilization of noise was just the beginning of an entire assemblage of research studies designed to help enhance the sensitivity of the cochlear implants used by profoundly-deaf patients (e.g., Chatterjee & Robert 2001). But is it possible that natural selection beat Morse and Evans to the punch?

Experimenting with amphibian, instead of human, cochlea, Jaramillo and Wiesenfeld (1998) examined the inner hair cells of the leopard frog (*Rana pipiens*) ear canal, and found that they were not attached to the canal's membrane quite as rigidly as more superficial hair cells. This allowed the inner hair cells to more easily undergo a type of Brownian motion as they fluttered in the surrounding medium. It was further shown that this extraneous Brownian motion stimulated the hairs at a level of noise which allowed the frogs to hear weak, sub-threshold sounds in the water through a stochastic resonance-like effect. This prompted the suggestion that the detachment of the inner hair cells from the typical membrane structure might have at one time provided a fitness advantage to a few lucky frogs. Natural selection, then, might have "detected" this advantage, and sustained it.

There is still a difference, though, between the detection of the effects of SR and its intentional exploitation. For instance, the noise levels that are presumed to be advantageous to *Daphnia* are different from the external noise utilized by the leopard frog in that, for *Daphnia*, the noise must somehow be generated internally. This may

happen either by a learned strategy, or through specific brain "circuitry", and very recent evidence suggests that both of these possibilities may be plausible. For instance, Li *et al.* (2008) have shown that the eukaryotic amoebae *Dictyostelium* and *Polysphondylium* exhibit exponential distributions of turning angles very similar to those employed by *Daphnia* when searching for food in the absence of apparent external stimuli. The amoebae's motion under this construct was shown through simulation to be more efficient than if they instead practiced a traditional random walk, since exponential distributions increased the probabilities that the cells would find their targets. Just like *Daphnia*, the noise that was observed in this case was found in the choices made by the organisms, but what is the internal origin of these habitual choices?

There is, indeed, the intriguing possibility that the brain of the organism may contain neurons specifically evolved to provide noisy accessory signals to functional stimulation. The first evidence for this phenomenon was found in the antennal lobe of the fruit fly, *Drosophila* (Shang *et al.* 2007). The antennal lobe in *Drosophila* is similar to the olfactory bulb of vertebrates in that it is used to facilitate the sense of smell. In addition to the typical olfactory neurons, the receptors of smells, *Drosophila's* antennal lobe contains other local excitatory neurons which respond to odors with increased activity, but this excitation does not have any noticeable odor-specific spatial structure across the lobe. If the total output of the antennal lobe were to be measured, the local excitatory activity would be detected as a form of noise being added to the typical olfactory stimulation. As it is, the neurons responsible for relaying sensory information from the antennal lobe to the rest of the brain are driven by this combined signal, and the overall sensitivity of the system is increased by the accessory noise in a SR effect similar to the example in Figure 2.2b. Furthermore, enhanced sensitivity – and, therefore, a competitive advantage - conveniently occurs at the particular levels of noise which the excitatory local neurons have evolved to produce.

So, for the fruit fly, it now seems possible that natural selection, or whichever other method of designing species one believes in, was successful in internalizing a source of noise and "purposefully" exploiting it. The following section will discuss a model designed to investigate whether or not the ancestors of *Daphnia* might also have benefited from the internalization of noise.

3.2. SIMULATION OF EVOLVING DISTRIBUTIONS

As shown in Section 2.3, the *Daphnia* foraging model resulted in classic stochastic resonance curves predicting optimum levels of noise in the *Daphnia's* turning angle and hop length distributions. A new simulation, EVO, will now be used to explore whether the process of natural selection might have been "guided" by the advantages provided by SR. In other words, EVO will help to determine whether or not *Daphnia* might have limited their collective parameter choices to narrow ranges of variance after many cycles of natural selection had affirmed the advantage of these choices. EVO's algorithm will employ the same general feeding mechanisms that were used in the *Daphnia* foraging model. Particularly, foragers will feed inside a uniformly-distributed, circular food patch for a finite amount of time, and they will travel along a trajectory made up of hops and turns. (Feeding during the pause times will not be investigated using this algorithm, per the discussion below.)

The main differences between the *Daphnia* foraging model and EVO are that the foragers in EVO will be assembled into sequential groups representing consecutive generations, and the movement parameter distributions from which the foragers construct their random trajectories will now be dynamic, changing by a small percentage after each use by a single generation of foragers. This can be contrasted with the *Daphnia* foraging model, in which foragers always used pre-defined distributions with specific noise levels. These evolving parameter distributions will act as the "parent", and the members of a generation, the "children", will choose their movement parameters randomly from this parent distribution. After a complete generation of children have eaten, each forager's rate of energy (food) intake will be judged and compared to the others in that generation. There will be a single "winner" who is the most efficient forager, and the rest of the population will be deemed "losers" and disregarded. The winner will then share its strategy for choosing movement parameters with future generations by providing an inheritance in the form of an update to the current, evolving, parental movement parameter distribution. This update will consist of adding some percentage (typically 2%) of a histogram of the successful child's movement parameters to the parent distribution. Also during the update, the same amount (2%) that was added will then be subtracted

from the parent parameter distribution, but this subtraction will be divided equally (percentage-wise) across each bar of the distribution. Thus, the total area of the distribution will always be preserved. The new distribution will then be used as the parent distribution for the next generation of foragers. In this manner, initially uniform and uncorrelated parameter distributions will be modified over and over, generation after generation, eventually evolving to what will presumably be an optimal result used by the most successful foragers. The full description of the EVO algorithm is presented in the Supplementary material of Appendix B.

Although EVO depends on the variability of parameters chosen randomly, too much variability can also erode the ability of the algorithm to effectively direct the evolution of the distributions. For instance, one might think that it would be extremely interesting to combine EVO with the basic patch model described in Section 1.2, where a forager encounters many patches along its trajectory, and must decide how to efficiently exploit them. A model like this was indeed attempted, and a typical layout of the patches, along with a sample trajectory, is shown in Figure 3.1. The competing agents begin foraging at the center of this group of patches. The most successful agent provides an inheritance as described above, but recall that it is only the distribution that is inherited, not the order of the choices. The next generations' choices of movement parameters may not have the same timing between the processes of investigating a patch (larger turning angles, smaller hop lengths) and traveling between patches (smaller turns, longer hops). Furthermore, in this model, the positions of the smaller patches are chosen randomly before each generation since food patches are not necessarily a constant in nature, so there is simply too much variability in what is required of the forager from generation to generation to effectively arrive at any significant improvement in the agents' foraging efficiencies. Evidence of this effect is seen in the plot of food gathered versus generation, Figure 3.2, where the amount of food gathered remains constant, showing little to no improvement over thousands of generations.

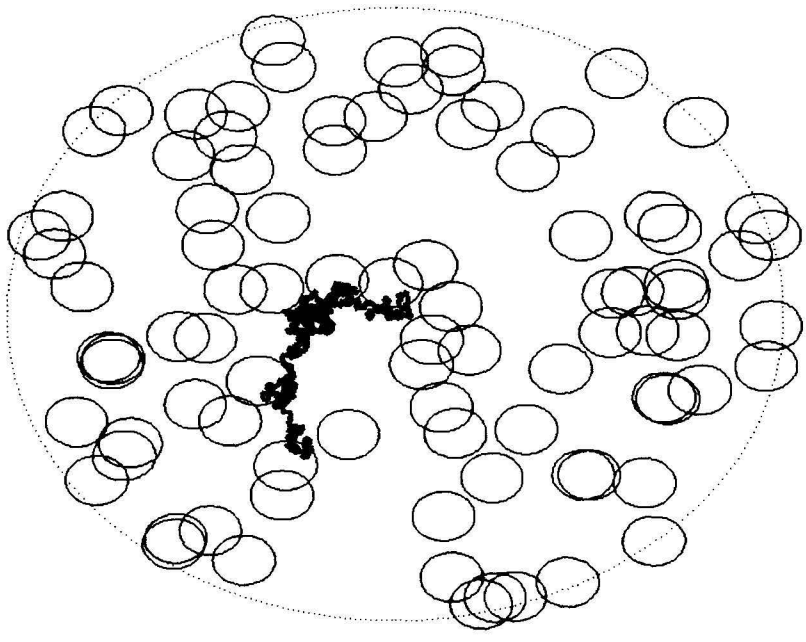

Figure 3.1. Layout of Many Small Patches

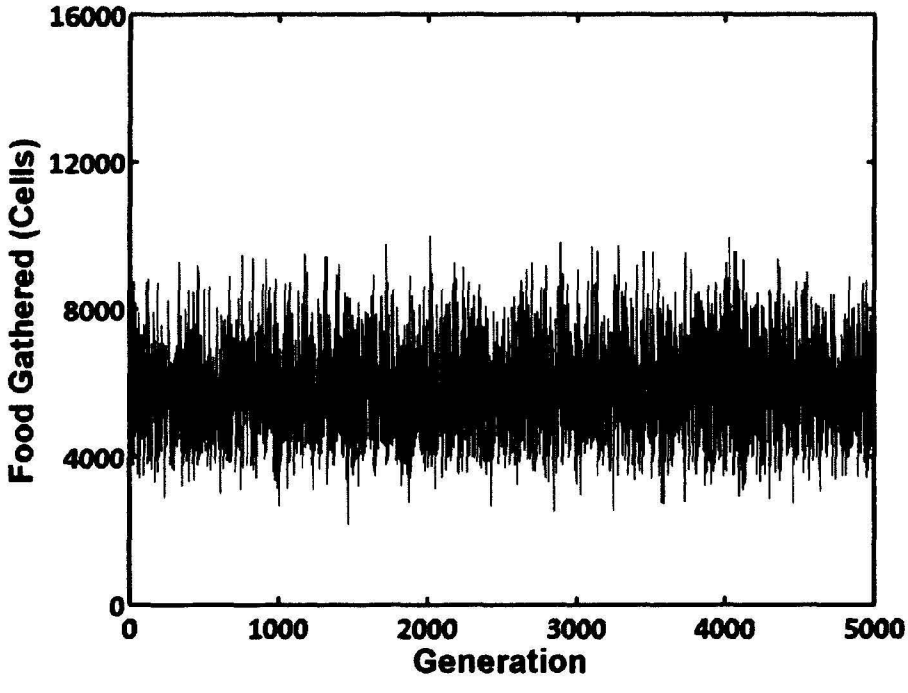

Figure 3.2. Food Gathered vs. Generation, Basic Patch Model

Another instance of having insufficient criteria for the evaluation of foragers occurs when more than one forager is allowed to participate in the inheritance. For example, suppose that 10 foragers are allowed to eat simultaneously, as in the *Daphnia*

foraging model, and 20 groups of 10 simultaneous foragers now compete with each other and are constituted as a generation. The foragers in this generation select movement parameters at random from an inherited parental distribution. The most efficient group of 10 foragers must be chosen to provide the inheritance to the next generation, but this choice becomes complicated when trying to account for the parameters used by each member of every group. When histograms of parameters are formed from groups of 10 foragers, they now represent quite a large number of angles. This is problematic because large numbers of angles chosen from the parent distribution means that the resultant grouped childrens' histograms will very closely resemble this parental distribution, and, in turn, they will also more closely resemble each other, regardless of their foraging success (or failure)! The results of food gathered by the most successful group under this algorithm are shown in Figure 3.3. Data from 8000 consecutive generations of foragers is shown. The efficiency hardly improves from beginning to end. The variability between the parents and the children, and between children and other children, has been lost, akin to the loss of random mutations in nature. Even in this case, when there are only 10,000 angles chosen from a 63-bin distribution, the inheritance is virtually meaningless, as the figure shows.

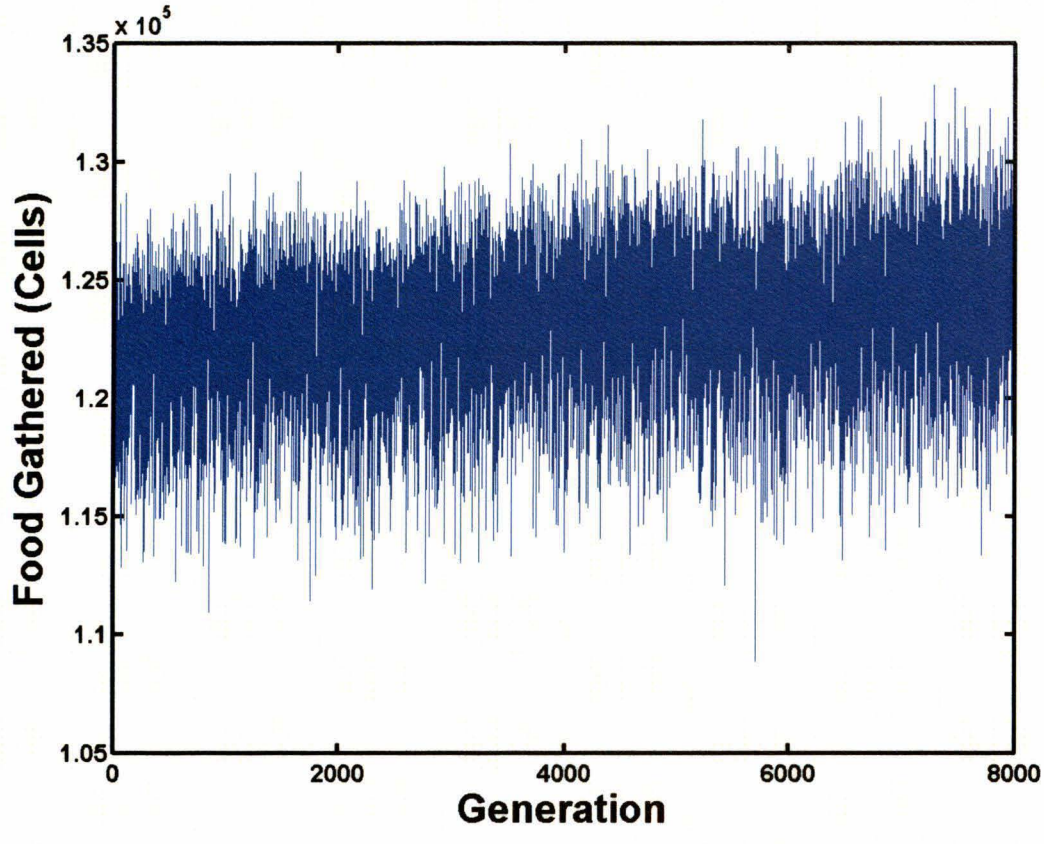

Figure 3.3. Food Gathered for 10 Simultaneous Foragers

EVO has been designed with constraints which should address these problems. Foragers in EVO operate one at a time, feeding independently inside a fully-populated food patch, and they begin their trajectories at the center of the patch instead of starting from random positions. The success of a forager will depend on its ability to stay inside of the food patch and avoid its own path. The forager's efficiency will *not* be affected by an unlucky random starting position or the trajectories of its neighbors. These rules offer the clearest, simplest view of the competition between foragers.

While the published results discuss only the evolution of turning angle distributions, hop length distributions were also evolved using this algorithm. They were evolved by themselves (while turning angle distributions remained uniform), and also simultaneously with the turning angle distributions. Hop length distributions of different ranges were tested, with some distributions limiting hop lengths to 25 units, and other distributions limiting hop lengths to only 5 units. (Note that the radii of the food patches

were held constant at 100 units.) One might expect this variety of scenarios to result in the evolution of diverse hop length distributions, but, in fact, this was not found to be the case.

For simulations in which the hop length distributions were evolved while the turning angle distributions were held constant and uniform, the hop lengths increased steadily to the largest available length (5 or 25 units, depending on the simulation). Foragers will not typically leave the food patch while choosing angles from a uniform distribution of angles, since the abundance of larger angles and sharper turns are not conducive to extended straight travel. The foragers in these simulations did, however, over many generations, attempt to develop strategies for avoiding their own paths through less-localized trajectories. Since less localized trajectories can always be achieved with larger hop lengths, larger hop lengths became advantageous. The resultant food gathered, the hop length distributions at 1500, 3000, 4500, and 6000 generations, and the winning trajectory at generation 6000 are shown in Figures 3.4 and 3.5 for maximum hop lengths of 5 units and 25 units, respectively. Notice that the plot of food gathered in Figure 3.4 shows much more improvement in efficiency than the same plot in Figure 3.5. This happens because the larger hop lengths (> 5 units) present in the uniform distribution at the beginning of the simulation in Figure 3.5 immediately provide less-localized trajectories, and, therefore, much higher quantities of food gathered, so that there is little room for improvement.

This tendency for hop lengths to steadily increase did not change when the turning angle distributions were allowed to evolve at the same time as the hop length distributions. These results are pictured in Figures 3.6 and 3.7, again with maximum hop lengths allowed being 5 units and 25 units, respectively. (Note that the turning angle distributions are plotted in absolute value form.) The hop length distributions at generation 10,000 appear to be very similar for both simulations, even though the turning angle distributions do not. These consistent results in hop length distribution warrant the decision to focus the reported work on the evolution of turning angle distributions only, while the hop lengths were held fixed at certain lengths.

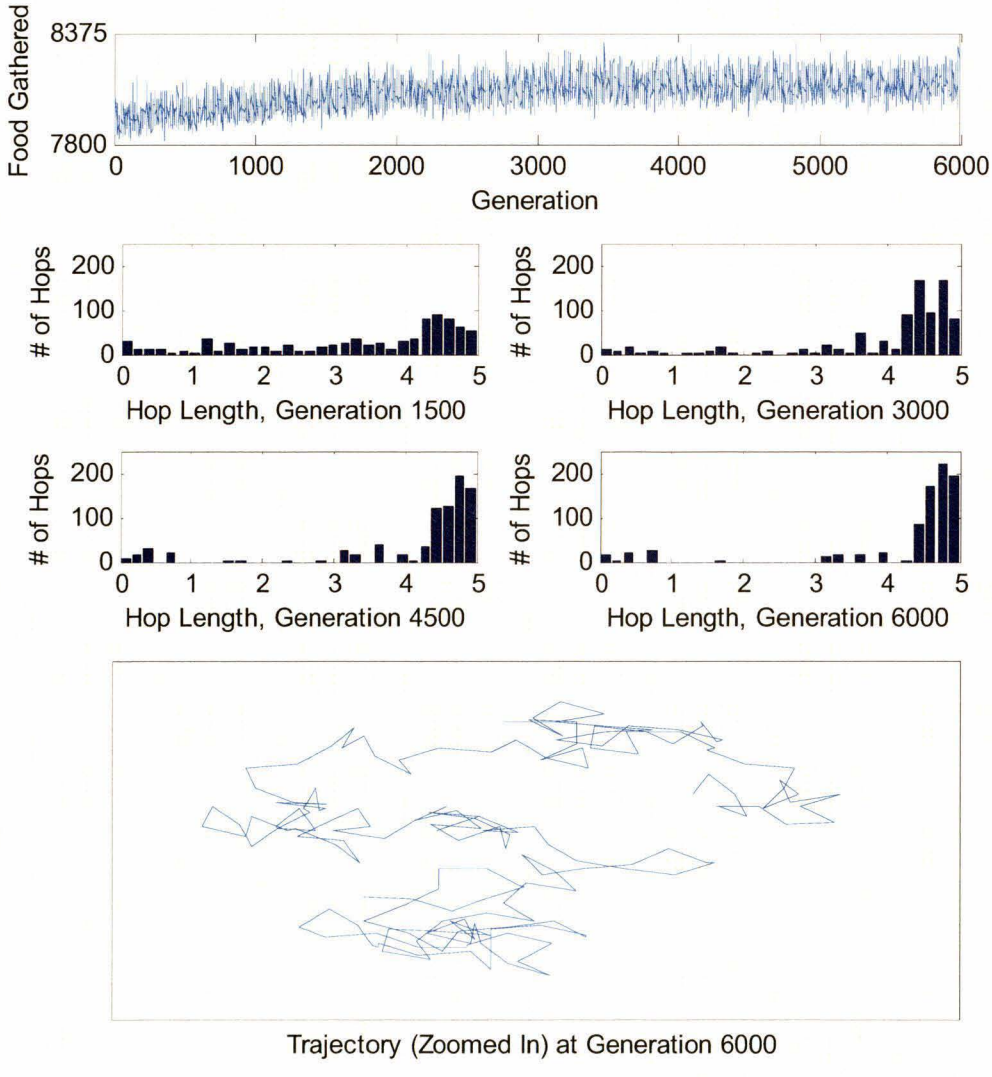

Figure 3.4. Evolving Hop Length Only, Max = 5 Units

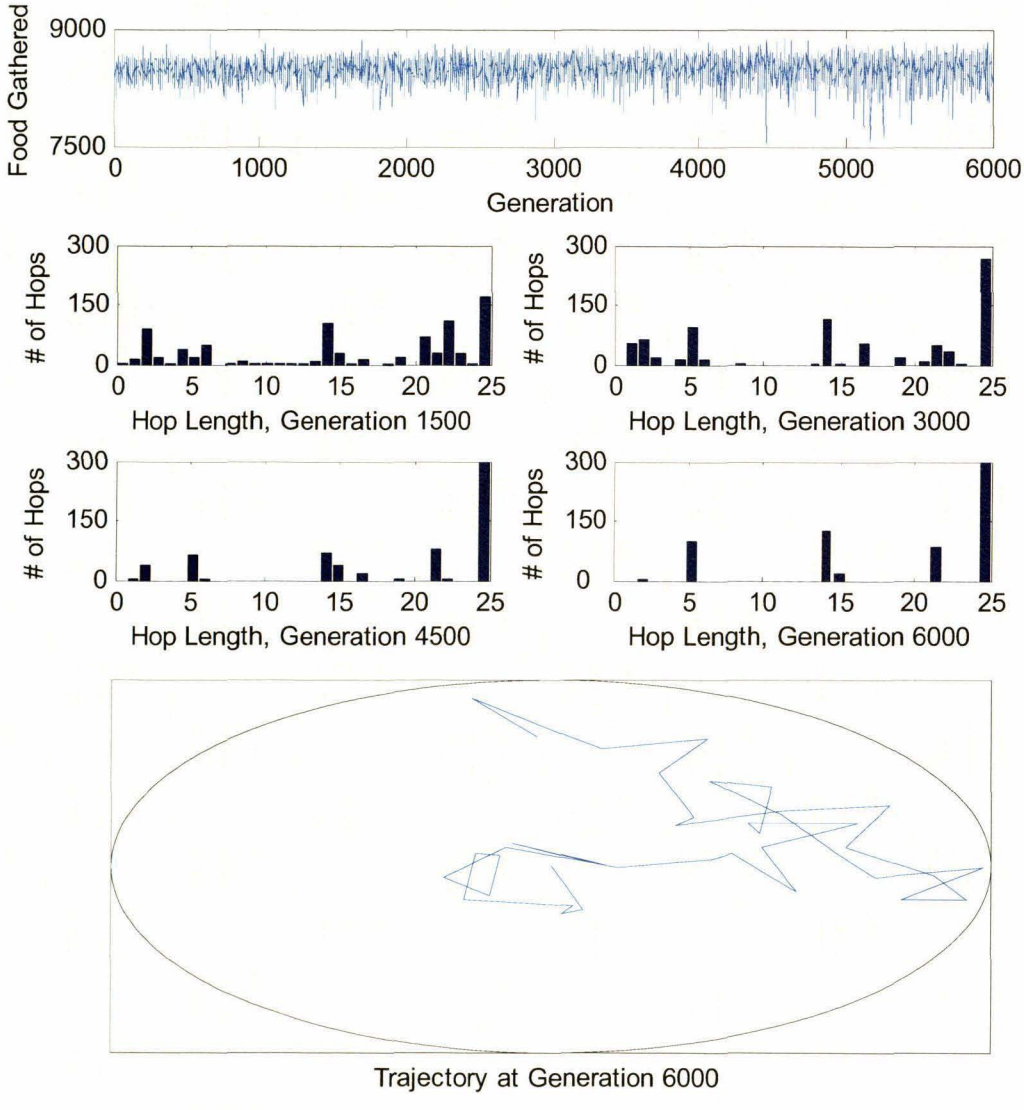

Figure 3.5. Evolving Hop Length Only, Max = 25 Units

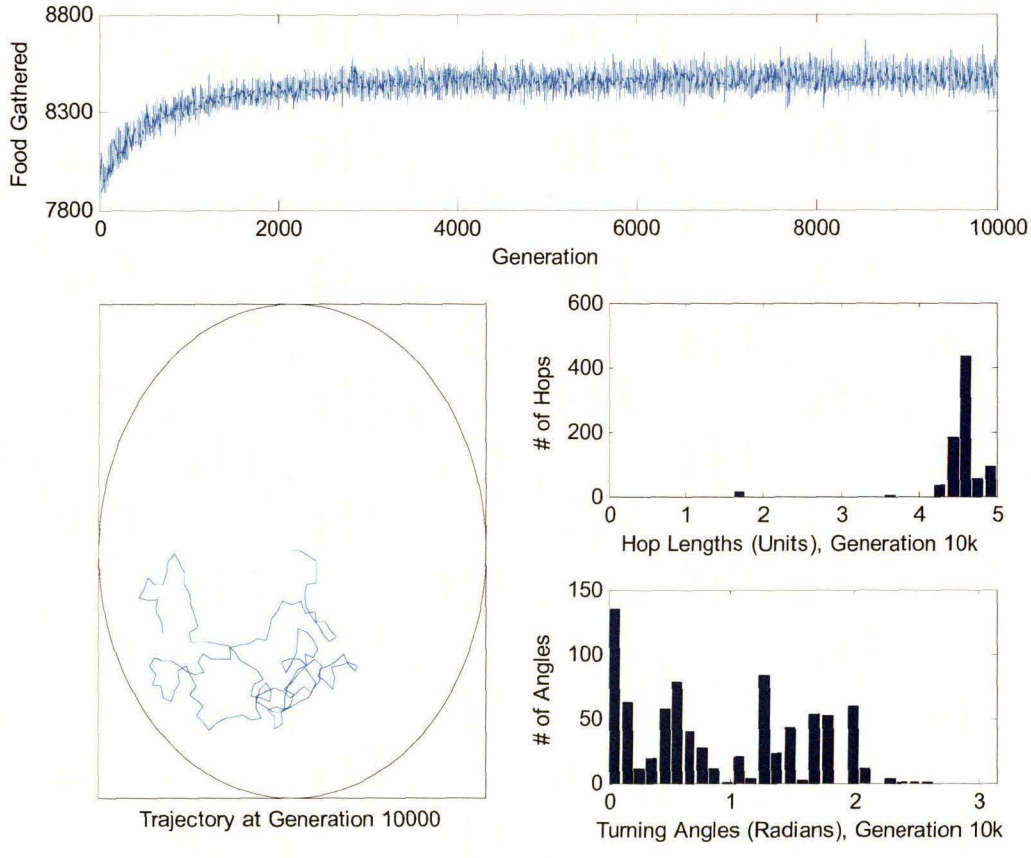

Figure 3.6. Evolving Hop Lengths (Max = 5 Units) and Turning Angles

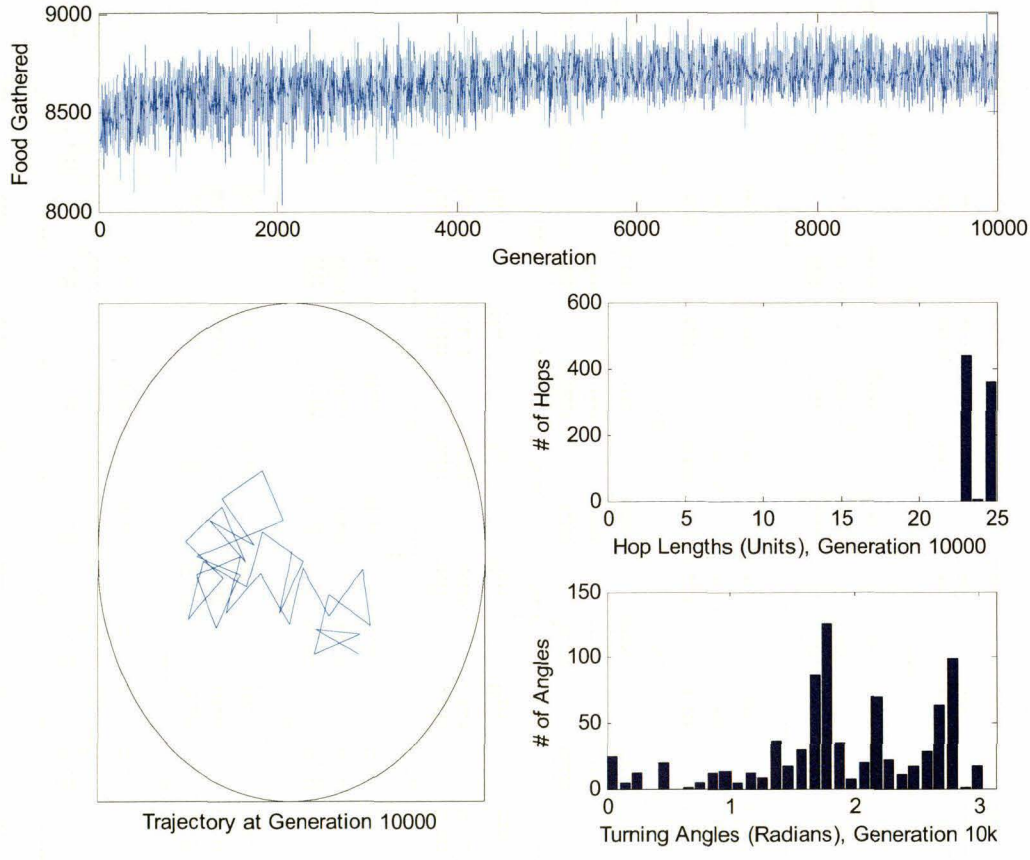

Figure 3.7. Evolving Hop Lengths (Max = 25 Units) and Turning Angles

The published results of EVO were further focused by limiting the analysis to just the first feeding protocol used in Appendix A, where foragers feed along their paths of travel. As mentioned in Appendix A, *Daphnia* may feed during their hops, during the pauses, or possibly at all times. There are no experimental reports which would prove that either protocol is more relevant than the other. The first feeding protocol, therefore, serves every intended purpose. For instance, in real systems, the concentration of food in a patch should decrease as foragers feed, thereby reducing their clearance rates (Hartgers 1999), while diffusion of the food particles should insure that as long as the animals remain inside of the patch, they should be consuming at least a little food as they strain the surrounding medium. The first feeding protocol is accurate in this sense as the food concentration decreases during foraging, but the foragers typically will still find food along at least some part of each individual hop. (Alternatively, see the large voids of food cleared from the patch using the second feeding protocol in Figure 11 of Garcia *et al.*

(2007).) Additionally, the algorithm of the first feeding protocol is very simple to understand, and offers a clear picture of the success of foraging agents.

3.3. THE RESULTS OF 'EVO'

Appendix B reports the comparison of the optimum turning angle distribution noise intensities predicted by the *Daphnia* foraging model and the "supposed" optimum turning angle distribution noise intensities derived by the evolution of these distributions. The experiment is designed to address question (2) proposed above (in Section 2.1), and to provide support for the hypotheses that, since the turning angle distribution noise levels are similar across several species, they might be evolved quantities, with SR having a role in this evolution.

For the sake of comparison, the *Daphnia* foraging model was modified slightly to match the constraints imposed in EVO. In other words, foragers in both models were programmed to operate independently, and to start their trajectories in the center of the food patch. As the distributions in EVO evolved, the noise intensities of the distributions steadily decreased from the large amount of noise present in the uniform distribution to a point of stasis, where the noise intensity then remained approximately constant for tens of thousands of generations thereafter. This supports the hypothesis that the noise intensities could have arisen via natural selection.

As fixed hop length values were increased, the *Daphnia* foraging model predicted increasing values for the optimal noise intensity. Strikingly, the EVO simulation showed the same effect – with increased hop lengths, the stasis values for the evolved turning angle distribution noise intensities were larger. Thus, EVO "tracks" the predictions of the *Daphnia* foraging model's SR-like curves, supporting the hypothesis that SR could have "guided" the selection of *Daphnia* over millions of generations.

The numerical values of the noise intensities evolved by EVO were very similar to those predicted by the *Daphnia* foraging model for the same hop length values. The average difference between the predicted and evolved noise intensities across all hop lengths reported was 0.083 radians. In each case, however, the evolved noise levels were slightly higher than those predicted by the *Daphnia* foraging model. As discussed in Appendix B, the differences between the perfect Gaussians used in the *Daphnia* foraging

model and the evolved distributions are most evident near the tails of the distributions. As also discussed in Appendix B, these differences are more easily seen when fewer trials are considered, rather than the averaged result of 10 trials, such as those presented in the Appendix. For example, Figure 3.8 shows an evolved turning angle distribution (grey bars) which is the averaged result of just two trials at hop length = 1.0 units. The distributions that make up this averaged result have evolved for 100,000 generations, and have had steady noise levels for almost 70,000 of those generations. The figure also shows a true Gaussian fit (red curve) at the noise level predicted by the *Daphnia* foraging model for this hop length. Notice that the evolved distribution lacks the gradual tapering present in the tails of the true Gaussian, potentially resulting in larger measurements of standard deviation (noise level), as seen in the experimental results (Appendix B – Results).

It is suggested in Appendix B that the EVO algorithm might have a slight problem sustaining histogram bins which have low bin heights (representing small probabilities). This could be due to the continual subtraction of the certain percentage of every bin's height before the addition of the inheritance at the frequent generational updates. If a bin height falls very close to zero, it will continue to have a certain percentage subtracted after each generation, but will be less and less likely to be added back through representation in the inheritance. On the other hand, the pre-defined distributions in the *Daphnia* foraging model have bins of every height, including low-height bins in the tails of the distributions. If foragers in the *Daphnia* foraging model need to select larger turning angles, they may choose them from the tails of the distributions with no problem. If foragers in EVO need these angles, however, they must preserve fairly large bins to select them from, such as the tall bins seen extending above the Gaussian fit in Figure 3.8 around ± 1 radian.

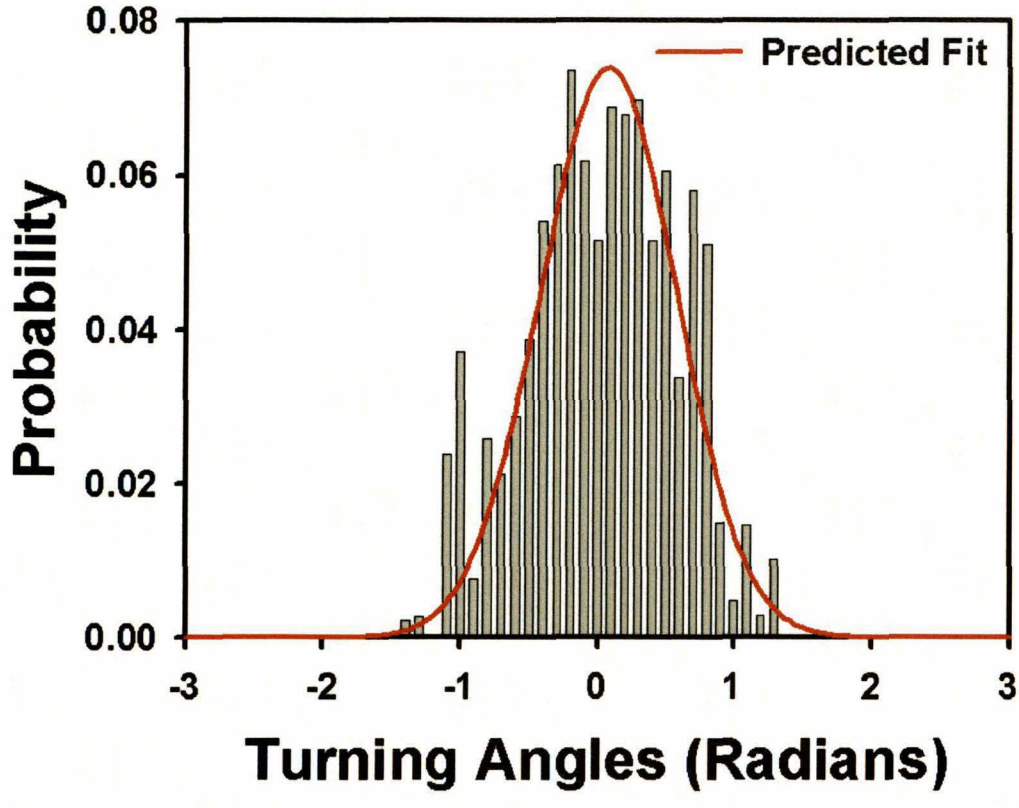

Figure 3.8. Errors in the Gaussian Fit of Evolved Distributions

The overall shapes of the evolved distributions may have also been affected by the ratio between the total trajectory length and the radius of the food patch. In Appendix B, a ratio of 15:1 was used. This ratio was chosen somewhat arbitrarily, as there are no previous studies which provide accurate information for how long or for how many hops a *Daphnia* in the wild traverses inside a single patch (or for how quickly the *Daphnia* might enter a second patch if it were to leave the first). It was verified, for instance, that when this ratio is changed to 1:1, the turning angle distribution will evolve into a delta function at zero radians. This is an effective strategy for the foragers at this ratio because it eliminates any chance of them crossing their own paths. And since there is zero possibility for any forager to actually leave the patch, crossing one's own path becomes the only judgment criterion available.

Another point, which was not discussed in Appendix B, is that the results of Garcia *et al.* (2007) showed that the noise levels found in the turning angle distributions of juvenile *Daphnia pulex* and juvenile *Daphnia magna* were 0.52 ± 0.05 and 1.0 ± 0.2

radians, respectively, while the noise levels exhibited by the adults in the same species were 20 and 58% larger, also respectively. Juveniles, being smaller in size than the adults, also have smaller hop lengths, and so it seems that the proportional relationship reported between the fixed hop lengths and the predicted and evolved noise intensities might actually have some biological basis.

4. THE CIRCLING TRAJECTORIES OF PADDLEFISH

4.1. PHYSICAL LAWS AFFECT ANIMAL BEHAVIOR

An animal's behavior is determined by many factors. Among them are the characteristics of the animal's predators and prey, the instincts and capabilities that the animal inherits, and also the environment in which it lives. There are many physical laws, too, which have a significant impact on animal behavior. Consider all of the actions that an animal must take to maintain its internal heat, energy, and fluid balances, balances which are typically described by simple physical input and output equations (Schmidt-Nielsen 1997). Other physical laws are more externally prevailing, such as the law of gravity. These physical laws cannot be ignored when attempting to analyze an animal's behavior.

The locomotion of animals is a very commonly studied physical activity due, in part, to the major associated energy costs. These energy costs are usually (and most easily) calculated by measuring the rate of oxygen consumption during the activity (Schmidt-Nielsen 1997). Horses offer a helpful comparative example in that they have three different modes of movement: walking, trotting, and unreserved running (galloping). An obvious assumption might be that the faster a horse travels, the more energy it must use to maintain its speed. This is actually *not* the case, as illustrated in Figure 4.1. This figure shows that, if a horse is specially trained to move at different speeds within a particular gait, a wide range of energy consumption rates are associated with these different speeds (for each gait, see the fitted data points in Figure 4.1). However, untrained horses moving at the different gaits upon their own volition are observed to move at the speeds indicated by the blue histograms below the curves in Figure 4.1. The histograms show that typical horses prefer the most efficient speed within the range for each gait. A horse's instinctual movements seem to be governed by some physical law of energy efficiency.

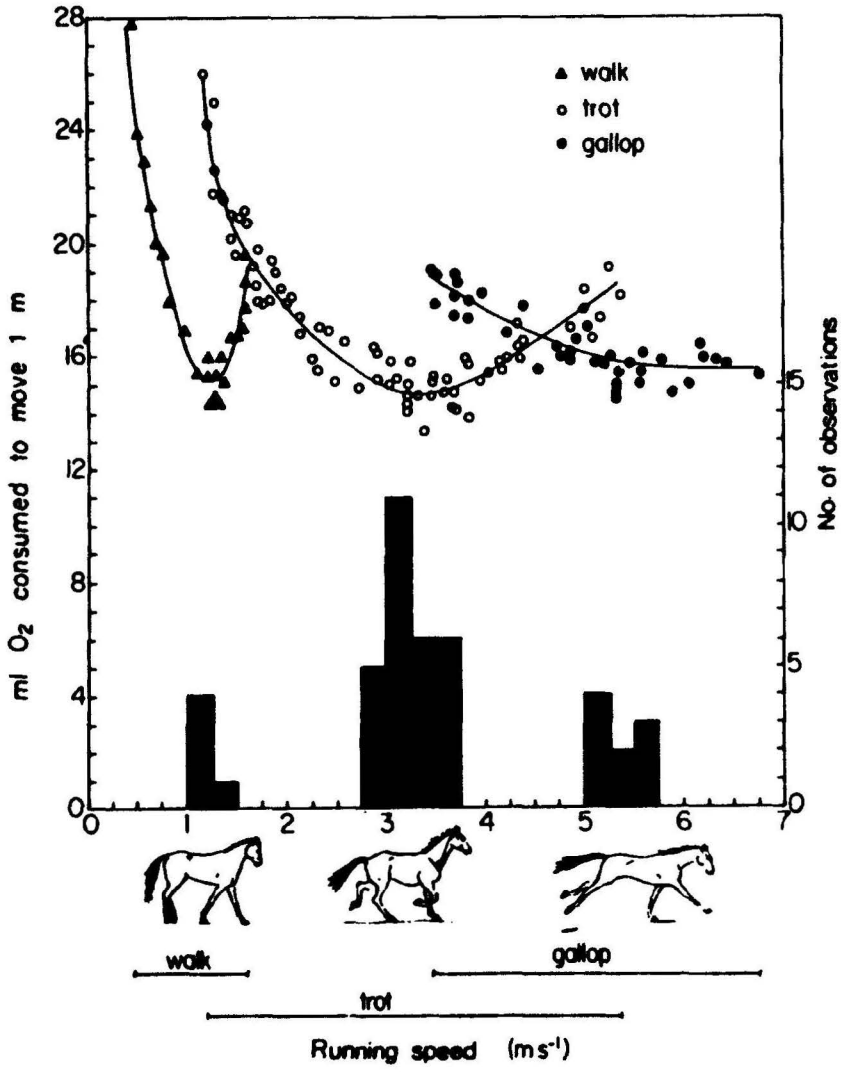

Figure 4.1. Energy Consumption vs. Running Speed for a Horse[3]

For a different perspective on the investigation of energy efficiency, consider the following question: what is the most efficient way to get from one place to the other, running, swimming, or flying? The answer to this question, of course, depends somewhat on what is between the two places, meaning that it would be hard to swim through a desert, and it would be hard for a swimming organism such as a fish to fly over a mountain. But, more generally, if an animal were equipped to move a certain distance across a featureless planar terrain using any of the three methods of locomotion - running on land, swimming in water, or flying through the air - which method should the animal

[3] Reprinted by permission from Macmillan Publishers Ltd: Nature, Hoyt & Taylor, copyright 1981.

choose? For a given body mass, the surprising answer is that swimming is the most efficient method of the three, even though a swimming organism must push through a much denser medium (Schmidt-Nielsen 1972). Running is actually the least efficient, to the surprise of those who might have thought that flying would be the most energetically demanding. To combat this idea, Schmidt-Nielsen (1997) reminds his readers that "migrating birds fly nonstop for more than 1000 km, and it would be difficult to imagine a small mammal such as a mouse that could run that far without stopping to eat and drink." The energy cost comparison of running, swimming, and flying is shown in Figure 4.2.

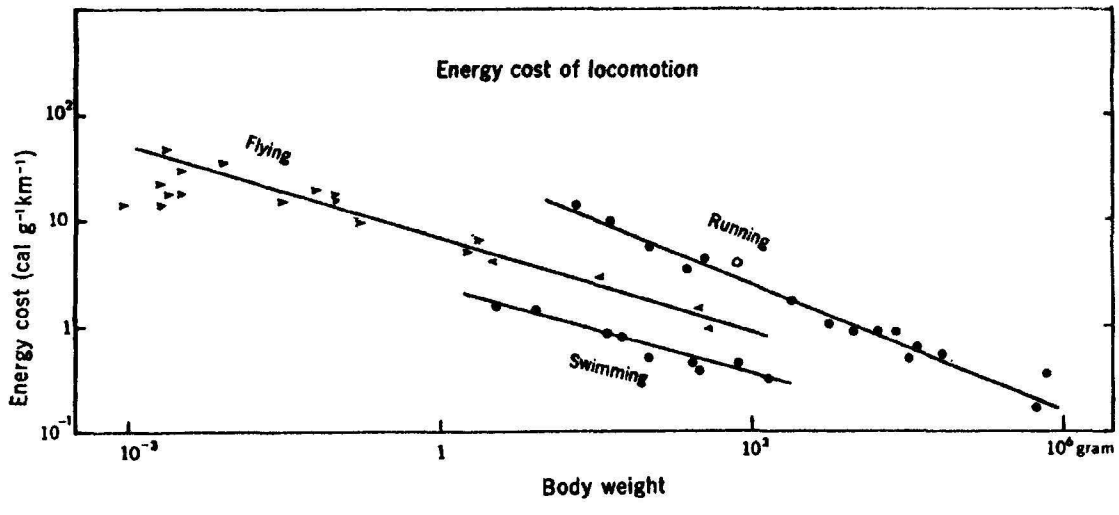

Figure 4.2. Energy Cost Comparison of Running, Swimming, and Flying[4]

One main reason for the high efficiency of swimming is that most swimming organisms are buoyancy-neutral, and therefore expend very little energy (if any at all) to support their own body weight vertically. They simply wiggle their streamlined bodies and easily propel themselves forward. But this is not the case for all aquatic organisms. Even in Figure 4.2, it is seen that as the body mass of the swimmer gets smaller, the energetic cost of swimming gets larger, and data is not even reported for tiny organisms such as *Daphnia*, with masses on the order of milligrams (Ward & Robinson 2005). The following sections will address the fact that the swimming efficiency of small organisms is affected quite differently from that of larger swimmers by the density of water. It will

[4] From Schmidt-Nielsen (1972), Reprinted with permission from AAAS.

be shown that if this difference is accounted for in foraging simulations, radically different foraging behaviors will occur.

4.2. *DAPHNIA* VS. PADDLEFISH

As described in Appendix C, *Daphnia* and paddlefish offer an interesting comparison by which to investigate the effects of the physical laws associated with swimming in a dense medium. Although both organisms are filter-feeders, and both feed on patchy food sources (see Folt & Burns (1999) for a discussion of the patchiness of paddlefish prey), the animals differ greatly in their size, and also, therefore, in the flow regimes in which they operate. *Daphnia* swim in the viscous flow regime, where, after each propelling stroke by their large second antennae, the surrounding fluid immediately stops their motion due to large frictional forces which easily overcome such a tiny momentum (Videler *et al.* 2002). *Daphnia* never build sustainable inertia that would allow them to coast in the water, and so for each hop and turn along their trajectory, they are starting from zero velocity.

Paddlefish, on the other hand, *do* operate in the inertial flow regime. They build linear momentum as they travel, a momentum which is significantly decreased when they decide to change direction (Weihs 1972). Regenerating this lost momentum is quite costly for the larger animal, so the single most inefficient motion for a paddlefish would be to make a sharp turn, or, in other words, to make a turn through a large angle. Large-angle turns affect *Daphnia* very little at all, however. It has been shown that due, to the *Daphnia's* nearly-round shape and small body volume, turns in the water are like rotations, a type of motion which does not seem to be impeded as they swim, and which incurs a near-zero cost to the organism (Videler *et al.* 2002). It is natural to hypothesize that these physical differences between the two animals must have some effect on their overall behavior as they search for food in similar environments.

4.3. THE PADDLEFISH MODEL

It is simple to imagine that the patchy swarms of *Daphnia* on which paddlefish feed have boundaries which are circular in shape when seen from above, reminiscent of the patches of zooplankton upon which *Daphnia* feed. Also, since most fish generally

swim in a limited horizontal plane (Webb 1991), the swimming trajectories of paddlefish can be easily modeled in a 2-dimensional environment. These constraints represent two of the most basic rules present in the *Daphnia* foraging model and EVO, immediately suggesting a simulated comparison between foraging *Daphnia* and foraging paddlefish. This comparison is further motivated by observations of the vastly different swimming trajectories of real *Daphnia* and real paddlefish. While *Daphnia* move in random walk-like trajectories, as mentioned above (see Uttieri *et al.* 2004 for pictures of 3-dimensionally-tracked trajectories), data from captive paddlefish reported in Appendix C show highly structured circling patterns in both clockwise and counter-clockwise directions. A model similar to the *Daphnia* foraging model and EVO, designed to incorporate the effects of swimming in different flow regimes, might offer an explanation for the distinct differences between the two types of trajectories.

As described in Appendix C, the EVO simulation was modified by the addition of a penalties which punish a swimmer in the inertial flow regime for turning. The incurred penalties reflect the use of extra resources to maintain swimming speed by generating momentum along the new heading after changing directions. Since the resource used in this case is energy, the modeled agents are punished by a subtraction of some of the food that they had collected while feeding. These penalties will not, of course, be applied to organisms in the viscous flow regime, thereby providing a point of differentiation between the modeled *Daphnia* and the modeled paddlefish.

Two different methods for the application of penalties were considered for the paddlefish simulation. The first method, P_1, was designed to account for the differences between the bodies of the paddlefish and the bodies of *Daphnia*. Unlike the small, roughly-spherical *Daphnia* which can easily execute a turn by rotating in the water, a larger, longer fish must bend its body to change direction, pushing the sides of its body against a viscous medium, thereby consuming some energy. It was assumed in the definition of P_1 that a fish uses very little strength to keep its flexible body bent, so that consecutive turns at the exact same angle would incur no penalty (due to a lack of further body-bending). However, even if the fish wanted to simply straighten its body out so as to discontinue turning, this movement would also require more pushing against the medium, and would therefore require a proportional amount of energy. Mathematically,

P_1 is directly proportional to the absolute value of the difference between each pair of consecutive turning angles, $\Delta\alpha = |\alpha_{n+1} - \alpha_n|$, and was applied accordingly.

The reader will obviously be thinking that the definition of P_1 is incomplete because consecutive turns through the same angle will still create a loss of linear momentum which must be replenished. The definition of a second penalty, P_2, addresses this problem. When it is applied, P_2 requires a subtraction of food gathered in an amount directly proportional to the absolute value of each turning angle used by the forager. This linear relationship is shown qualitatively in Figure 4.3, and the results of applying both penalties are discussed in the following section.

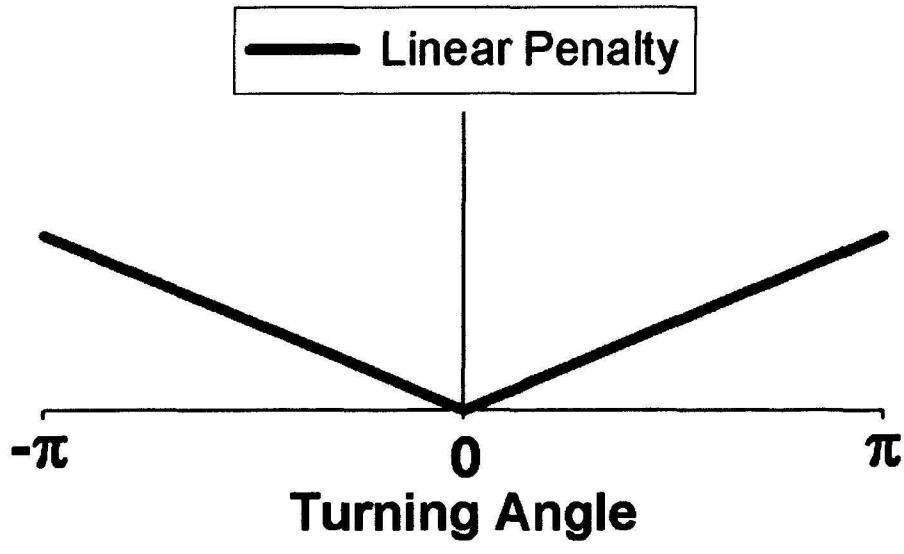

Figure 4.3. Linear Penalty Relationship (P_2)

4.4. RESULTS OF THE PADDLEFISH MODEL

The results of the preliminary trials of the paddlefish model (Figure 4.4) were qualitatively the same whether just P_1, P_2, or a combination of both penalties was assessed on the simulated foragers. The first column in Figure 4.4 shows the average result of food gathered over 50,000 generations and 10 trials; the second column shows the trajectory of a single forager at generation 50,000, and the third column shows the mean turning angle of the evolving distribution in each of 10 trials over 50,000

generations. The bold black line in the plot of mean turning angle represents the absolute value of the average result of mean turning angle for the 10 trials (which appear individually as multicolored lines). Circling trajectories are predicted for all combinations of penalties applied, matching explicitly with the experimental paddlefish data presented in Appendix C - Results. This suggests that, in the model, the energy costs attributed to turning dictate that the most efficient method for a larger filter-feeding forager to exploit a patchy food source is by swimming in circles.

See Appendix C for many other variations of this model, all of which produce a circling behavior for foragers in the inertial flow regime, and never for foragers in the viscous flow regime. Note that, in the appendix, only penalty P_2 was applied to inertial swimmers, being that it is the simplest (yet still effective) definition of energy costs associated with turning.

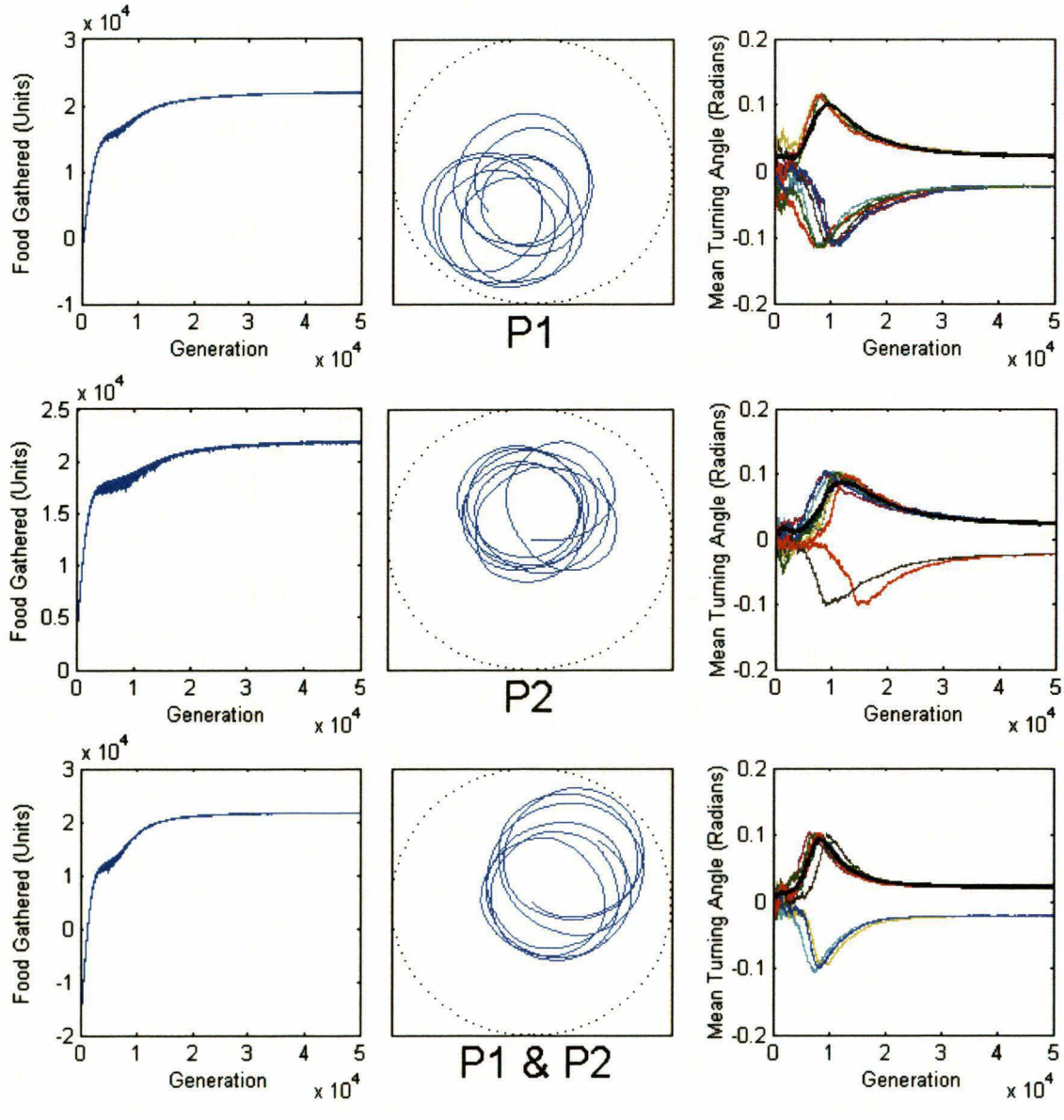

Figure 4.4. Paddlefish Model Results

4.5. CIRCLING

The extent of the circling behavior found in the trajectories of the modeled *Daphnia*, the modeled paddlefish, and the live paddlefish were quantified in the Mathematical analysis section of Appendix C using a "circling index". This measure was invented for the study, and is described in more detail in the Appendix. Briefly, the circling index is a measurement of the frequency within a given trajectory that left-hand turns follow other left-hand turns, and that right-hand turns follow other right-hand turns.

The index is based upon the notion that trajectories containing numerous consecutive turns in either the left-hand or right-hand direction will contain lengthy segments of spiraling or circling motions. Trajectories that exhibit *perfect* circles, for instance, will never have a random "mixing" of right and left-hand turns. These highly-ordered trajectories will be defined by a circling index value of 1. On the other hand, trajectories in which the directions of turns are chosen completely at random and in no noticeable patterns will appear to resemble traditional random walks. Trajectories of this type will have circling index values of very nearly 0.

A table of circling index values, not given in Appendix C, is shown below (Table 4.1). Simulations of foraging *Daphnia* are compared, using a two-tailed, unequal-variance t-test, to what is called the "*Daphnia* control" simulation. In the control simulations, the inheritances for the evolving turning angle distributions are provided by a random forager rather than the most successful forager. This leads the evolving distributions to remain uniform and uncorrelated throughout the trial. Both the *Daphnia* and the *Daphnia* control simulations have very low (near-zero) circling index values which are statistically similar, indicating that the modeled *Daphnia* change directions randomly, and confirming once again that the modeled *Daphnia* exhibit random walks.

The t-test between the paddlefish simulation and the paddlefish control simulations tells a different story. The paddlefish simulation shows an average circling index of 0.99, while the paddlefish control simulation's index is similar to those of the *Daphnia* and the *Daphnia* control simulations, averaging only 0.09. The statistically significant difference between the paddlefish simulation and the paddlefish control simulation (as well as the significant difference between the modeled paddlefish and the modeled *Daphnia*) proves that the assessment of energy expenditure penalties due to turning in this model leads to distinct circling behavior.

In addition to the simulated values, Table 4.1 also shows the circling index values for 19 real paddlefish. Some of these animals obviously circled more than others, but an average circling index value of 0.60 is indicative of a general tendency to exhibit distinct circling behavior. Further details about comparisons of the turning angles measured in the trajectories of the real paddlefish to surrogate sequences of these turning angles are given in Appendix C – Mathematical analysis.

Table 4.1. Circling Index Values for Simulated Data and Real Animals

	Daphnia Simulation	*Daphnia* Control	Paddlefish Simulation	Paddlefish Control		Captive Paddlefish
	0.0906	0.0187	0.9975	0.0201		0.5809
	0.0059	0.0015	0.9975	0.0179		0.8741
	0.0121	0.0495	0.9975	0.1121		0.4722
	0.0116	0.0099	0.9975	0.0777		0.5944
	0.1473	0.1616	0.9772	0.0946		0.5954
	0.1021	0.1282	0.9974	0.0041		0.8085
	0.0366	0.0865	0.9975	0.0930		0.2139
	0.1450	0.0077	0.9949	0.1080		0.7541
	0.1008	0.1564	0.9873	0.3905		0.8545
	0.0637	0.1851	0.9874	0.0146		0.8261
Mean	0.0716	0.0805	0.9932	0.0933		0.1962
Std. Dev.	0.0537	0.0722	0.0070	0.1127		0.3166
T-test		0.7574		0.0000		0.8443
						0.6642
						0.7553
T-test between *Daphnia* and Paddlefish simulations				0.0000		0.6348
						0.5318
						0.3439
						0.6578
					Mean	0.6063
					Std. Dev.	0.2147

At this point, an observant reader might point out the fact that in Appendix C, the holding tank for the real paddlefish is described as square-shaped, while the modeled agents swim in circular patches. However, it has been verified that simulated agents foraging in a square food patch while turning penalties are assessed do indeed exhibit circling behavior (data not shown). In fact, it could be argued that since the real fish swim in a square tank, it is quite remarkable that they still circle, even though they are not able to follow along the side of a tank to do so.

5. PERSPECTIVES AND FUTURE WORK

5.1. INHERITED BEHAVIOR

There is an open question in biology that has been hotly debated since before the time of Charles Darwin, and which looms in the background of many of the assumptions and conclusions presented in this manuscript. Can behavior be inherited?

Even the definition of behavior itself seems to be debatable. Clark and Grunstein (2000) mention the following two definitions within 4 pages of their text: 1) perception of a stimulus in the environment, followed by the integration of this perception with previous experiences and a reaction to the stimulus, and 2) whatever it is that an animal does to stay alive and reproduce. The second definition obviously seems analogous to the definition of an "instinct", and conjures images of animals working as machines, performing their duty without question and without reasoned logic. But, the first definition seems to involve, at minimum, learning and thinking, if not also analysis and invention. Behavior which must be learned, though, is obviously not inherited, so the second definition seems most appropriate for this discussion. Clark and Grunstein (2000) mention, for instance, that a newborn human baby with no prior experience will withdraw its hand from a harmful flame. They also successfully argue that even a single-celled paramecia use Na^+, K^+, and Ca^{++} pumps and channels to manipulate the polarization of their cell membrane in order to align themselves with certain fields and currents, avoid extreme temperatures or UV light, and find food and mates, all without having a brain or nervous system. Surely, their behavior must be inherited genetically.

Darwin did not promote the inheritance of behaviors, per se, but he did believe in the inheritance of instincts, and perhaps in mutations of these instincts. He touched on this in his notebooks regarding the transmutations of species, which were later published in the 1960s. In trying to understand why species which diverge into separate groups are eventually unable to produce offspring, he wrote "Instinct goes before structure... hence aversion to generation, before great difficulty in propagation" (Burkhardt 1975). Darwin was acknowledging here that instincts could somehow change, but he did not give a clear indication of why. Darwin also used this explanation to discuss changes in other behaviors as well. He stated, for instance, that if the instincts of a particular species of

bird urged the birds to begin feeding solely by fishing, those birds which were best adapted to fishing would end up being the ones to reproduce, and then the structure of the bird would adjust accordingly.

Opponents of the possibility of inherited behavior argue that it is only genes that are inherited, and they present analogies which disassociate genes from behavior, such as this one: Imagine a series of 26 dominos, labeled A to Z, standing upright and in a straight line across a tabletop. Now, imagine that toppling domino A towards the others represents having a specific gene, and toppling domino Z represents the outward expression of some trait or a behavior. Toppling A is sufficient for topping Z, but not necessary. Z could be toppled in 25 other ways, including directly knocking over domino Z. And while it is essentially agreed upon by biologists that a single gene is typically not responsible for something as complex as a behavior, but rather that several, or more likely, many genes may be involved, it is very hard to prove that the only way a given behavior can occur (or be inherited) is through a specific set of genes (Moore 2001).

There are many examples from current research, however, which lead to the opposite conclusion. A striking example from the field of foraging behavior involves the gene-dependent regulation of foraging habits in the roundworm (*Caenorhaditis elegans*). The patch exploitation of roundworms hinges on expressions of the alleles of a single gene, *npr-1* (Clark & Grunstein 2000; Gloria-Soria & Azevedo 2008). If the 215F allele of *npr-1* is represented in a group of worms, the worms will tend to clump together in a small area of a larger food patch as they feed. If the 215V allele is represented in the group, the worms will avoid contact with one another and spread out evenly across the food patch. Thus, in this case, foraging behavior is proven to be inherited.

5.2. FUTURE WORK

The study in Appendix A relies heavily on experimental observations performed by Garcia *et al.* (2008). The measurements of movement parameters in this study were taken from the trajectories of several different *Daphnia* that moved across the field of view of the digital camera during the experiment. While this method avoided any edge effects that the aquarium might have induced, it did not allow for the collection of long sequences of consecutive movement parameters used by any particular organism. If,

instead, one single *Daphnia* were monitored for a longer period of time in a larger aquarium to accumulate a chronological sequence of measurements of turning angles, hop lengths, and pause times, the analysis of the trajectory could include time-sensitive measurements such as auto-correlation of the measurements of a single parameter, or correlation between different parameters. Such time series data might inspire a re-design of the simulations, and also might transform the interpretations of *Daphnia's* foraging strategy. This data would also allow the circling index to be calculated for the real *Daphnia* trajectories, a measurement which was unfortunately not able to be included in Appendix C.

The work in Appendix B could be extended further by performing the same analysis while using the second feeding protocol described in Appendix A. In the second feeding protocol, foragers consumed food during the pauses in between each hop rather than along the line of the hop. After each hop, the simulated agent is imagined to be straining the surrounding medium, consuming all food particles in the surrounding area at a speed which is based on a clearance-rate factor. This phenomenon is modeled as a steadily increasing circular area in the food patch where the food particles have been consumed. As in most other cases, the food was not replaced under the description of destructive foraging. This feeding protocol has not yet been applied to EVO in any capacity, but an effort to do so may offer new, interesting information, or robustness to the current results.

And lastly, a major improvement to the study of paddlefish circling behavior would be the observations of paddlefish circling in their natural environment. This is a very complicated task to perform, however. Radio-tracking is a great technology for detecting long-range migrations, but it is not superior for detecting circling, due to its poor spatial resolution. Ultrasound tracking could be used over shorter ranges and would offer better resolution, but it is thought that, in the wild, a paddlefish would most likely swim too far away from a researcher once a transmitter is implanted and the fish is released (Michael Hofmann, personal communication). Direct observations by divers would be useful and possible, but again, the paddlefish might be scared by the diver and quickly swim away. A feasible place to observe paddlefish might be industrial hatchery ponds. There are still drawbacks to this idea, however, as the environment would only be

semi-natural, and the scientist would have to contend with poor visibility and possibly overpopulation. This type of observation must be accomplished, however, to confirm the validity of the paddlefish model, as so pointedly argued by Stephens and Krebs (1986).

APPENDIX A

Dees *et al.* 2008a[5]

[5] Reprinted from the Journal of Theoretical Biology, Volume 252, Dees *et al.*, Patch exploitation in two dimensions: From *Daphnia* to simulated foragers, Pages 69-76, Copyright 2008, with permission from Elsevier.

Available online at www.sciencedirect.com
ScienceDirect
Journal of Theoretical Biology 252 (2008) 69–76
Journal of Theoretical Biology
www.elsevier.com/locate/yjtbi

Patch exploitation in two dimensions: From *Daphnia* to simulated foragers

Nathan D. Dees*, Sonya Bahar, Ricardo Garcia, Frank Moss

Department of Physics and Astronomy, Center for Neurodynamics, University of Missouri at St. Louis, 503J Benton Hall, One University Boulevard, St. Louis, MO 63121, USA

Received 7 August 2007; received in revised form 22 January 2008; accepted 28 January 2008
Available online 6 February 2008

Abstract

We explore the variability that animals display in their movement choices as they forage in a finite-sized food patch with a uniform food distribution, and present a framework for how these choices may be adjusted to optimize foraging efficiency. Inspired by experimental studies of the zooplankton *Daphnia*, we model foraging animals as "agents" moving in two dimensions in repeated and successive sequences of hops, pauses, and turns. For *Daphnia* and other species, critical movement parameters such as hop lengths, pause times, and turning angles are typically reported as probability density functions. Similarly, the agents in our simulations choose their movement parameters at random from such distributions. Each distribution is defined by a characteristic width, which we interpret as a "noise width," available to be tuned for increased foraging efficiency. We investigate the sensitivity of the system by measuring the food gathered by the agents as the turning angle and hop length noise widths are varied. In all cases, we find a maximum in food gathered at some particular value of the noise width in question, suggesting that these results can be considered robust examples of *natural stochastic resonance*.

Keywords: Turning angle; Hop length; Foraging; Natural stochastic resonance

1. Introduction

Studies of successful foraging have attracted the attention of researchers for several decades (e.g., Kamil and Sargent, 1981; Kamil et al., 1987; Stephens and Krebs, 1986; Okubo and Levin, 2001). For many animals, research has focused on particular types of random searches within environments that offer a specified distribution of resources. The conditions and responses that optimize foraging success are crucial to the forager's survival, and are therefore of particular interest. For instance, it is well known that, in order to maximize their advantage, animals will often modify their patterns of movement when favorable "patches" of resources are discovered (Bell, 1991). As an example, zooplankton, which provide the inspiration for the present study, have been shown to adjust their swimming trajectories when they encounter their prey (e.g., Cowles and Strickler, 1983; Buskey, 1984; Tiselius, 1992; Bundy et al., 1993; Larsson and Kleiven, 1996; Dodson et al., 1997; Uttieri et al., 2004; Menden-Deuer and Grünbaum, 2006).

Patterns of movement are created by particular choices of movement parameters, such as hop lengths and turning angles. These parameter choices can be assembled into representative distributions; modifications of these patterns entail changes in the distributions. In the present paper, we represent critical movement parameters with probability density functions whose definitions include *characteristic widths*. Adjustment of these widths can be interpreted as an organism's means of "tuning" its range of possible of choices in order to improve, or even optimize, its foraging efficiency. The idea of adjusting variance in order to achieve a beneficial outcome has been discussed in recent years under the name of *stochastic resonance* (Douglass et al., 1993; Wiesenfeld and Moss, 1995; Levin and Miller, 1996). In classical stochastic resonance, an optimal amount of variance, or noise, can enhance the signal-to-noise ratio

*Corresponding author. Tel.: +1 314 516 5015; fax: +1 314 516 6152.
E-mail address: nathan.dees@umsl.edu (N.D. Dees).

0022-5193/$ - see front matter © 2008 Elsevier Ltd. All rights reserved.
doi:10.1016/j.jtbi.2008.01.026

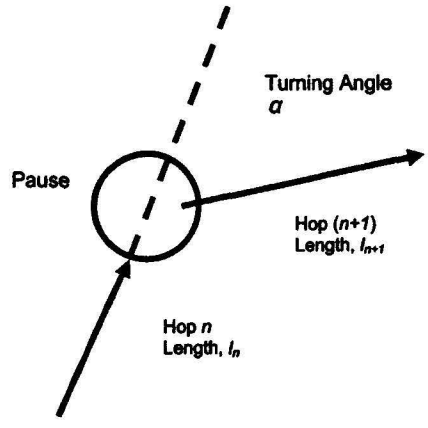

Fig. 1. Schematic diagram of the two-dimensional hop–pause–turn sequences used to simulate random walkers.

of a weak, subthreshold periodic signal. More generally, stochastic resonance is a phenomenon in which an intermediate amount of noise can optimize some behavior of the system in question.

In the present study, we consider how an animal searching for food could use a certain amount of noise, or "jitter", in its choices of turning angles or hop lengths to exploit the maximum amount of resources in a localized food patch. We model such searches using simulations, first suggested by Garcia et al. (2007), in which "agents" move about and feed in food patches of finite size for a fixed feeding time. The food is plentiful and uniformly distributed over the patch, and we use experimentally motivated correlated random walks consisting of repeated and successive sequences of hops, pauses, and turns (hereafter called "hop pause turn" sequences) to simulate the motion.

Fig. 1 illustrates the movement parameters used by an agent in each step of the hop pause turn sequence. In the simulation, these parameters are chosen at random from distributions, whose characteristic widths we describe as "noise widths," or "noise intensities." We find that the noise width of both the turning angle and hop length distributions can be tuned to give a maximum in the agent's foraging efficiency under various conditions and for various feeding strategies, providing a robust example of *natural stochastic resonance.*

2. Experimental results and distribution functions

Here, we present the results of experimental studies of *Daphnia pulex* and *Daphnia magna* movement. Experiments were performed as described in Garcia et al. (2007). Briefly, a very low density of daphnias (typically 8 12 individuals) was placed in a Perspex aquarium measuring $26 \times 26 \times 5\,\mathrm{cm}^3$ and containing a uniformly distributed feeding solution of freeze-dried *Spirolina.* The depth of the solution was limited to 1.5 2 cm, so that *Daphnia* motion could be approximated in two dimensions. This approximation is biologically motivated, since, in the wild, *Daphnia* feed on phytoplankton or algae, which are typically found in patches confined to a thin horizontal plane (Derenbach et al., 1979; Lampert, 1989; Cowles et al., 1993; Franks and Jaffe, 2001).

Swimming zooplankton alter their patterns of movement when encountering many different stimuli, including light sources in the visible range (Ringelberg, 1987). Therefore, visible light was eliminated from the room during the experiment. The motion of the animals was illuminated by infrared light, and recorded digitally by a Sony DCR-TRV80 camera operating at 30 frames per second. The videos were captured directly onto a computer for further processing. The videos were analyzed as described in Garcia et al. (2007) to create histograms of turning angles, hop lengths, and pause times of traveling daphnias. Edge effects of the aquarium were avoided in data collection by following the trajectories of animals near the center of the aquarium, and switching focus to another animal if the initial daphnia of interest neared the edge of the tank. Thus, data in each histogram below are gathered from multiple animals, typically three to four.

After data collection, we fitted the experimentally measured histograms with various distributions, each of which contains a clearly defined *width parameter* (available for "tuning" in the simulations). We narrowed the selection to those fits with the highest *R*-squared values, which are presented in Table 1 for each parameter and species.

We selected distributions for use in our simulations based on Table 1 in combination with real biological constraints of zooplankton movement, as discussed below.

2.1. Hop lengths

Although some relatively long hop lengths do appear in the recorded data, a three-parameter Lorentzian distribution allows for *extremely* large values of the hop length parameter, which are completely unrealistic for the hop pause turn sequences of *Daphnia* movement. Furthermore, the two-parameter exponential decay fit shows significantly lower *R*-squared values than all other results; so this fit was excluded as well. Therefore, the three-parameter Gaussian,

$$P(l) = K \exp\left[-0.5\left(\frac{l - l_0}{\lambda_0}\right)^2\right], \quad (1)$$

Table 1
R-squared values are given for different fits to the experimental hop length and pause time data

R-squared values distributions	Hop lengths		Pause times	
	D. pulex	*D. magna*	*D. pulex*	*D. magna*
Three-parameter Gaussian	0.88	0.94	0.87	0.94
Three-parameter Lorentzian	0.84	0.89	0.89	0.94
Two-parameter exponential decay	0.82	0.65	0.88	0.85

was chosen to represent the hop length data, where l is the hop length, l_0 is the peak of the distribution (i.e., the most probable hop length), λ_0 is the noise width of the hop length distribution, and K is a normalization constant. Experimentally recorded hop length data are shown in Fig. 2A and B for the two species respectively.

2.2. Pause times

Although a range of pause times was observed experimentally, as shown in Fig. 3, *extremely* long pause times are not observed in actual *Daphnia* movement, and thus the three-parameter Lorentzian distribution was excluded because it allows unrealistically long pauses. For representation of the pause time data, both the Gaussian and exponential decay fits show high R-squared values. Indeed, the Gaussian and exponential fit overlay each other exactly

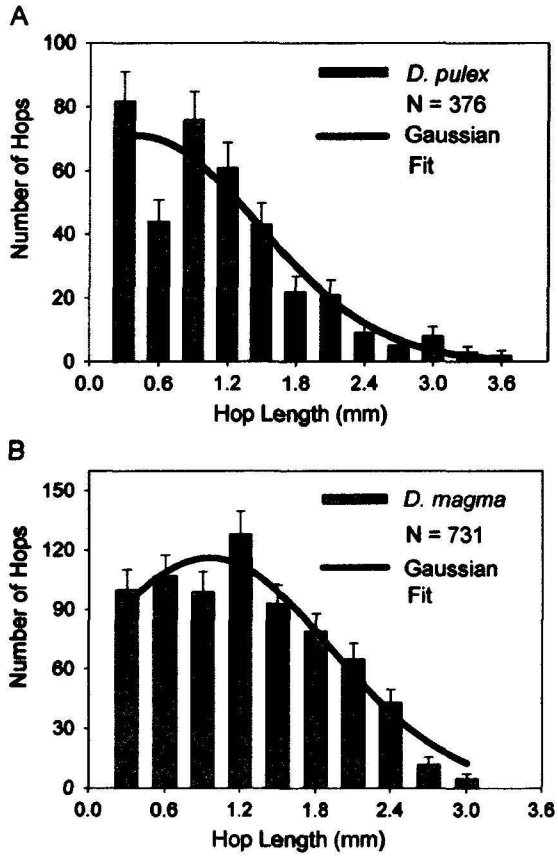

Fig. 2. (A) Hop length histogram for *D. pulex*, where the solid line is a fit using Eq. (1) with $K = 71$, $\lambda_0 = 1.06 \pm 0.29$ mm, and $l_0 = 0.41 \pm 0.4$ mm. (B) Hop length histogram for *D. magna*, with $K = 116.0$, $\lambda_0 = 0.97 \pm 0.1$ mm, and $l_0 = 0.95 \pm 0.1$ mm. N is the total number of hops gathered from multiple animals, typically three to four. Error bars show the square root of the number of counts in each histogram column.

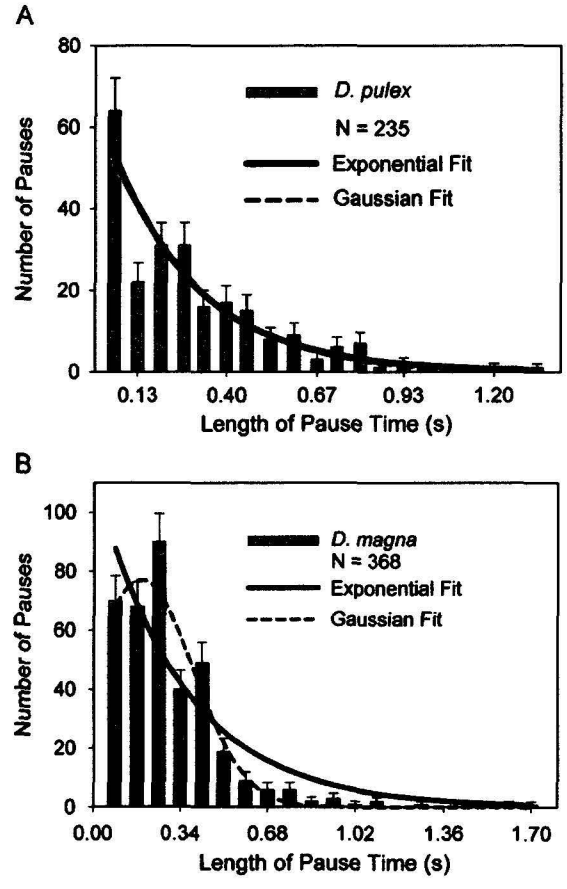

Fig. 3. (A) Pause time histogram for *D. pulex*, where the solid line is a fit using Eq. (2) with $N_0 = 66.9$ and $\tau_0 = 0.26 \pm .04$ s. In this case, a Gaussian fit to the data is completely covered by the exponential fit (solid line). (B) Pause time histogram for *D. magna* with the solid line showing an exponential fit (Eq. (2)) with $N_0 = 112.1$ and $\tau_0 = 0.35 \pm .06$ s; dotted line shows a Gaussian fit. N is the total number of pauses gathered from multiple animals, typically three to four. Error bars show the square root of the number of counts in each histogram column.

in the *D. pulex* histogram (see Fig. 3A). The Gaussian fit to the *D. magna* data (Fig. 3B) does not, however, allow for the several longer pause times which appear, and which could be observed experimentally as a result of the "hop and sink" motions *Daphnia* use when searching in a food patch (Larsson and Kleiven, 1996). Therefore, the exponential decay fit (2)

$$P(T) = N_0 \exp\left[\frac{-T}{\tau_0}\right], \tag{2}$$

was chosen, where T is the pause time, τ_0 the noise width of the distribution, and N_0 is a normalization constant. In Fig. 3, we show the histograms of the pause times recorded for the two species.

2.3. Turning angles

The distributions of unsigned turning angles were described in Garcia et al. (2007) using exponential distributions,

$$P(\alpha) = N_0 \exp\left[-\frac{\alpha}{\sigma_0}\right], \quad (3)$$

where α is the turning angle, and σ_0 is the noise width of the distribution. Noise widths were found to be $\sigma_0 = 0.74 \pm 0.1$ rad for *D. pulex*, and $\sigma_0 = 1.2 \pm 0.1$ rad for *D. magna*. In the actual experiments, the *Daphnia* turning angle distributions were symmetrical about the vertical axis, with approximately as many left turns (negative) as right turns (positive). In the simulations described below, a random sequence of positive and negative turning angles is generated from the distribution (3), with either sign (i.e., direction) equally probable. In order to study the effects of different noise widths, we generate such distributions and sequences for a variety of values of σ_0.

3. Simulation methods

We simulate the movement of "agents", or virtual animals, foraging in circular food patches of radius R within an unlimited, continuous two-dimensional space. For each simulation trial, 10 agents starting from random locations within the patch move simultaneously as random walkers in a hop pause turn sequence. They traverse the patch, and compete for resources that they find either along their path (first feeding protocol), or during the pauses between hops (second feeding protocol). The total amount of food eaten by the 10 agents is tabulated, and then averaged over thousands of separate trials.

The food patch is covered with a grid of 2.5×10^6 "food cells". Each cell is represented by a row and column index, and is considered as containing a food particle which is available to be "eaten" by an agent. Once an agent eats a food particle in a particular row and column, the particle is removed (no longer available to be "eaten" by any of the agents) and tabulated as part of the total food gathered by the group of agents. However, notice that it is not advantageous for agents to travel too closely to their own paths or the paths of other agents, as the food in these areas will have been removed. Also, if the agents travel outside of the food patch, they will not find food there either, though their movement is unimpeded.

Two different feeding protocols have been used in the simulations, inspired by the traits of real *Daphnia*. In order to feed, *Daphnia* "hop" along by intermittently pulling themselves forward with strokes of their large second antennae. Meanwhile, bristly thoracic legs flutter constantly inside the carapace (outside shell) of the animal, creating a constant current flow of the surrounding medium through the carapace cavity (Pennak, 1953). The bristles filter food particles from the medium whenever the legs are beating. This can occur, for instance, along the path as the animals hop (first feeding protocol used in the simulations) or as the animals siphon the medium while pausing between hops (second feeding protocol).

3.1. First feeding protocol

The agents feed during the hop segment of a hop pause turn sequence. The length of travel for each agent is always fixed, and is therefore proportional to the total foraging time. Pauses in this case are irrelevant. During the walk, each cell (food particle) touched by an agent is removed (eaten) and tabulated; this food particle is subsequently not available to be eaten by that or any other agent.

For simulations in which the turning angle noise width is varied, the hop length l is fixed, and turning angles α are chosen at random from the distribution (3). Each agent executes N total hops, eating along the hops, and with total travel length Nl. When an agent reaches the end of the fixed length of travel, the walk is terminated. The output of the simulation is the total food gathered as a function of the noise width of the turning angle distribution.

In another group of simulations, the turning angle distribution is fixed; it is defined by a noise width which had produced a maximum in food gathered as the turning angle noise width had been varied. Hop lengths are chosen at random from the distribution (1), while the hop length noise width is varied. The total length traveled is again fixed, and quantified as $\sum_{i=1}^{N} l_i$. The output of the simulation is the total food gathered as a function of the noise width of the hop length distribution.

3.2. Second feeding protocol

In our second feeding protocol, agents feed only during pauses in the hop pause turn sequence. Each hop is therefore separated from the next hop by a pause time T_i taken from the distribution (2). At the end of each hop, the agent feeds within a small circle of area $A_i = \rho T_i$, where ρ is the ingestion (feeding) rate. During a pause, all food cells located within the area A_i are removed from the food patch (eaten) and tabulated. Therefore, the area cleared, and hence, the amount of food consumed, is proportional to the pause time, T_i. When consecutive pause times T_i accumulate to the total fixed feeding time for each agent in a trial, the agents' walks are terminated.

4. Simulation results

Using the first feeding protocol (feed during hops, fixed hop length, no pause, random turning angles) we studied the amounts of food gathered as a function of the turning angle distribution width (turning angle noise width). Here we have assigned the dimension mm to the hop length and to the radius of the circle, because these numbers are realistic for real foraging *Daphnia*. (For example, $\langle l \rangle = 0.97$ mm for *D. magna*.) In Fig. 4A, we show the

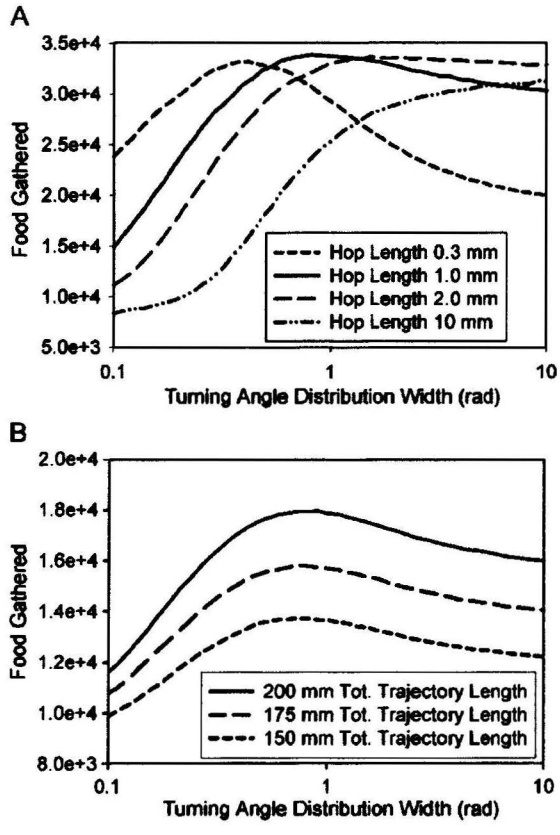

Fig. 4. First feeding protocol, hop length fixed. Food gathered versus turning angle noise width. In each trial, 10 agents are started at random locations within the food patch all feeding simultaneously. Five thousand trials were performed for each turning angle noise width σ_0. The statistical precision is approximately the size of the symbols, and hence error bars are omitted. (A) Food gathered versus turning angle noise width for the four fixed hop lengths indicated, with food patch radius $R = 100$ mm and total distance traveled $Nl = 400$ mm. (B) shows the same measure for three different total trajectory lengths, with hop length fixed at $l = 1$ mm.

food gathered as a function of turning angle noise width for four values of fixed hop length. Other conditions of the simulation are given in the figure caption. Fig. 4B shows the food gathered versus turning angle noise width for three values of the total distance traveled (proportional to feeding time) using an identical hop length of 1 mm. Both panels show that a maximum in food gathered occurs at particular values of the turning angle noise width.

In the next simulation, we vary the hop length noise width, λ_0, defined in Eq. (1). The values of l_0 and K in Eq. (1) are held fixed at the average fit values of these parameters for the two species, as reported above. For each hop, a turning angle is chosen from the distribution given in Eq. (3), with the turning angle noise width fixed at $\sigma_0 = 0.82$ rad. This is the value which had resulted in the maximum food gathered in Fig. 4A. We truncate the choice

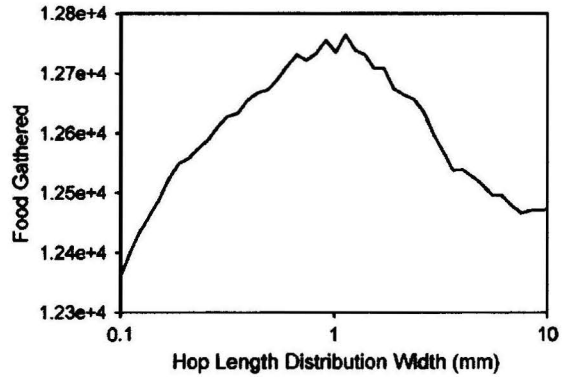

Fig. 5. First feeding protocol, hop length random. Food gathered versus hop length noise width. Turning angles were chosen from a distribution in the form of Eq. (3) with noise width $\sigma_0 = 0.82$ rad. Hop lengths were chosen from the distribution described by Eq. (1), for various values of λ_0, with $l_0 = 0.68$ mm and $K = 93.5$ (the averages of the values for the two species; see Fig. 2). $R = 100$ mm, and $Nl = 140$ mm. Seventy-five thousand trials (10 agents each trial) were accomplished for each value of λ_0.

of hop lengths at 5.0 mm because, as shown in Fig. 2, this limit is close to the experimentally observed upper limits for *D. magna* and *D. pulex*. The results shown in Fig. 5, therefore, reflect hop lengths chosen from the distribution Eq. (1) ranging from 0.1 to 5.0 mm.

We note that again there is a maximum in food gathered at a particular noise width. In this case, the food gathered peaked at a hop length distribution with $\lambda_0 = 1.13$ mm. Although the results of this simulation show less variation in total food gathered than in other simulations, it should be noted that the turning angles are chosen from *already* "optimized" distributions. The smaller percentage increase in food gathered near the maximum in this case suggests that there is little room left for improvement after the turning angle noise width has been tuned. Nonetheless, the observation of any peak at all in Fig. 5 provides a proof-of-principle demonstration of a stochastic resonance effect as the noise width of the hop length distribution is varied.

We now turn to the second feeding protocol, in which the agents feed during pause times only. First, we repeat the simulations of food gathered versus turning angle noise width, just as we did for the first feeding protocol as shown in Fig. 4, except that the foragers now feed during pause times. The results are shown in Fig. 6A for several different fixed hop lengths. Fig. 6B shows the effects of different ingestion rates at a fixed hop length. The ingestion rate is given as food cells consumed per second; recall that there are initially 2.5×10^6 total food cells in the entire food patch. As with the first protocol, we find maxima in the amount of in food gathered as turning angle and hop length noise widths are "tuned".

In order to complete the comparison between the two feeding protocols, we investigate the food gathered under the second feeding protocol while varying the hop length

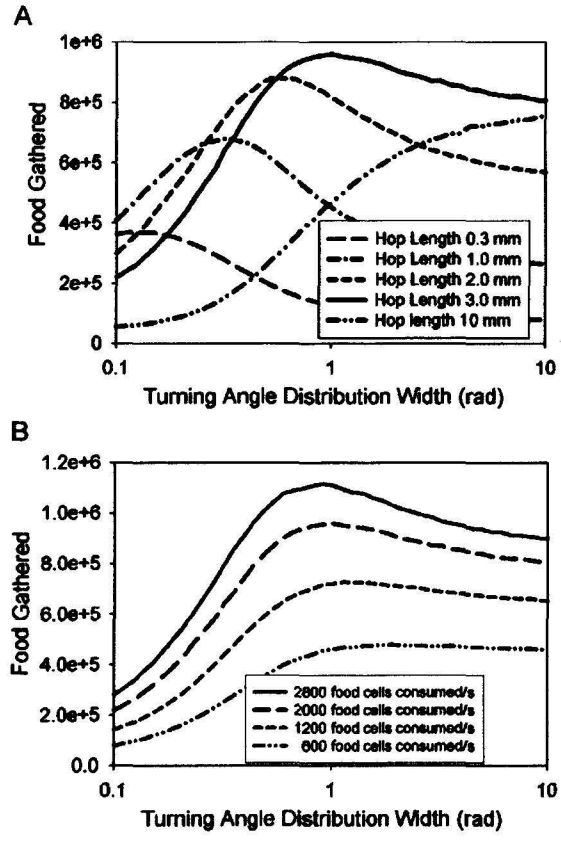

Fig. 6. Second feeding protocol (feeding during pauses). Food gathered is shown as a function of turning angle noise width for a total feeding time of 140 s. (A) Results for several fixed hop lengths with a fixed ingestion rate of 2000 food cells consumed per second. One thousand and five hundred trials were accomplished (10 agents per trial) for each value of the turning angle noise width, σ_0. (B) Simulations with four different ingestion rates, using a fixed hop length of 3.0 mm. Two thousand and five hundred trials were accomplished (10 agents per trial) for each chosen value of the turning angle noise width, σ_0.

noise width. Again, the choices of hop length are truncated to a range of 0.1 5.0 mm. The turning angle is selected at random from the distribution (3), with $\sigma_0 = 1.01$ rad, corresponding to the value at which maximal food was gathered in Fig. 6A. As before, l_0 and K in Eq. (1) are fixed as the average values of these fit parameters between the two species. The results are shown in Fig. 7.

Again, we find a clear peak in the amount of food gathered. In the following section we discuss the implications of these observations.

5. Discussion

It is not difficult to understand, from a purely mathematical standpoint, why there are maxima in the

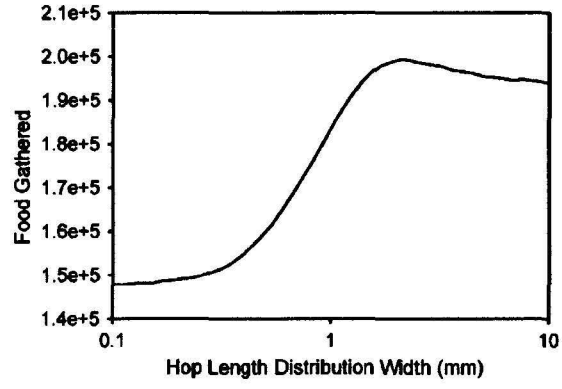

Fig. 7. Second feeding protocol (feeding during pauses). Food gathered versus hop length noise width. Turning angles were chosen from the distribution given in Eq. (3) with the noise width $\sigma_0 = 1.01$ rad. Hop lengths were chosen from the distribution Eq. (1) for various values of λ_0, with $l_0 = 0.68$ mm and $K = 93.5$. The ingestion rate used was 2000 food cells consumed/s. $R = 100$ mm, and $Nl = 140$ mm. Twenty-five thousand trials were accomplished (10 agents each trial) for each value of λ_0.

amount of food gathered, at least in the case of the turning angle distribution. Consider three possible turning angle distributions as sketched in Fig. 8A. At the extremes are very wide (far left panel) and very narrow (delta function, far right panel) distributions. Now consider three example trajectories (illustrated in Fig. 8B) generated with turning angles taken from the distribution (3), with three different values of the noise width σ_0. Foragers using trajectories with $\sigma_0 = 0.3$ rad (very narrow, delta function-like) or $\sigma_0 = 5.0$ rad (very wide, nearly uncorrelated Brownian-like), will gather less food than those utilizing distributions with the intermediate noise width. The wide distribution leads to too many path-recrossing events, and the agent spends too much time in a localized region, thus depleting the resources there, while leaving the outer regions of the food patch unexplored. The narrow distribution, on the other hand, leads to nearly straight line motion over considerable distances, and the agent escapes the food patch too quickly to exploit the resources. Clearly, there must be a preferred width of the turning angle distribution between these two extremes.

As a further illustration of a preferred noise width, our simulations have shown that maxima exist for each characteristic of the motion investigated (turning angles and hop lengths), and for both feeding protocols. The locations of these maxima, however, shift slightly depending on the conditions of each simulation. It is qualitatively possible to understand the displacements of these maxima. For example, Fig. 4A shows that the peak in food gathered exists at higher values of the turning angle noise width when the (fixed) hop length is increased. We note from Fig. 8 that larger turning angles, on average, lead to tighter, more localized trajectories (blue trajectory). The converse is also true; small turning angles lead to

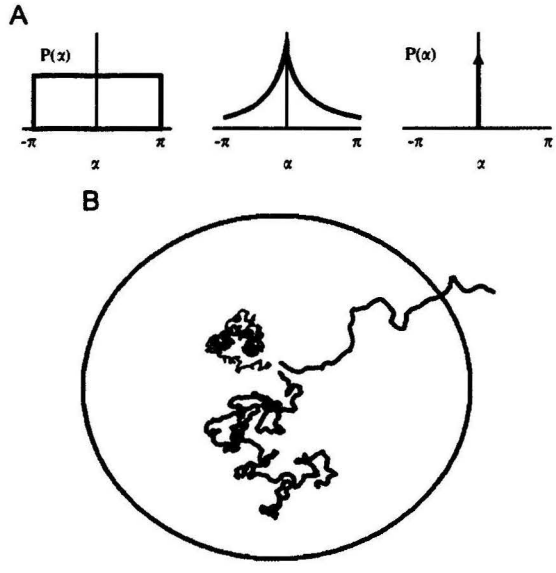

Fig. 8. (A) Idealized wide, intermediate, and narrow turning angle distributions. (B) Three example trajectories for narrow ($\sigma_0 = 0.3$ rad, red trajectory), preferred ($\sigma_0 = 0.8$ rad, black trajectory), and wide ($\sigma_0 = 5.0$ rad, blue trajectory) noise widths of the turning angle distribution.

straighter, more directed motions (red trajectory). Increasing the hop length by itself would simply lead to less compact trajectories. The system compensated by shifting the peak towards higher values of the turning angle noise width. Fig. 4B shows that the location of the peak in food gathered does not move horizontally with increasing total length traveled (increased feeding time). Since no statistical characteristics of the trajectories are changed, we do not expect the preferred noise width value to change. The amplitude of the maximum (in food gathered) simply increases with feeding time, as one would expect. Fig. 6 shows that these characteristics are preserved with the second feeding protocol. However, Fig. 6B indicates that the preferred turning angle noise width decreases slightly as the feeding rate increases. This is also possible to understand. As the circles where food is gathered increase in area (larger feeding rates during similar pause times), the agent must reduce, on average, its turning angles in order to achieve more directed trajectories. These allow the agent to escape localities where, at large feeding rates, resources are depleted more rapidly.

Much like the agents in the simulations, real zooplankton also show signs of adjusting their trajectories in response to foraging conditions. Light intensities (e.g., Ringelberg, 1987), odors of predators (e.g., Pijanowska and Kowalczewski, 1997), odors of prey (e.g., Buskey, 1984; van Gool and Ringelberg, 1996), visual or chemosensory perception of possible mates (e.g., Strickler, 1998), and turbulence (e.g., Saiz et al., 1992; Kiørboe and Visser, 1999) have all been noted to elicit specific behavior. Copepods often decrease their swimming speed (Strickler, 1982; Cowles and Strickler, 1983; Buskey, 1984; Tiselius, 1992; Bundy et al., 1993) or increase their turning rate (Tiselius, 1992; Bundy et al., 1993) in areas of high food concentration. *Daphnia* also slow down when encountering abundant prey (Cuddington and McCauley, 1994; Larsson and Kleiven, 1996); they decrease their path lengths (over time) and travel in a hop-and-sink motion rather than a hop pause turn sequence. Zooplankton may also, presumably, be forcing larger quantities of the surrounding medium through their bodies in these environments (Strickler, 1982); everything works together to increase the prey encounter rate.

In the case of a high density of uniformly distributed food, it has been shown that uncorrelated purely Brownian motions are less than optimum; instead, correlated random walks have often been found to result in optimal foraging (e.g., Kareiva and Shigesada, 1983; Berg, 1993; Byers, 2001). The Lévy statistic has also been applied to foraging trajectories observed for microzooplankton (Bartumeus et al., 2002), which, interestingly, transition from Brownian statistics when resources are plentiful and uniformly distributed to Lévy statistics when resources become sparse or patchy (Bartumeus et al., 2003, 2005; Bartumeus, 2007). Our results provide a mathematical context for these behavioral adjustments.

It has been argued in a variety of cases that success in foraging for food enhances an animal's fitness. This theory was applied most notably to Darwin's famous finches (Sulloway, 1982; Grant, 2003), and has continued through more modern applications such as Parker and Maynard Smith (1990) and Lemon (1991). Dodson et al. (1997), studying the effects of light and food on individual organisms (clones) of *D. pulex* and *D. magna*, suggested that "[a]mong-clone differences in food and light effects may be the result of natural selection." We suggest that, as an example of natural stochastic resonance, the distributions which represent the choices of foraging movement parameters of an organism have characteristic noise widths which may be "tuned" to more advantageous values by natural selection over many generations.

Acknowledgments

S.B. gratefully acknowledges support from start-up funds provided by the University of Missouri at St. Louis. N.D. offers special thanks to Lon A. Wilkens for literature and discussions concerning zooplankton.

References

Bartumeus, F., 2007. Lévy processes in animal movement: an evolutionary hypothesis. Fractals 15 (2), 151–162.

Bartumeus, F., Catalan, J., Fulco, U.L., Lyra, M.L., Viswanathan, G.M., 2002. Optimizing the encounter rate in biological interactions: Lévy versus Brownian strategies. Phys. Rev. Lett. 88, 097901 (and 89, 109902).

Bartumeus, F., Peters, F., Pueyo, S., Marrasé, C., Catalan, J., 2003. Helical Lévy walks: adjusting searching statistics to resource availability in microzooplankton. PNAS 100, 12771–12775.

Bartumeus, F., da Luz, M.G.E., Viswanathan, G.M., Catalan, J., 2005. Animal search strategies: a quantitative random-walk analysis. Ecology 86, 3078–3087.

Bell, W.J., 1991. Searching Behaviour: The Behavioural Ecology of Finding Resources. Chapman & Hall, New York.

Berg, H.C., 1993. Random Walks in Biology. Princeton University Press, Princeton, New Jersey.

Bundy, M.H., Gross, T.F., Coughlin, D.J., Strickler, J.R., 1998. Quantifying copepod searching efficiency using swimming pattern and perceptive ability. Bull. Mar. Sci. 63 (1), 15–28.

Buskey, E.J., 1984. Swimming pattern as an indicator of the roles of copepod sensory systems in the recognition of food. Mar. Biol. 79, 165–175.

Byers, J.A., 2001. Correlated random walk equations of animal dispersal resolved by simulation. Ecology 82, 1680–1690.

Cowles, T.J., Strickler, J.R., 1983. Characterization of feeding activity patterns in the planktonic copepod centropages typicus Kroyer under various food conditions. Limnol. Oceanogr. 28 (1), 106–115.

Cowles, T.J., Desiderio, R.A., Neuer, S., 1993. In situ characterization of phytoplankton from vertical profiles of fluorescence emission spectra. Mar. Biol. 115, 217–222.

Cuddington, K.M., McCauley, E., 1994. Food-dependent aggregation and mobility of water fleas *Ceriodaphnia dubia* and *Daphnia pulex*. Can. J. Zool. 72, 1217–1226.

Darnbach, J.B., Astheimer, H., Hanson, H.P., Leach, H., 1979. Vertical microscale distribution of phytoplankton in relation to the thermocline. Mar. Ecol. Prog. Ser. 1, 187–193.

Dodson, S.I., Ryan, S., Tollrian, R., Lampert, W., 1997. Individual swimming behavior of *Daphnia*: effects of food, light, and container size in four clones. J. Plankton Res. 19 (10), 1537–1552.

Douglass, J., Wilkens, L.A., Pantazelou, E., Moss, F., 1993. Noise enhancement of information transfer in crayfish mechanoreceptors by stochastic resonance. Nature 365, 337–340.

Franks, P.J.S., Jaffe, J.S., 2001. Microscale distributions of phytoplankton: initial results from a two-dimensional imaging fluorometer, OSST. Mar. Ecol. Prog. Ser. 220, 59–72.

Garcia, R., Moss, F., Nihongi, A., Strickler, J.R., Göllar, S., Erdmann, U., Schimansky-Geier, L., Sokolov, I.M., 2007. Optimum foraging by zooplankton within patches: the case of *Daphnia*. Math. Biosci. 207, 165–188.

Grant, B.R., 2003. Evolution in Darwin's finches: a review of a study on Isla Daphne Major in the Galapagos archipelago. Zoology (Jena) 106 (4), 255–259.

Kamil, A.C., Sargent, T.D., 1981. Foraging Behavior: Ecological, Ethological, and Psychological Approaches. STPM Press, Garland, New York.

Kamil, A.C., Drebs, J.R., Pulliam, H.R. (Eds.), 1987. Foraging Behavior. Springer, Berlin.

Karciva, P.M., Shigesada, N., 1983. Analyzing insect movement as a correlated random walk. Oecologia 56, 234–238.

Kiørboe, T., Visser, A.W., 1999. Predator and prey perception in copepods due to hydromechanical signals. Mar. Ecol. Prog. Ser. 179, 81–95.

Lampert, W., 1989. The adaptive significance of diel vertical migration of zooplankton. Funct. Ecol. 3 (1), 21–27.

Larsson, P., Kleiven, O.T., 1996. Food search and swimming speed in *Daphnia*. In: Lenz, P.H., Hartline, D.K., Purcell, J.E., Macmillan, D.L. (Eds.), Zooplankton: Sensory Ecology and Physiology. Gordon & Breach, Amsterdam, the Netherlands, pp. 375–387.

Lemon, W.C., 1991. Fitness consequences of foraging behaviour in the zebra finch. Nature 352, 153–155.

Levin, J., Miller, J., 1996. Broadband neural encoding in the cricket cercal sensory system by stochastic resonance. Nature 380, 165–168.

Mendan-Deuer, S., Grünbaum, D., 2006. Individual foraging behaviors and population distributions of a planktonic predator aggregating to phytoplankton thinn layers. Limnol. Oceanogr. 51 (1), 106–116.

Okubo, A., Levin, S.A. (Eds.), 2001. Diffusion and Ecological Problems. Modern Perspectives, second ed. Springer, New York.

Parker, G.A., Maynard Smith, J., 1990. Optimality theory in evolutionary biology. Nature 348, 27–33.

Pennak, R.W., 1953. Fresh-Water Invertebrates of the United States. Ronald Press Company, New York.

Pijanowska, J., Kowalczewski, A., 1997. Predators can induce swarming behaviour and locomotory responses in *Daphnia*. Freshwater Biol. 37, 649–656.

Ringelberg, J., 1987. Light induced behaviour in *Daphnia*. In: Peters, R.H., de Bernardi, R. (Eds.), *Daphnia*. Mem. Inst. Ital. Idrobiol. (45), 285–323.

Saiz, E., Alcaraz, M., Paffenhofer, G.A., 1992. Effects of small-scale turbulence on feeding rate and gross-growth efficiency of three *Acartia* species (Copepoda: California). J. Plankton Res. (14), 1085–1097.

Stephens, D.W., Krebs, J.R., 1986. Foraging Theory. Princeton University Press, Princeton, NJ.

Strickler, J.R., 1982. Calanoid copepods, feeding currents, and the role of gravity. Science 218 (4568), 158–160.

Strickler, J.R., 1998. Observing free-swimming copepods mating. Philos. Trans.: Biol. Sci. 353 (1369), 671–680.

Sulloway, F.J., 1982. Darwin and his finches: the evolution of a legend. J. Hist. Biol. 15 (1), 1–53.

Tiselius, P., 1992. Behavior of *Acartia tonsa* in patchy food environments. Limnol. Oceanogr. 37 (8), 1640–1651.

Uttieri, M., Mazzocchi, M.G., Nihongi, A., D'Alcalà, M.R., Strickler, J.R., Zambianchi, E., 2004. Lagrangian description of zooplankton swimming trajectories. J. Plankton Res. 26 (1), 99–105.

van Gool, E., Ringelberg, J., 1996. Daphnids respond to algae-associated odours. J. Plankton Res. 18 (2), 197–202.

Wiesenfeld, K., Moss, F., 1995. Stochastic resonance and the benefits of noise: from ice ages to crayfish and SQUIDs. Nature 373, 33–36.

APPENDIX B

Dees *et al.* 2008b[6]

[6] Reprinted from Physical Biology (www.iop.org/journals/physbio), Dees *et al.*, Stochastic resonance and the evolution of *Daphnia* foraging strategy, Copyright 2008, with permission from IOP Publishing Ltd.

IOP PUBLISHING PHYSICAL BIOLOGY
Phys. Biol. 5 (2008) 044001 (6pp) doi:10.1088/1478-3975/5/4/044001

COMMUNICATION

Stochastic resonance and the evolution of *Daphnia* foraging strategy

Nathan D Dees, Sonya Bahar and Frank Moss

Center for Neurodynamics, Department of Physics and Astronomy, University of Missouri at St Louis, St Louis, MO 63121, USA

E-mail: nathan.dees@umsl.edu

Received 22 July 2008
Accepted for publication 27 October 2008
Published 24 November 2008
Online at stacks.iop.org/PhysBio/5/044001

Abstract
Search strategies are currently of great interest, with reports on foraging ranging from albatrosses and spider monkeys to microzooplankton. Here, we investigate the role of noise in optimizing search strategies. We focus on the zooplankton *Daphnia*, which move in successive sequences consisting of a hop, a pause and a turn through an angle. Recent experiments have shown that their turning angle distributions (TADs) and underlying noise intensities are similar across species and age groups, suggesting an evolutionary origin of this internal noise. We explore this hypothesis further with a digital simulation (EVO) based solely on the three central Darwinian themes: inheritability, variability and survivability. Separate simulations utilizing stochastic resonance (SR) indicate that foraging success, and hence fitness, is maximized at an optimum TAD noise intensity, which is represented by the distribution's characteristic width, σ. In both the EVO and SR simulations, foraging success is the criterion, and the results are the predicted characteristic widths of the TADs that maximize success. Our results are twofold: (1) the evolving characteristic widths achieve stasis after many generations; (2) as a hop length parameter is changed, variations in the evolved widths generated by EVO parallel those predicted by SR. These findings provide support for the hypotheses that (1) σ is an evolved quantity and that (2) SR plays a role in evolution.

[M] This article features online multimedia enhancements

(Some figures in this article are in colour only in the electronic version)

Introduction

In its most general form, stochastic resonance (SR) is a process whereby the addition of a random function, or 'noise', can optimize a physical or biological process (Wiesenfeld and Moss 1995). SR has been studied for many years and was discovered in sensory biology well over a decade ago (Douglass *et al* 1993). In nearly all experiments with SR, the noise was added from an external source, such as environmental noise. However, considering the evolution of organisms, if such external noise is, or was, beneficial to sensory systems, one might expect natural selection to have exploited it, as suggested by Jaramillo and Wiesenfeld (1998). If the advantageous use of noise was subsequently internalized, one might also expect to find neural circuits in the central nervous system specifically designed to make use of SR. Indeed, experimental evidence for such a circuit in the *Drosophila* olfactory system has recently been reported (Shang *et al* 2007). Such circuits, as yet undiscovered elsewhere, may, however, be widespread.

Here, we investigate the nexus between SR and animal foraging behavior, a topic of great recent interest (e.g., Viswanathan *et al* 1996, Bartumeus *et al* 2003, Boyer *et al* 2004, Shlesinger 2006, Buchanan 2008). As a behavior, foraging is subject to noise in the form of a presumably internally-generated variability in an animal's

choice of movements. Animal behavior mediated by internal noise has been reported in two other experiments with *Drosophila* (Maye *et al* 2007, Reynolds and Frye 2007), and more recently in human psychophysics experiments (Emberson *et al* 2007). In our previous experiments, *Daphnia* foraged in a patch with uniformly distributed food, moving in approximately two dimensions. In the absence of directional stimuli (such as visible light or non-uniform food distribution), their turning angle distributions (TADs) $[-\pi$ to $\pi]$, with left-hand and right-hand turns equally probable, were well described by an exponential function (Garcia *et al* 2007), $P(\alpha) = N_o \exp[-|\alpha|/\sigma]$, where α is the turning angle, N_o is the number of angles observed and σ is the noise intensity (characteristic angle or width) of the TAD, the primary quantity measured in the experiment. Since the values of σ were quite similar across five different species, including adults and juveniles of two species, we suggested that the noise intensity is an evolved property (Garcia *et al* 2007). Additional evidence for an evolutionary origin of σ has recently emerged from experiments with single cells of two different species of slime mold searching for a chemical signal in a two-dimensional space. In the absence of directional stimuli, both species exhibited exponential TADs (Liang *et al* 2008) similar to those we observed in *Daphnia* (Garcia *et al* 2007).

To further study the hypothesis that the characteristic widths of TADs are evolved quantities, we have developed a *model-free* simulation, EVO, of natural selection using the simplest and fewest possible assumptions. We compare the results of EVO with simulations of SR similar to those performed by Garcia *et al* (2007) and Dees *et al* (2008) which indicate the values of σ that are optimum for foraging success. These simulations are designed to answer the question: how might the observed exponential TADs and their characteristic widths have arisen?

Methods

EVO simulation

EVO updates an evolving TAD at each generation, commencing with a uniform and uncorrelated distribution of turning angles ranging from $-\pi$ to $+\pi$. This initial distribution represents the 'primordial noise', or variability, that is available at the beginning of the natural selection process as originally discussed in detail by Darwin (Gould 2002). Twenty agents forage independently in circular food patches of radius $R = 100$ units. The patches are covered with a uniform grid of $\pi \cdot 10^6$ square cells, 0.1×0.1 units in size. The cells represent food particles to be 'consumed' by the agents. Each agent traverses a total distance of 1500 units (simulating a fixed feeding time). The agents can move within or outside the patch, randomly choosing a new turning angle at each hop from the current TAD. All food particles that the agents cross directly while completing their trajectories are removed from the food patch, 'consumed', and tabulated. After all agents have completed feeding, the single agent that collected the most food is identified. Only this most successful agent is allowed to supply information critical to fitness to the next generation of agents. A distribution is created from its choices of turning angles, and a fraction, h, the inheritance of this distribution, is added to the evolving TAD. The next generation of foragers chooses random angles from this modified TAD, and the updating process continues indefinitely.

We emphasize that the 'inheritance' consists only of a slight bias in the next generation toward the set of choices made by the most successful feeder in the preceding generation. This does not mean that all members of the next generation will acquire the feeding strategy of the ancestral 'winner', as the angles are chosen randomly from the evolving distribution. Indeed, due to the random nature of the simulation, a number of the 'children' will perform even *worse* than their gluttonous ancestor.

Daphnia in the wild exhibit so-called *diel vertical migration* (Zaret and Suffern 1976, Ringelberg 1993), avoiding predators by spending the daylight hours near the bottom of a lake or pond (Bollens and Frost 1989) while thin patches of photosynthetic algae (Derenbach *et al* 1979, Lampert 1989, Cowles *et al* 1993, Franks and Jaffe 2001) develop near the surface. At night, *Daphnia* rise to the surface to feed on this algae, and therefore are forced to swim in approximately two-dimensional planes. Also, fractal characterization of three-dimensional *Daphnia pulex* swimming trajectories has shown that their paths are much less vertically complex than pure three-dimensional random walks, and also that they typically travel within 4 cm vertical planes (Uttieri *et al* 2005). We thus justify our two-dimensional approximation in this regard.

In our simulations, the hop length is treated as a fixed parameter. The ratio of hop length to food patch radius is a dimensionless parameter. We hold the radius fixed at 100 units as described above, and perform simulations for three values of the hop length. The results can be compared to experimental studies of *Daphnia* foraging if we take one unit in our simulation as equal to 1 mm, comparable with the average hop length for *D. magna* of 0.95 mm (Dees *et al* 2008). Following this analogy, we can consider the food patches used in our simulations as circles of radius 100 mm. This choice is in agreement with high density food (phytoplankton/prey) patch sizes measured in freshwater (Doubell 2008, personal communication) as well as in marine environments (Doubell *et al* 2006, Franks and Jaffe 2001).

SR simulation

In the SR simulation, agents again forage in food patches as defined in the EVO simulation while traversing a fixed distance (1500 units). Apart from these two constraints, the EVO and SR simulations are completely independent.

At the end of each hop during the SR simulation, an agent chooses a new turning angle at random from a normal distribution (see discussion below) using a predetermined width, σ. Any food particles touched by the agent along its trajectory are removed from the patch and tabulated. Twenty agents feed in this manner for the chosen value of σ. The maximum food gathered by the agents in this population of 20 is then recorded, disregarding extreme outliers (values $\geqslant 3$

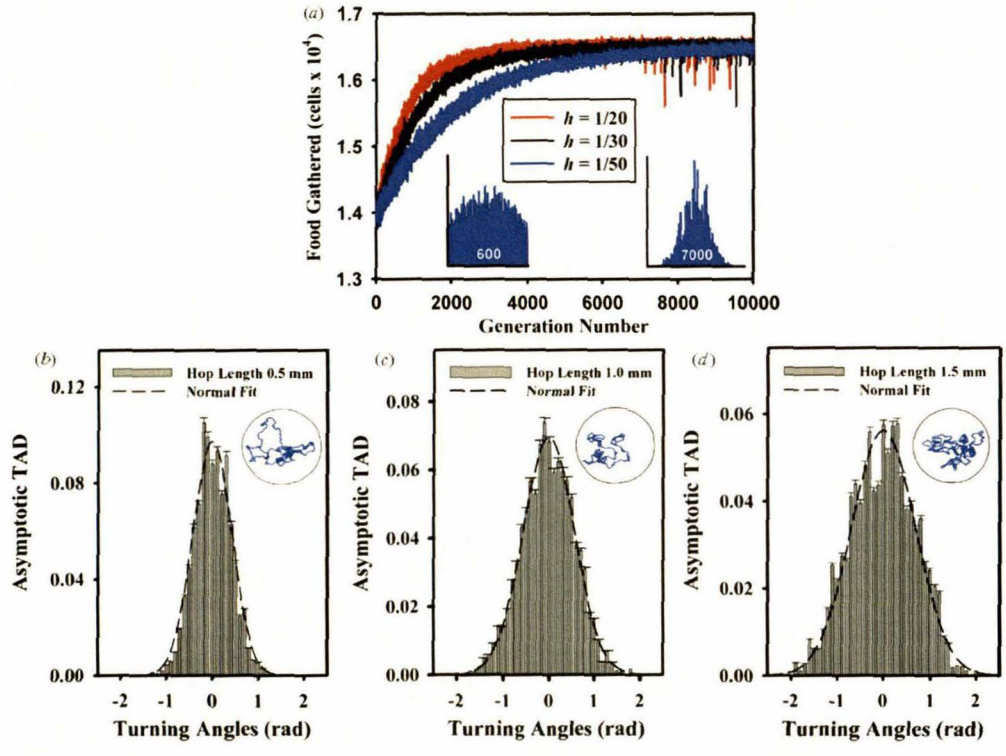

Figure 1. (*a*) Food gathered by the most successful agent in each generation of the EVO simulation versus generation number for three values of the inheritance parameter h as indicated. Insets show normalized turning angle distributions ($P(\alpha)$ versus α, with α ranging from $-\pi$ to π) for $h = 1/50$ at generation 600 (wide distribution) and generation 7000 (narrow distribution). Asymptotic TADs averaged across ten trials with the hop lengths indicated for $h = 1/50$ are shown in (*b*)–(*d*). The dashed lines are fits to the normal distribution with parameters determined by maximum likelihood estimation. The width of each distribution yields a value σ, as listed in table 1. (*b*) $\sigma = 0.42 \pm 0.01$ rad, (*c*) $\sigma = 0.57 \pm 0.02$ rad and (*d*) $\sigma = 0.70 \pm 0.02$ rad. Error bars represent the inheritance, h (1/50), multiplied by the bin height, representing the maximum possible inter-generational change in bin height. The insets in (*b*)–(*d*) show example trajectories inside circular patches.

Table 1. Asymptotic, optimal and measured values of σ.

Hop length (mm)	Asymptotic noise intensity (EVO)[a] (rad)	Optimal noise intensity (SR)[b] (rad)	Average experimental noise intensity[c] (rad)
0.5	0.42 ± 0.01	0.33 ± 0.06	
1.0	0.57 ± 0.02	0.50 ± 0.09	1.06 ± 0.1
1.5	0.70 ± 0.02	0.61 ± 0.10	

[a] Values are the mean and standard deviation of ten trials; $h = 1/50$.
[b] Values are the mean and standard deviation of 100 trials.
[c] Value is averaged over data from 5 species, as well as juveniles from 2 of these species. Precision is estimated; see Garcia *et al* (2007).

inter-quartile ranges from the third quartile). Next, a second value of σ is chosen, and a second population of 20 agents feed, with the maximum food gathered again recorded. This process continues for 46 values of σ ranging from 0.1 to 10 rad, constituting a single trial. The result of a trial is a curve of maximum food gathered as a function of σ. We perform 100 such trials, and then calculate the particular value of σ which results in the peak of the curve for each trial. These 100 values of σ are averaged, and the average (and standard deviation) is reported in table 1 as the optimal SR noise intensity.

For a more detailed description of the EVO and SR algorithms, see the supplementary material stacks.iop.org/PhysBio/5/044001.

Results

Figure 1(*a*) shows the food gathered by the most successful agent in the EVO simulation as a function of the number of generations. The food gathered plateaus after a number of generations depending on the value of inheritance parameter h, with larger values of h leading to stasis in earlier generations,

as expected. Insets show examples of the evolving TADs which begin with wide characteristic widths (large σ) and become narrower (smaller σ) in later generations. Similar plateaus arise often in both natural and artificial selection (Falconer 1981, Robertson 1980). Note that these plateaus are achieved in remarkably few generations, a testament to the power of natural selection (Endler 1986). Surprisingly rapid evolutionary processes have also been shown in other natural selection-based (albeit model-dependent) simulations, such as Nilsson and Pelger's model for the evolution of the fish eye (1994).

Asymptotically achieved TADs, together with Gaussian fits and representative trajectories, are shown in figures 1(*b*)–(*d*). The choice of normal fitting curves is the result of statistical analysis of the asymptotic distributions. The shapes of the evolving and asymptotic distributions, and consideration of the experimental data, suggest null hypotheses that correct fits would either be Laplacian (double-exponential) or normal. We calculated the Cramér–von Mises W^2, the Watson U^2, the Anderson–Darling A^2 and the Kolmogorov–Smirnov D statistics (D'Agostino and Stephens 1986, Efron and Tibshirani 1993, Puig and Stephens 2000) for the empirical distribution functions to help discern between the two possibilities. Although one might immediately expect normal distributions based on the central-limit-theorem, we point out that this applies only in the limit of a large number of observations, which may not apply to the foraging situation under investigation here. Our model, for instance, does not involve an infinite number of experiments with infinite sets of turning angles; nor do we model either an infinite feeding time or a food patch of infinite size.

A table detailing the results of our statistical analysis is provided in the supplementary material. Briefly, assessment of the Laplacian null hypotheses for the hop length value 1.0 mm gave $W^2 = 0.191$, $U^2 = 0.151$, $A^2 = 1.191$ and $D = 1.102$, qualifying the null hypothesis to be rejected at the 0.025, 0.01, 0.025 and 0.01 levels, respectively. However, for the normal distribution, the statistic values of $W^2 = 0.084$, $U^2 = 0.080$, $A^2 = 0.512$, and $D = 0.814$ reject the normal null hypothesis at the 0.25 level for the first three statistics, and at the 0.1 level for D. The significance levels we report show that neither distribution has been rejected outright by all tests, although there is convincingly less evidence that our resultant distribution is Laplacian.

Figure 2(*a*) shows σ as a function of generation for three different values of h, while (*b*) shows σ as a function of generation for different hop lengths. In each case, as in figure 1(*a*), stasis is achieved as the number of generations increases. Note that, in figure 2(*b*), the evolved value of σ increases as hop length increases. Stasis values of σ shown in figure 2(*b*) are reported in table 1. It is these final asymptotic values of σ that we consider to be evolved quantities. But the question immediately arises: are these evolved quantities optimal for foraging success? If they indeed arise from natural selection, then we expect that they might in fact be optimal as consistent with a 'strict Darwinian' interpretation of natural selection. We independently test this assertion using the stochastic resonance simulation to extract optimal values of

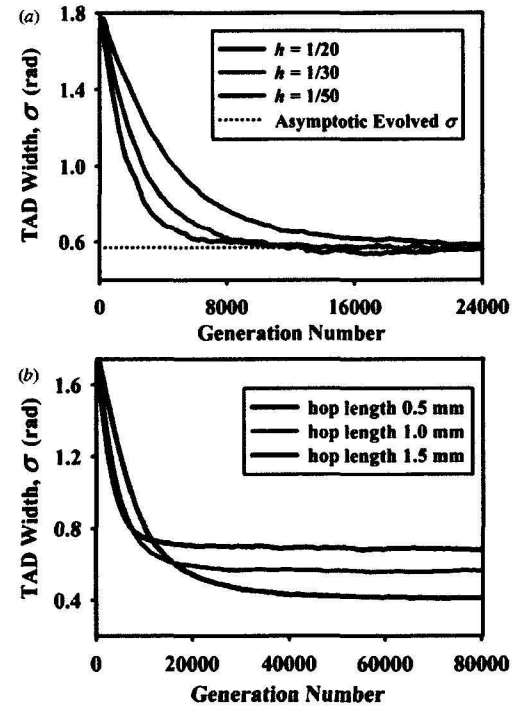

Figure 2. (*a*) Evolution of σ using different values of the inheritance, h, with the hop length parameter fixed at 1 mm shows an asymptotic approach to similar values of σ. Note lessening variability in curves with lesser inheritance. Curves represent averages over two trials. (*b*) Evolution of σ using different values of fixed hop length shows asymptotic behavior to different values of σ. Curves represent averages over ten trials.

σ, which are then compared with the experimental findings of Garcia *et al* (2007), and with the predictions of EVO, in table 1.

In the SR simulation, the maximum value of food gathered was averaged over 100 trials for each value of σ. Plotting these values for food gathered versus σ results in classic SR curves, shown in figure 3, wherein a beneficial feature (food gathered) is maximized at optimum noise intensity (σ). We find that the optimum noise intensities for SR are typically intermediate values of σ; in other words, TADs that are either too narrow or too wide lead to less than optimal foraging efficiency. We also note that the optimum noise intensity increases as hop length increases, a result that 'tracks' similar findings from the EVO simulation (see figures 1(*b*)–(*d*), 2(*b*) and table 1).

Discussion

Comparison of figures 2(*b*) and 3 (and the first three columns in table 1) shows that our evolutionary simulation converges on a solution to the foraging problem similar to that achieved with the SR algorithm. Optimal foraging is achieved at increasing values of σ for increasing hop length. This is found both in the values of σ for which the SR algorithm achieves maximum food gathered, and in the asymptotic values of σ achieved with

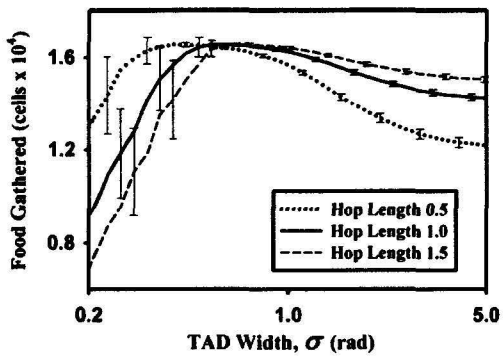

Figure 3. Food gathered versus σ for the three hop lengths indicated, calculated using the SR simulation. Curves are averaged results from 100 trials; error bars, shown every third point on each curve, represent the standard deviation. Each trial incorporates 20 independent determinations of the food gathered by an agent for each of 46 values of σ. Here, we only show values of σ from 0.2 to 5 rad on the horizontal axis.

EVO. Furthermore, the two algorithms lead to very similar optimal noise intensities. While these results do not *prove* the two hypotheses stated above, they offer substantial support in their favor.

Since both algorithms are performing optimizations independently, it is quite remarkable that they converge on similar solutions. The result that both optimal (SR) and asymptotically achieved (EVO) values of σ increase with hop length can be explained at a 'geometrical' level with the following argument (see also the discussion in Dees *et al* (2008)). It is clear that larger turning angles (distributions with larger σ) lead to more compact trajectories, while smaller turning angles lead to straighter trajectories. The latter case, combined with larger hop lengths, leads to the feeding agent quickly leaving the food patch, and hence to a decreased feeding efficiency. Thus, optimal feeding will be achieved at wider turning angle distributions for longer hop lengths, a result shown both in the SR and the EVO simulations.

How does one interpret the shapes of the evolved distributions? Higher animals, such as albatrosses (Viswanathan *et al* 1996), monkeys (Boyer *et al* 2006) and marine predators (Sims *et al* 2008), including humans (Bertrand *et al* 2007), searching in *non-uniform* environments can make complex cognitive decisions about where food is located (Boyer *et al* 2006). Their foraging behavior has been described using Lévy-shaped distributions, though this description has recently been revised in the cases of some animals (Edwards *et al* 2007). Trajectories of smaller animals such as *Daphnia* cannot be described using Lévy statistics since the animals move through short hops of limited distance. In contrast, experimental studies of slime mold cells (Liang *et al* 2008), and the studies of foraging *Daphnia* (Garcia *et al* 2007, Dees *et al* 2008) which motivated our present paper suggested exponential turning angle distributions. Maxima can be obtained from the SR algorithm regardless of whether it is based on exponential distributions as in Dees *et al* (2008), or based on normal distributions as in the present study. Our model-free approach in EVO, however, seems to 'prefer' the Gaussian distribution.

The areas of largest disagreement between the Gaussian fits and the evolved distributions in figures 1(*b*)–(*d*) lie near the extremities of the distributions. This is even more apparent when looking at individual rather than averaged distributions (data not shown). This may be a result of the algorithm itself, which consists of repeated percentage-wise subtractions from the 'parent' distribution followed by the addition of the inheritance. This may lead to a gradual tapering of the evolving distribution in low-percentage areas, possibly diminishing the outer edges of the tails. Furthermore, looking at the final results, for each hop length tested, the peak noise intensities extracted by SR are slightly less than those predicted by EVO. We suggest that because foragers in SR are selecting angles from perfectly formed TADs, they have access to all angles throughout the entire distribution $[-\pi$ to $\pi]$, including the furthest reaches of the tail. If EVO does indeed systematically diminish some of the tail, the only way that foragers in EVO will have access to these angles is to foster slightly wider distributions, where the angles they need are no longer in the outer tail regions. Still, the values of table 1 show definite agreement between the two models.

Our results follow the conventional view of natural selection as an 'optimizing' mechanism, famously critiqued by Gould and Lewontin (1979). Ultimately, however, the problem is deeper—and evolution more subtle—than that. Natural selection is constrained by the physical limitations of animal morphologies, as well as by historical contingencies that may privilege less-than-optimal solutions. Nonetheless, traces of optimization remain, as, perhaps, in the observed turning angle distributions of real *Daphnia* and the single cells of slime molds.

Acknowledgments

We are grateful to Lutz Schimansky-Geier, Udo Erdmann and Sebastian Göller of Humboldt University in Berlin for useful discussions. An early version of an evolutionary simulation was written by SG. ND would like to thank Professor Haiyan Cai for discussions concerning the statistical analysis.

References

Bartumeus F, Peters F, Pueyo S, Marrasé C and Catalan J 2003 Helical Lévy walks: adjusting searching statistics to resource availability in microzooplankton *PNAS* **100** 12771–5

Bertrand S, Bertrand A, Guevara-Corrasco R and Gerlotto F 2007 Scale-invariant movements of fishermen: the same foraging strategy as natural predators *Ecol. Appl.* **17** 331–7

Bollens S M and Frost D W 1989 Predator-induced diel vertical migration in a planktonic copepod *J. Plankton Res.* **11** 1047–65

Boyer D, Miramontes O, Ramos-Fernández G, Mateos J L and Cocho G 2004 Modeling the searching behavior of social monkeys *Physica* A **342** 329–35

Boyer D, Ramos-Fernández G, Miramontes O, Mateos J L, Cocho G, Larralde H, Ramos H and Rojas F 2006 Scale-free foraging by primates emerges from their interaction with a complex environment *Proc. R. Soc. Lond.* B **273** 1743–50

Buchanan M 2008 Ecological modeling: the mathematical mirror to animal nature *Nature* **435** 714–6

Cowles T J, Desiderio R A and Neuer S 1993 *In situ* characterization of phytoplankton from vertical profiles of fluorescence emission spectra *Mar. Biol.* **115** 217–22

D'Agostino R B and Stephens M A 1986 *Goodness-of-Fit Techniques* (Burnaby, BC, Canada: Marcel Dekker)

Dees N D, Bahar S, Garcia R and Moss F 2008 Patch exploitation in two dimensions: from *Daphnia* to simulated foragers *J. Theor. Biol.* **252** 69–76 (DOI 10.1016/j.jtbi.200801.026)

Derenbach J B, Astheimer H, Hansen H P and Leach H 1979 Vertical microscale distribution of phytoplankton in relation to the thermocline *Mar. Ecol. Prog. Ser.* **1** 187–93

Doubell M J, Seuront L, Seymour J R, Patten N L and Mitchell J G 2006 High-resolution fluorometer for mapping microscale phytoplankton distributions *Appl. Environ. Microbiol.* **72** 4475–8

Douglass J, Wilkens L A, Pantazelou E and Moss F 1993 Noise enhancement of information transfer in crayfish mechanoreceptors by stochastic resonance *Nature* **365** 337–40

Edwards A M *et al* 2007 Revisiting Lévy flight search patterns of wandering albatrosses, bumblebees and deer *Nature* **449** 1044–8

Efron B and Tibshirani R J 1993 *An Introduction to the Bootstrap* (New York: Chapman & Hall)

Emberson L, Kitajo K and Ward L M 2007 Endogenous neural noise and stochastic resonance *Noise and Fluctuations in Biological, Biophysical, and Biomedical Systems (Proc. SPIE* Vol 6602–25*)* ed S M Bezrukov

Endler J A 1986 *Natural Selection in the Wild* (Princeton, NJ: Princeton University Press) pp 210–29

Falconer D S 1981 *Introduction to Quantitative Genetics* 2nd edn (New York: Longmans)

Franks P J S and Jaffe J S 2001 Microscale distributions of phytoplankton: initial results from a two-dimensional imaging fluorometer, OSST *Mar. Ecol. Prog. Ser.* **220** 59–72

Garcia R, Moss F, Nihongi A, Strickler J R, Göller S, Erdmann U, Schimansky-Geier L and Sokolov I M 2007 Optimal foraging by zooplankton within patches: the case of *Daphnia Math. Biosci.* **207** 165–88 (DOI 10.1016/j.mbs.200611.014)

Gould S J 2002 *The Structure of Evolutionary Theory* (Cambridge, MA: Harvard University Press) pp 144–6 1035–7

Gould S J and Lewontin R C 1979 The spandrels of San Marco and the Panglossian paradigm: a critique of the adaptationist programme *Proc. R. Soc. Lond.* B **205** 581–98

Jaramillo F and Wiesenfeld K 1998 Mechanoelectrical transduction assisted by Brownian motion: a role for noise in the auditory system *Nat. Neurosci.* **1** 384–8

Lampert W 1989 The adaptive significance of diel vertical migration of zooplankton *Funct. Ecol.* **3** 21–7

Liang L, Nørrelykke S F and Cox E C 2008 Persistent cell motion in the absence of external signals: a search strategy for eukaryotic cells *PLoS ONE* **3** e2093 (DOI 10.1371/journal.pone.0002093)

Maye A, Hsieh C-H, Sugihara G and Brembs B 2007 Order in spontaneous behavior *PLoS ONE* **2** e443 (DOI 10.1371/journal.pone.0000443)

Nilsson D-E and Pelger S 1994 A pessimistic estimate of the time required for an eye to evolve *Proc. R. Soc. Lond.* B **256** 53–8

Puig P and Stephens M A 2000 Tests of fit for the Laplace distribution, with applications *Technometrics* **42** 417–24

Reynolds A M and Frye M A 2007 Free-flight odor tracking in *Drosophila* is consistent with an optimal intermittent scale-free search *PLoS ONE* **2** e354 (DOI 10.1371/journal.pone.0000354)

Ringelberg J 1993 Diel vertical migration of zooplankton *Arch. F. Hydrobiol.—Adv. Limnol.* **39** 1–222

Robertson A 1980 *Selection Experiments in Laboratory and Domestic Animals* (Slough: Commonwealth Agricultural Bureau)

Shang Y, Claridge-Chang A, Sjulson L, Pypaert M and Miesenböck G 2007 Excitatory local circuits and their implications for olfactory processing in the fly antennal lobe *Cell* **128** 601–2 (DOI 10.1016/j.cell.200612.034)

Shlesinger M F 2006 Search research *Nature* **443** 281–2

Sims D W *et al* 2008 Scaling laws of marine predator search behavior *Nature* **451** 1098–102 (DOI 10.1038/nature06518)

Uttieri M, Zambianchi E, Strickler J R and Mazzochi M G 2005 Fractal characterization of three-dimensional zooplankton swimming trajectories *Eco. Model.* **185** 51–63

Viswanathan G M, Afanasyev V, Buldyrev S V, Murphy E J, Prince P A and Stanley H E 1996 Lévy flight search patterns of wandering albatrosses *Nature* **381** 413–5

Wiesenfeld K and Moss F 1995 Stochastic resonance: from ice ages to crayfish and squids *Nature* **373** 33–6

Zaret T M and Suffern J S 1976 Vertical migration in zooplankton as a predator avoidance mechanism *Limnol. Oceanogr.* **21** 804–13

Supplementary Material

EVO Simulation

The EVO simulation begins with an initially uncorrelated distribution of turning angles, $D_1(\alpha)$, ranging from $-\pi$ to $+\pi$. This represents the "primordial noise" that is available at the beginning of the natural selection process as originally discussed in detail by Darwin (Gould 2002). We divide the angular space into 63 bins and initially write $N/63$ into each bin, where N is the total number of angles to be chosen for a given agent's trajectory. A population of 20 agents represents the initial, or first generation of foragers. Each agent in this population begins to forage from the center of an independent food patch. (There are 20 separate food patches, one for each forager.) Each food patch is a circle of radius 100 units containing a uniform distribution of $\pi \cdot 10^6$ food particles. The food particles are laid out in a grid of small boxes measuring 0.1 by 0.1 units. One box represents the radius of absorption of a forager. An agent independently chooses an angle at random from $D_1(\alpha)$, and this angle is tabulated in a register identified with that agent. The agent hops for a fixed hop length in the direction dictated by its choice of α. Along the hop, the position of the forager is determined every 0.05 units, and any food particle being directly touched by the agent at that time is removed from the patch and tabulated in a second register identified with that agent. Upon the end of the first hop, the agent again chooses another angle from $D_1(\alpha)$, and hops for a second time in a different direction determined by the new α. The new angle and any food particles touched by the agent during this hop are tabulated in the registers. After the trajectory extends to 1500 total units, the movement is terminated, and a new forager begins to feed in a new food patch. After this process is repeated for the entire population of 20, the registers for food collection are surveyed. The agent who gathered the most food particles is identified as the most successful and all other agents together with their registers are discarded. The turning angles chosen by the successful agent are used to modify the turning angle distribution using the formula $D_2(\alpha) = (1\text{-}h)D_1(\alpha) + hC_1(\alpha)$, where $C_1(\alpha)$ represents the histogram of angles chosen by the most successful agent as distributed among the bins of $D_1(\alpha)$, and normalized to 1.0. $C_1(\alpha)$ is attenuated by the inheritance, h (typically = 1/50), ensuring a gradual change, and the addition of $D_1(\alpha)$ multiplied by $(1\text{-}h)$ preserves the total area (1.0) represented in the evolving probability distribution. Through this algorithm, information critical to survival is passed on to the next generation. A second generation of agents is created exactly as the first, and the iterative process commences again as before. However, the second generation chooses its turning angles from the modified distribution, $D_2(\alpha)$. At the end of the second generation, the turning angle distribution is updated again with survival information from the second generation's most successful agent to make $D_3(\alpha)$. The turning angle distribution evolves from generation to generation accordingly.

After 10 trials of EVO have been performed, the asymptotic noise intensities were determined for each hop length value as follows: The distributions for 10 trials of EVO at each hop length were averaged together at every generation. For this averaged set of TADs, the distribution width σ versus generation number was calculated using the MLE technique; this data is shown in figure 2b. Along these curves, we used a sliding window of 10,000 generations, and calculated the slope within each window. At the first window in which the slope changed sign from negative to positive, the first generation in the window was considered to be the first generation in the stasis state. The asymptotic noise intensity is the MLE value at this generation. We also mention that the same result can be achieved this way: σ can be calculated generation by generation for each trial *independently*, and the first generation in the stasis state for each trial can be determined via the same windowing method. Then, the values of sigma for each generation following the onset of stasis can be averaged for each trial, and then across all 10 trials, giving the same asymptotic result as before. It is these asymptotic values of σ that we call evolved quantities and compare

with the optimum widths predicted by stochastic resonance and with the experimental findings of Garcia *et al.* (2007) in table 1.

SR Simulation

In each trial of the SR simulation, 100 trials of 20 agents feed independently in a food patch for a range of predetermined values of σ. The food patch is identical to that in the EVO simulation. It consists of a circle of radius 100 units containing a uniform distribution of $\pi \times 10^6$ food particles, each represented by a small square of size 0.1 by 0.1 units. Each agent starts at the center of a fully-populated food patch and travels for a fixed distance of 1500 units. For each trajectory, a value of σ is chosen, and by extension a normal probability distribution of turning angles, $P_\sigma(\alpha) = N_0 / (\sigma\sqrt{2\pi}) \cdot \exp[-\frac{1}{2}(\alpha - \mu)^2 / \sigma^2]$, is defined, where α represents a set of turning angles with mean μ, N_0 is the number of angles to be observed, and σ is the noise intensity of the distribution. The choices of turning angle range from $-\pi$ to $+\pi$, with the constraining provision that left and right-hand turns are equally probable ($\mu = 0$, as seen in the experimental data (Garcia *et al.* 2007)). After N_0 random turning angles are chosen from the defined distribution, the agent then executes N_0 hops using the chosen angles until the trajectory is terminated after the last hop. Any food particles directly crossed by the agent along this trajectory are removed from the patch and tabulated. The maximum value of food gathered (within three interquartile ranges from the third quartile, in order to exclude extreme outliers) amongst the 20 foragers is then recorded, and the process begins again with a second value of σ. This process continues for 46 values of σ ranging from 0.1 to 10 radians (including the value of σ predicted by EVO), constituting a single trial. The result of the trial is a set of values of maximum food gathered for each value of σ tested, which, when plotted, results in a curve similar to that in figure 3. After 100 trials are completed, we calculate the value of σ which results in the peak of the curve for each trial. These 100 values of σ are averaged, and this average value and its standard deviation are reported in table 1 as the optimal SR noise intensity. The curves from these 100 trials are averaged and plotted in figure 3, with the standard deviation at each point of the curve represented by the error bars.

Statistical Analysis

Goodness-of-fit tests were performed on the asymptotic evolving distributions in EVO. We test the averaged asymptotic results from 10 evolved distributions for each hop length. Our first null hypothesis, H_L, was that the empirical distribution functions (EDFs) were Laplacian distributions, and our second null hypothesis, H_N, was that the EDFs were normal distributions. We then used a bootstrap method (Efron & Tibshirani 1993), creating 1000 samples of 100 random angles chosen from the averaged EDF in question, and for each sample calculated the Cramér-von Mises W^2, the Watson U^2, the Anderson-Darling A^2, and the Kolmogorov-Smirnov D statistic. (These statistical tests are outlined in Puig & Stephens (2000) for the Laplacian distribution, and in D'Agostino & Stephens (1986) for the normal distribution.) We then determined the mean percentage points calculated from the 1000 samples, and compared these values to the significance level tables in the above references. The results are as follows:

Statistic, 0.5 mm	Laplacian Point	%	Significance Level	Normal Point	%	Significance Level
W^2	0.251 ± .11		0.01	0.128 ± .05		0.10
U^2	0.182 ± .05		0.01	0.123 ± .05		0.10
A^2	1.501 ± .68		0.01	.793 ± .36		0.10
D	1.268 ± .21		0.01	.971 ± .18		0.05
Statistic, 1.0 mm	**Laplacian Point**	**%**	**Significance Level**	**Normal Point**	**%**	**Significance Level**
W^2	0.191 ± .08		0.025	0.084 ± .04		0.25
U^2	0.151 ± .05		0.01	0.080 ± .03		0.25
A^2	1.191 ± .47		0.025	.512 ± .20		0.25
D	1.102 ± .21		0.01	.814 ± .16		0.10
Statistic, 1.5 mm	**Laplacian Point**	**%**	**Significance Level**	**Normal Point**	**%**	**Significance Level**
W^2	0.202 ± .07		0.025	0.085 ± .04		0.25
U^2	0.165 ± .05		0.01	0.081 ± .04		0.25
A^2	1.31 ± .45		0.025	0.530 ± .22		0.25
D	1.11 ± .20		0.01	0.802 ± .17		0.15

APPENDIX C

Living With Different Reynolds Numbers

Living with different Reynolds numbers: Physical constraints drive evolution of different foraging strategies in water fleas and paddlefish

Nathan D. Dees[1], Michael Hofmann[2], and Sonya Bahar[1]
[1]*Department of Physics and Astronomy and Center for Neurodynamics, University of Missouri at St. Louis, St. Louis, MO 63121, USA*
[2]*Department of Biology and Center for Neurodynamics, University of Missouri at St. Louis, St. Louis, MO 63121, USA*

Email: nathan.dees@umsl.edu

Summary

Optimal balance between energy usage and feeding is crucial to an animal's fitness, and thus is a driving force in the evolution of species. Animals show varieties of different foraging strategies, each adapted to particular ecological and physical constraints. For example, while paddlefish and zooplankton *Daphnia* both filter-feed on patchy food sources, they have enormous differences in size, and therefore in Reynolds numbers and the flow regimes in which they operate. To examine the effects of these physical constraints on the evolution of foraging strategies, we have modified a recent evolution simulation written for *Daphnia* by adding an energy penalty proportional to each turning angle used by modeled foraging agents. This modification accounts for the loss of linear momentum of undulatory swimmers as they change direction, a loss which *Daphnia* do not experience in the viscous flow regime. In stark contrast to the random-walk-like trajectories predicted for *Daphnia*, the model now predicts distinct circling trajectories and non-zero peaks in the turning angle distributions of larger species such as paddlefish. These results may explain the experimental data also reported here: the circling patterns and bimodal turning angle distributions observed in juvenile paddlefish.

Keywords:

Reynolds number, foraging strategy, evolution model, turning angle, paddlefish, *Daphnia*

1. Introduction

In a recently developed a model, EVO (Dees *et al.* 2008), we used the central principles of Darwinian natural selection to simulate the evolution of the turning angle distributions (TADs) of the filter-feeding zooplankton species *Daphnia*. The model features computer-generated agents foraging in a continuous two-dimensional space containing a finite circular food patch. The freely changing (evolving) parameter is the TAD of the foraging agents, and the agents' fitness levels are determined by the quantity of food they gather in a specified amount of time. After thousands of generations, the evolved TADs resemble those of the real animals in shape and width, and the trajectories which result are very similar to those of the real animals. Here, we investigate the predictions of EVO

when considering the physical constraints encountered by larger aquatic filter-feeders, such as the paddlefish. The comparison of the two models has significant implications regarding the role of physical constraints in driving the evolution of foraging strategies.

Filter-feeders collect food by straining large volumes of their surrounding medium as it flows through some part of their bodies, usually their mouth. Feeding, therefore, requires this flow, and is almost always accompanied by locomotion of some sort. While both real (Garcia *et al.* 2007) and modeled (Dees *et al.* 2008) *Daphnia* travel in trajectories resembling random walks resulting from single-peak zero-mean TADs, experimental and observational studies show that many filter feeders swim in circular or elliptical trajectories as they feed or search for food, particularly when the food is patchy. The behavior is typically suggested to be an effective method of staying within a food-rich area, and extends from smaller fish species, such as anchovy (Hunter & Dorr 1982), and medium-sized species, such as herring (Batty *et al.* 1986), to the largest living fish species, the whale shark (Nelson & Eckert 2007). With regard to turning angles and distributions, traversing a circle would be achieved by using many consecutive positive (or negative) turning angles, resulting in clockwise (or counterclockwise) circling. Each set of consecutive positive or negative angles would appear on a TAD as a non-zero peak, in strong contrast to the TADs of *Daphnia*.

Why do *Daphnia* swim so differently from other filter-feeders? One obvious reason is that the fish species and *Daphnia* operate in radically different flow regimes. Reynolds numbers (*Re*) for zooplankton have been measured to be between 0.1 and 100, depending on their velocity (Videler *et al.* 2002; Catton *et al.* 2007). However, *Re* for small fish are typically one or two orders of magnitude higher, and those of larger fish and whales are up to a half-dozen orders of magnitude higher (Videler *et al.* 2002). As a result, zooplankton swim in the viscous flow regime, while all of the other species mentioned operate in the inertial flow regime. *Daphnia* also use a different mode of propulsion than fish species. The propulsive efficiency of the undulatory swimming used in the inertial regime diminishes at very low *Re* (Uchiyama & Kikuyama 2008), so most zooplankters are "rowing" creatures. *Daphnia*, for example, move in repeated and successive sequences of a hop, a pause, and a turn through an angle, stroking their large second antennae like oars to lunge forward during each hop (Pennak 1953).

Locomotion is a major component of the energetic budget for most species (Domenici *et al.* 2007). This would seem to be particularly true for filter-feeders, whose energy output (locomotion and metabolism) is so intricately connected to energy input (feeding). We report here the evidence of another filter-feeding species, the paddlefish (juveniles), circling in captivity. Experimentally, the fish exhibit bimodal TADs with non-zero peaks, consistent with the reasoning outlined above for circular swimming. To model the possible evolutionary origin of this circling behavior, we have modified EVO for larger *Re* by applying a slight energy cost proportional to each change in direction made by the inertial swimmers. While significant inertia is never achieved by organisms in the viscous flow regime (Anderson 1992), previous findings show that turning motions increase drag forces and decrease momentum for fish in the inertial flow regime (Weihs 1973). We assume that lost momentum can only be recovered by additional energy expenditure, so the penalty we impose affects the agents' food-gathering efficiencies proportionately. With this simple modification to EVO, we obtain fully-evolved TADs

which display non-zero peaks and the simulated foragers demonstrate circling trajectories which strongly resemble the experimental results we present for the paddlefish.

2. Methods

Paddlefish swimming behavior

Swimming behavior was measured in 19 paddlefish *(Polyodon spatula)* of length of 15-35 cm. The paddlefish were obtained from the Blind Pony and Hunnewell Fish Hatchery of the Missouri Department of Conservation. The fish were kept in large bio-filtered and aerated tanks containing dechlorinated water raised to a salinity of 2% by the addition of stock salt (Gunther Co., St. Louis). Fish were fed daily and kept under a 12:12 hour light regime. All experiments were conducted in compliance with the guidelines of the International Animal Care and Use Committee of the University of Missouri at St. Louis.

To record the swimming activity, individual fish were transferred to a rectangular monitoring tank of 1 x 1 m or 1 x 1.5 m. A video camera was placed above the tank and the fish were monitored for 10 to 120 min. Videos were directly digitized by a computer at a rate of 2-5 frames per second and at a resolution of 320 x 240 pixels. The swimming path was determined by the program Vidana (www.vidana.net). Each frame was analyzed automatically by tracing the outline of the fish and calculating the center coordinates and direction (heading) of the fish. Thus, for each frame, the coordinates (x, y) and an angle representing the fish's heading were recorded. These data were further analyzed with the software Igor 6.0 (Wavemetrics). Turning angles, calculated as the changes in heading, were plotted as a function of time; histograms of turning angles were also generated.

Paddlefish model

To model the evolution of paddlefish TADs (and the resultant foraging trajectories), we began with an initially uniform and uncorrelated probability distribution of angles, $D_1(\alpha)$, representing the "primordial noise" available at the beginning of the natural selection process (see Gould 2002). The range of $D_1(\alpha)$ is $-\pi$ to $+\pi$, and we divide this angular space into B bins (typically, $B = 200$). The distribution is normalized to 1.0, with the probability of choosing an angle from a given bin being $1/B$. The arena devised for feeding is a circular food patch of radius R units (typically, $R = 100$) overlaid by an evenly dispersed grid of π x $(10R)^2$ food particles. Each feeding agent begins at the center of an independent, fully-populated food patch, and travels for N steps of unit length (typically $N = 2000$) while consuming every food particle that lies along the trajectory. The food particles are not replaced as the agent is foraging, following the definition of destructive foraging (Viswanathan *et al.* 1999); in other words, if the agent visits any space in the grid more than once, food will no longer be found there.

A population of 20 agents represents the initial generation of foragers. The first agent in the population begins by choosing an angle at random from $D_1(\alpha)$, and moves 1 unit in the direction dictated by this choice of α. The agent gathers every food particle in the grid touched along this step. The agent then chooses another angle from $D_1(\alpha)$, and moves for a second time in a different direction determined by the new α. Upon using this second angle, the agent has made a turn, or some change in direction. In general, as a

fish swims straight ahead, it has a linear momentum (*mass* · *velocity*) in the direction that it is swimming. For the fish to maintain a constant swimming speed, any change in direction requires some accelerating force (thrust) along the new heading in order to restore the original velocity (see Discussion). We assume that these momentum-building thrusts after each turn require energy outputs directly proportional to the angular amounts of directional change (Weihs 1973), or, in terms of the model's parameters, the required energy output for each turn is directly proportional to the absolute value of the turning angle used. We assess this energy cost after each turn by subtracting a proportional amount of food gathered, $P = 5 \cdot |\alpha|$, from the agent's existing food collection.

The agent feeds as described above until the trajectory extends to N units, upon which the movement is terminated. Every turning angle used along the trajectory and every particle of food collected is recorded. Next, a new forager begins to feed in a new, fully-populated food patch. This feeding process continues for the entire population of 20 agents. The agent who gathered the most food particles is identified as the most successful (efficient) agent, and all other agents, together with their recorded quantities, are discarded.

Next, the turning angles chosen by the most successful agent are used to generate a new TAD,

$$D_2(\alpha) = (1-h)D_1(\alpha) + h \cdot H_1(\alpha), \qquad (2.1)$$

where $H_1(\alpha)$ is a normalized (to 1.0) histogram of the angles chosen by the most successful agent as distributed among the bins of $D_1(\alpha)$. $H_1(\alpha)$ is multiplied in (2.1) by the inheritance value, h, a small fraction (typically $h = 1/50$) governing the magnitude of adjustment from one generation to the next. $D_1(\alpha)$ is attenuated slightly in (2.1) by the value $(1-h)$, and then added to $h \cdot H_1(\alpha)$, preserving the total area of the evolving distribution. Through this modification of the "parent" distribution, $D_1(\alpha)$, information critical to efficient foraging is passed on from one generation to the next. A second generation of agents feeds exactly as the first, this time using turning angles chosen randomly from the modified distribution, $D_2(\alpha)$. After the second generation has finished feeding, the evolving TAD is updated with survival information from the second generation's most successful agent in order to generate the distribution $D_3(\alpha)$, and so on. The TAD evolves for thousands of generations in this manner.

Daphnia model

To simulate the swimming behavior of foraging zooplankton, we apply an algorithm very similar to that described above for the paddlefish, but we must consider the different flow regimes in which the organisms operate. Tiny organisms like *Daphnia* do not develop a conservable momentum as they swim. Instead, after each stroke, the surrounding fluid immediately stops their motion and dissipates their kinetic energy (Videler 2002). Changes in direction made by these organisms are more like rotations in the water, a type of movement that is not inhibited at such low *Re* (Videler 2002).

To account for this, we simply remove the energy penalty, P, assessed on changes in direction in the paddlefish model, while leaving the rest of the algorithm intact: the *Daphnia* feed in a circular food patch of the same size and density as do the paddlefish;

they remove food particles along their trajectory; they are simulated using the same number of bins, B, steps, N, and agents (20). Also, $D_1(\alpha)$ is again the evolving parameter, evolved using the same inheritance value, h, and the same updating algorithm. This ensures a direct comparison between the two organisms based solely on the aforementioned energy considerations.

Control simulations

For both the paddlefish and *Daphnia* simulations, controls were performed as follows. Controls were identical to the simulations described above, except that the evolving TAD was updated after each generation using a set of angles chosen by a *random* agent in the population rather than those chosen by the most successful agent. This means that the evolving distribution progressed in no particular direction, and by no particular criteria.

Mathematical analysis of turning angle sequences

In order to quantify the amount of circling in both our real and modeled data, we have developed a circling index, C, to analyze the measured sequences of turning angles. C was determined as follows. Circling is the result of using a large number of consecutive turning angles that have the same sign, meaning that the same direction of turning is used repeatedly. As a consequence, during circling, there should be a low number of changes in direction from clockwise to counterclockwise (and vice-versa) and, consequently, a low number of differently-signed angles chosen one after the other over time. We will call these instances of positive turning angles followed by negative turning angles (and vice-versa) "zero-crossings".

For each sequence of turning angles measured, we first calculated the number of zero-crossings that occurred during the sequence, n_{zc}. For comparison, we then randomized the order of the turning angles in the sequence, creating a "surrogate" sequence, and determined the number of surrogate zero-crossings, s_{zc}. We note that for each surrogate sequence, the distribution of the turning angles remains identical to that of the original run. We also note that in extreme cases where this distribution is characterized by either all-positive or all-negative turning angles, any randomized sequence will show no zero-crossings. In this situation, typically found in the model data only, we modified the original sequence of turning angles by concatenating it with a copy of the identical angles, but with reversed sign. This assures that we have an equal number of positive and negative turning angles while preserving the temporal structure of the original sequence.

From each original turning angle sequence, 100 different surrogate sequences were created, and a range of s_{zc} was found. The mean of the 100 values of s_{zc}, $\bar{s}_{zc}$, reflects the typical number of zero-crossings that would appear if an animal or agent chose angles at random from the distribution. We define C as

$$C = \frac{\left|\bar{s}_{zc} - n_{zc}\right|}{\bar{s}_{zc}}. \qquad (2.2)$$

This result gives us the degree of non-randomness of the original turning angle sequence used by the forager. A circling index of 0 indicates that the number of zero-crossing in

the original sequence is similar to the case in which angles were chosen randomly from the distribution, while a value close to 1 indicates a high degree of non-randomness, or consecutively chosen positive (or negative) angles, resulting in circling.

Lastly, since there is no "control" group for comparison with the real paddlefish data, we tested for significant differences in the zero-crossing values between the original turning angle sequences and those of the surrogate sequences. If n_{zc} is lower than the lowest value of s_{zc}, the probability for the null hypothesis is <0.01, i.e., the resolution of the p-value for 100 iterations of the randomized data (see Kajikawa & Hackett 2005).

3. Results

Paddlefish swimming behavior

The normal swimming behavior of 19 paddlefish was monitored in open field conditions (defined as a featureless arena) for a period of 10 to 120 minutes. Fish were constantly swimming with a speed of 5-10 cm s^{-1}. Most fish showed long periods of using either consecutive positive or consecutive negative turning angles resulting in clockwise or counterclockwise circling, respectively. Circling was sometimes interrupted by more erratic swimming, mostly along the walls. To quantify the amount of circling, we calculated C and found values of 0.61 ± 0.21, with the numbers of zero-crossings in the original sequences of turning angles being significantly different from those of the surrogate sequences ($p<0.01$).

Histograms of turning angles of most fish were bimodal and showed negative and positive peaks corresponding to periods of clockwise and counterclockwise circling. Turning angles roughly equaled ±0.4 rad, which means the fish needed about 15 seconds for a full circle. These values varied with the size of the fish; smaller fish made smaller circles, but this was not quantified systematically. The data in figure 1 shows an example of a fish monitored for about 1 hour. Figure 1*a* shows the swimming path during a five-minute section of the recording. For the entire hour, the turning angles were ± 0.4 rad (figure 1*c*) with a few zero crossings indicating a change in direction. The TAD (figure 1*b*) shows two non-zero peaks of equal height, demonstrating that the fish was circling for the same amount of time in the clockwise and counterclockwise directions. Many fish, however, showed an uneven bimodal distribution and circled longer in one direction than in the other. Often, circling was interrupted by periods of erratic swimming, particularly at the beginning, just after transferring the fish to the experimental tank. In some cases, erratic swimming continued for a long time and pronounced circling was not seen. These were interpreted as attempts to escape the experimental setup, and were accompanied by a rapid and unsteady swimming speed.

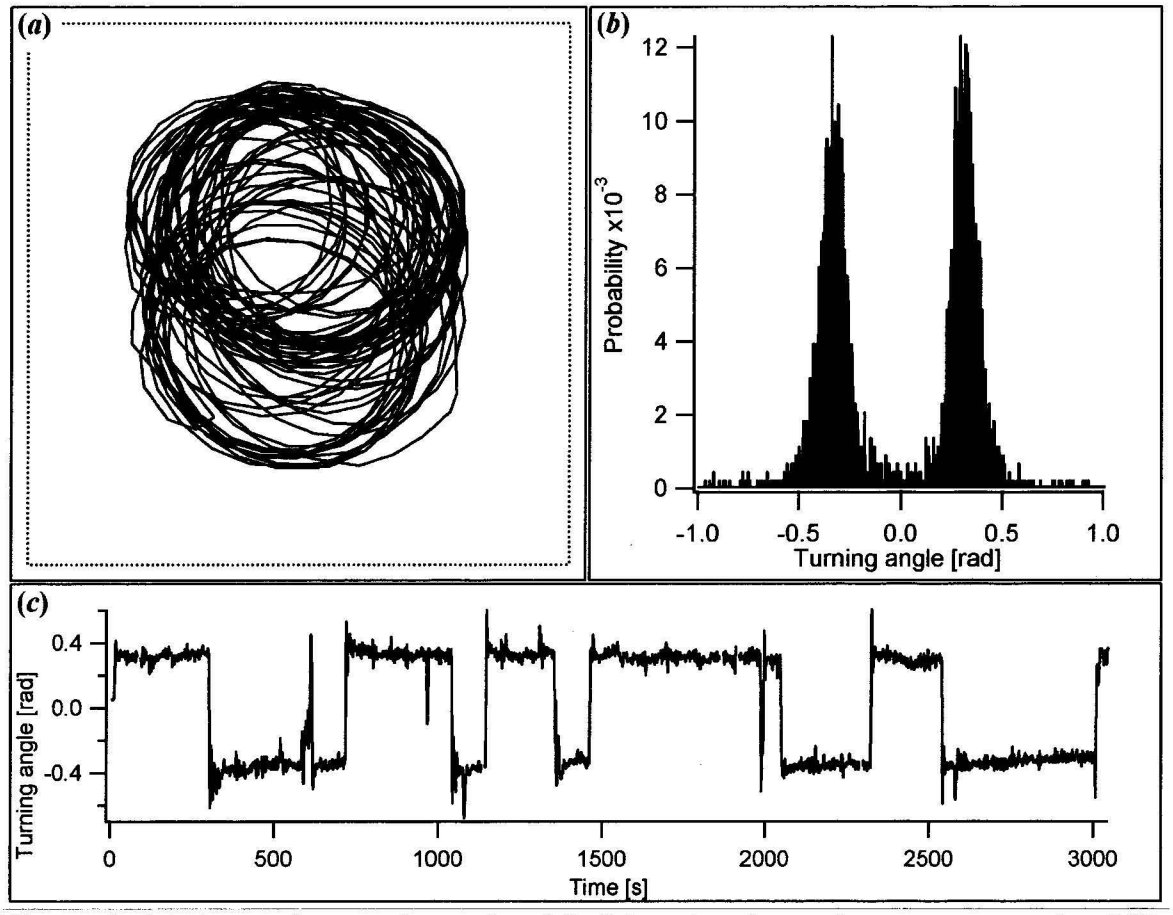

Figure 1. (*a*) A sample experimental paddlefish swimming trajectory representing 250s of continuous data shows evident circling behavior. (*b*) A histogram of turning angles from a real paddlefish trajectory shows a bimodal distribution with a positive and a negative peak, suggesting the animal utilizes both clockwise and counterclockwise circling. (*c*) A sequence of turning angles used by the real animal plotted over time shows prolonged periods of using either positive or negative turning angles with few sporadic zero-crossings, again indicating circling behavior.

Daphnia model

The first row of panels in figure 2 shows the results of the *Daphnia* simulation, originally introduced in Dees *et al.* (2008). Note the labels in the upper and lower left corners of each panel. The first panel ("Daphnia-FG") shows a gently rising curve of food gathered representing the steadily increasing efficiency of the foragers, and then a period of stasis indicating the maximum efficiency has been achieved. Probabilities shown in the "Daphnia-TAD" panel appear to be divided equally between the positive and negative turning angles, a feature confirmed by the near-zero result in the mean turning angle $\overline{\alpha}$ over the 50,000 generations shown ("Daphnia-MTA" panel; the final value of $\overline{\alpha}$, $\overline{\alpha}_f$, is 0.0369 ± 0.0652 radians over ten trials, 100,000 generations per trial). These features lead to a trajectory which resembles a traditional random walk, displaying uncorrelated left-hand and right-hand turns in equal amounts, but the somewhat exponential nature of

the distribution leads to less compact trajectories which weave around the food patch. The distribution allows the forager to explore the entire patch strategically, remaining inside the patch while also avoiding its own path (where food has been removed) as much as possible.

The control simulation for the *Daphnia* model (figure 2, second row) shows no evolution in the efficiency of food gathered, as one might expect. This result is echoed by a final TAD which is not significantly altered from its original highly noisy state. The mean turning angle curve remains near zero for the entire 100,000 generations ($\overline{\alpha}_f$ = -0.0287 ± 0.2458 radians over ten trials), and the resultant trajectories are tight, localized tracks in the center of the circle. These trajectories show a stark contrast to the meandering, exploratory, open trajectories produced by the original *Daphnia* simulation. The original *Daphnia* model showed circling index values of 0.072 ± 0.050, while the Daphnia control circling index was 0.080 ± 0.070. These results are not significantly different (t-test, $p>0.05$, $n=10$).

Paddlefish model

The simple addition of the energy cost P for inertial flow regimes changes the dynamics of the evolution model tremendously, as shown in the middle row of panels in figure 2. In the early phases of the paddlefish simulation, the initial pressure to reduce the occurrences of large positive ($\sim\pi$) and negative ($-\pi$) turning angles is elevated in comparison to the *Daphnia* simulation since, in addition to avoiding one's own path, the imposed penalty, P, proportional to $|\alpha|$, punishes these large angles heavily. Consequently, the plot of food gathered for the paddlefish (figure 2, panel "Paddlefish-FG") shows a slightly steeper initial increase than that of the same plot describing the *Daphnia* agents.

The plot of the mean turning angle for the paddlefish (panel "Paddlefish-MTA") hovers near zero for several thousand generations while the larger angles are eliminated from each side of the evolving distribution, due to the pressure from the penalty P and the need to avoid path-recrossing events in the center of the food patch. Correspondingly, the agents are carried further and further away from the center of the food patch as they utilize smaller turning angles from a narrowed distribution. As a limiting case, one can imagine an extremely narrow TAD, a delta function at zero radians. This delta function would guide the agents directly away from the center of the food patch, and then quickly beyond its edges, resulting in a near-minimum amount of food gathered. To avoid this limiting case, the distribution must stop narrowing as the agents begin to reach the edge of the food patch. The solution to this problem is the next phase of the evolution; the TAD shifts towards either the positive or the negative side, and the agents begin to choose similarly-signed angles consecutively, causing their trajectories to curve away from the edges of the food patch before they cross these edges and leave the patch. As the distribution shifts, the mean turning angle begins to swing sharply away from zero, as shown in the "Paddlefish-MTA" panel, and the food gathered ("Paddlefish-FG" panel) begins to level off just as it does in the *Daphnia* simulation, as all of the agents are beginning to remain inside the patch. The paddlefish trajectories at this point have short periods where they resemble those of the fully-evolved *Daphnia*, meandering and

weaving while staying inside the food patch. (An example of this can be seen in the generation 3000 path in figure 4.)

With a shifted distribution and many consecutive right-hand or left-hand turns being randomly selected, the agents begin to show signs of tight, smooth spiraling in between periods of *Daphnia*-like meandering. This occurs near the peak of the mean turning angle curve, and when the distribution is shifted as much as possible, circles begin to emerge (see the generation 11,000 path in figure 4). There is still some pressure for agents to avoid their own paths as they circle tightly, and furthermore, this initially tight circling requires larger turning angles (and therefore larger subtractions due to *P*) than wider circles would. The agents respond by slowly expanding the diameter of their circles, shifting the mean of the TAD slowly back towards zero while still preserving the efficient circling motion.

The food gathered again begins to increase during this final shift in the TAD mean until, again, a period of stasis is reached. The circles in the trajectories expand to the point where their diameters stretch from the starting point at the center of the food patch to the very edge of the food patch. This result provides a minimal amount of incurred subtractions of *P*, and a minimal amount of path-recrossing events. Note that the result is the same whether the motion is clockwise or counterclockwise, and we achieve both results at random. We report (and plot) the results of the mean turning angle in absolute value form. For 10 trials, $|\overline{\alpha}_f| = 0.0219 \pm 0.0002$ radians.

Circling indices, as calculated from ten fully-evolved distributions, had values of 0.990 ± 0.070, which are significantly different from the ones calculated from the paddlefish control simulations described below (t-test, $p<0.0001$, $n=10$) and also from the *Daphnia* model, which does not have a penalty for large turning angles (t-test, $p<0.0001$, $n=10$).

To achieve a more precise estimate of the final TAD and $|\overline{\alpha}_f|$ in the paddlefish simulation, we ran a high-resolution version of the model, in which the angular space was limited to $[-\pi/5$ to $\pi/5]$ while the number of bins remained at 200. In this case, the width of each bin was one-fifth the original size. This method of limiting the initial range of angles to a smaller set is justified by the fact that all other paddlefish simulations discussed above resulted in very narrow evolved distributions with final widths of less than 0.4 radians (< 7% of 2π). The initial trajectories in this implementation of the model (data not shown) resemble the meandering *Daphnia* trajectories, as the larger-valued turning angles had already been "removed" before the simulation began. Therefore, the period of eliminating larger turning angles is not necessary, and the plot of food gathered does not include the initial rise usually accompanying this phase of the evolution, as in figure 2, panel "Paddlefish-FG". Additionally, the mean turning angle shifts more rapidly away from zero, and shows no initial oscillations (compare the figure 2 panels "Paddlefish HiRes-MTA" with "Paddlefish MTA"). The dynamics from this point forward are the essentially identical to those described above for the regular paddlefish simulation, with $|\overline{\alpha}_f| = 0.0466 \pm 0.0012$ radians for a food patch of radius 50 units, and $|\overline{\alpha}_f| = 0.0219 \pm 0.0002$ radians for patch radius 100 units. See below for additional discussion of the role of patch size in the original paddlefish simulations.

The paddlefish control simulation (bottom row in figure 2) displays many of the same features as the *Daphnia* control simulation. The amount of food gathered does not evolve over time, the mean turning angle remains near zero for the entire 100,000 generations ($|\overline{\alpha}_f| = 0.0433 \pm 0.2206$ radians), and the final TAD consists of uncorrelated noise. The final trajectory (figure 2, "Paddlefish control-Path") is indistinguishable from its *Daphnia* control counterpart, showing the same very tight, localized shape.

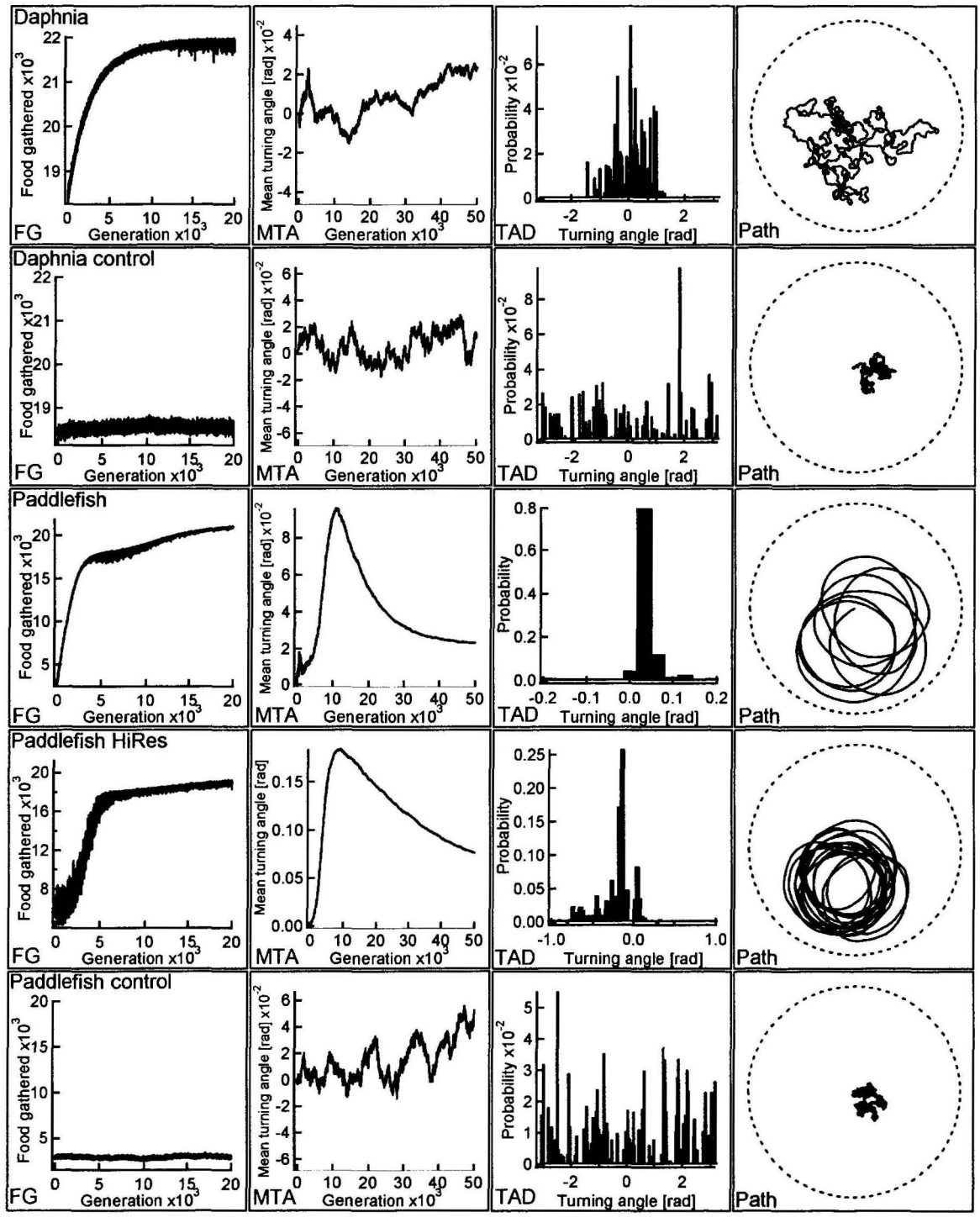

Figure 2. The results of EVO are shown for 5 variations of the model: the *Daphnia* model, the *Daphnia* control, the paddlefish, the high-resolution paddlefish, and the paddlefish control. Agents feed over a trajectory of 2000 unit-length hops. Food patch radii are 100 units, except in the high-resolution paddlefish case, where the patch radius is 50 units. The inheritance value, h, is 1/50. Column 1 (FG) represents the evolution of food gathered in a given feeding time plotted over 20,000 generations (out of 100,000 generations completed for each variation of the model). The plot represents the average value of evolving food gathered over 10 trials. Column 2 (MTA) shows the evolution of the mean turning angle of the evolving distribution over 50,000 (out of 100,000) generations. For the *Daphnia* model and the two control cases, the plots represent the average result over 10 trials. For the paddlefish and high-resolution paddlefish variations, the plot represents the average of the absolute values of the results for each of 10 trials. Column 3 (TAD) shows examples of final evolved TADs for a single run after 100,000 generations of evolution. Column 4 (Path) shows trajectories corresponding to the TADs in Column 3. The dotted circle represents the boundary of the food patch.

Non-destructive foraging

In order to further isolate the role of energy considerations in the evolution of circling trajectories, we tested versions of the paddlefish and *Daphnia* models in which the destructive foraging element was removed. For the paddlefish agents, this means that there are now only two main objectives: stay inside the patch, and avoid larger turning angles. For the *Daphnia*, however, excluding the need to avoid one's own path means that there is now only one objective: stay inside the patch. With the rest of the two algorithms being identical, this exercise offers a direct comparison of the role of the penalty P in the development of paddlefish foraging strategy as they feed inside the food patch.

The results are easy to see – the *Daphnia*'s behavior is drastically affected by this change, while the paddlefish agents again discover circling, as illustrated in figure 3. This illustrates the strength of the energy penalty as a determining criterion of the paddlefish's foraging strategy.

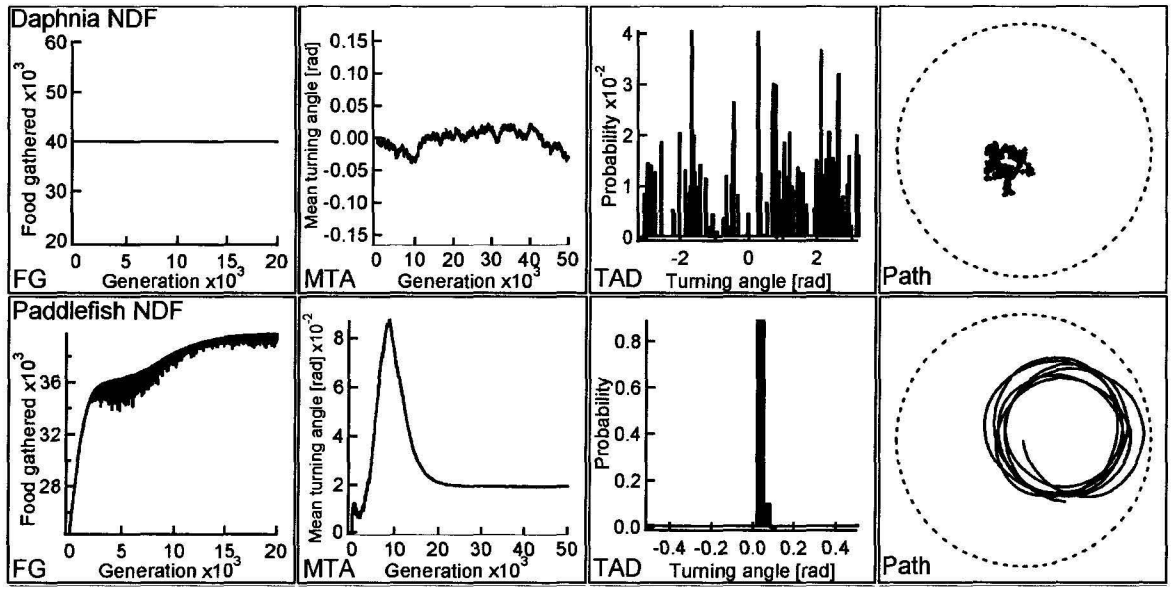

Figure 3. Results are shown for the *Daphnia* and paddlefish variations of the model where non-destructive foraging (NDF) is utilized. Fixed hop lengths are 1 unit. Agents feed over a trajectory of total length 2000 hops. Food patch radii are 100 units, and h = 1/50. Descriptions of columns are the same as in figure 2. In Column 2 (MTA), the mean turning angle is shown for the Daphnia NDF case (not an absolute value), while the absolute value of the mean turning angle is shown for paddlefish NDF (average over 10 trials for both variations).

Effects of food patch size

Lastly, with all other parameters in the paddlefish model held fixed, we investigated the effects of patch size on the dynamics. The results, shown in figure 4, indicate that the dynamics are qualitatively similar for each patch size tested. However, there are some quantitative differences. For the largest patch sizes, the foragers are able to travel further away from the center before reaching the edge of the food patch. As a result, the steep initial rise in food gathered extends higher for larger patches (figure 4*a*). Also, the initial reduction of large turning angles lasts longer, narrowing the distribution more quickly than in the smaller patch sizes. This more rapidly narrowing distribution leads to a less substantial shift of the distribution to one side - the shift occurs quickly, and the plot of mean turning angle peaks sooner (figure 4*b*). It takes longer for foragers in smaller patches to achieve the balance of staying inside the patch (by using *less* straight travel), while avoiding one's own path during spiraling (by using *more* straight travel). For example, the peak in $|\overline{\alpha}|$ for a patch of radius 150 units occurs around 8,000 generations while the peak in $|\overline{\alpha}|$ for a patch of radius 50 units occurs around 30,000 generations. Also, for every patch size tested, the simulation eventually results in trajectories which circle between the starting point and the outer edge of the patch, so it becomes obvious that smaller patch sizes should lead to larger resultant mean turning angles (tighter circles), and this is indeed the case (figure 4b). The values for $|\overline{\alpha}_f|$ for patches of radii

50, 75, and 150 units were 0.0537 ± 0.0046, 0.0293 ± 0.0004, and 0.0150 ± 0.0003 radians, respectively. Lastly, we note that smaller food patches evolved to slightly lesser amounts of food gathered, as tighter circles led to more path-recrossing events where the animals do not find food. For example, the final value of food gathered for patch size 150 was 22102 ± 42 food particles, while for patch size, it was only 20977 ± 211 food particles.

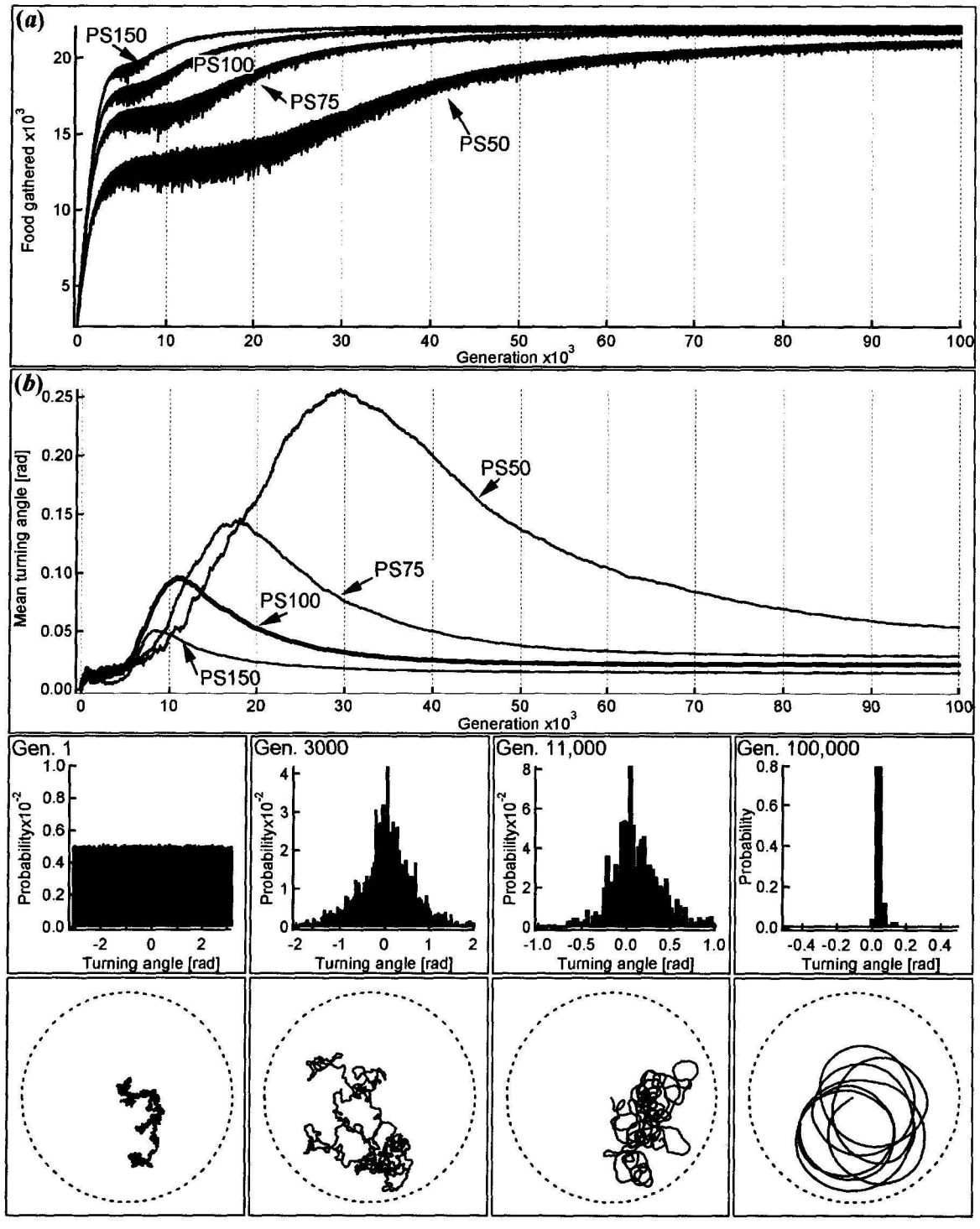

Figure 4. The effects of four different patch sizes (PS) are shown here with all other parameters left the same. As before, agents feed over a trajectory of 2000 unit-length hops, and $h = 1/50$. 100,000 generations are completed for each patch size. (*a*) A plot of food gathered for each generation over 100,000 generations is shown for each PS. Results are the average values over 10 trials. (*b*) The absolute value of the mean turning angle over 100,000 generations is plotted for each PS (average result over 10 trials shown). The bottom two rows in the figure show TADs and trajectories at different generations during a single run with patch radius 100 units. The generations at which these "snapshots" are taken are labeled above the distributions. The distributions are shown at different scales relevant to the data, with the angular space originally divided into 200 bins. Dotted circles represent the edges of the food patch.

Discussion

We have investigated two filter-feeding aquatic animals, where one, the zooplankton *Daphnia*, is the typical meal for the other, the paddlefish. This fact is only important when one considers that it demands that the organisms live in the same environments, subject to similar ecological conditions. It has also been shown that both organisms feed on patchy food (Folt *et al.* 1993); yet, the swimming behaviors and TADs of the two organisms are remarkably different.

As discussed above, organisms like *Daphnia* are not able to coast after a propulsive stroke; they do not operate with any considerable inertia. Clearly, momentum and the loss thereof would not be a factor when analyzing their hydrodynamic efficiency. Alternatively, when fish in the inertial flow regime bend their bodies to turn, this causes an increase in the added mass on the central part of the fish's body (Weihs 1972). (Added mass is the mass of the water carried forward by a fish during locomotion.) Extra power is required to accelerate this water, both in the direction of motion and in all other directions. The greater the amount of water acted on by the fish, the greater the amount of energy it will need to propel itself in the new direction after a turn (Frith & Blake 1995). In addition to the water, the fish's mass must also be accelerated in these cases.

Our analysis suggests a particular strategy – circling – which may optimally balance the food gathered with the energy expended when feeding in a patchy environment. The propulsive behaviors of fish, however, and the metabolic costs of these behaviors are quite complex (see Blake (2004) for a review). Three relevant types of swimming were compared in Boisclair and Tang (1993): "forced swimming", "directed swimming", and "routine swimming". Forced swimming involves undulatory propulsion against a constant current at a steady rectilinear speed, a very common method of swimming imposed on fish being investigated in laboratory experiments. Directed swimmers are trained to follow shadows around a circular aquarium, and therefore are constantly turning (circling) in stationary water (e.g., Muir *et al.* 1965). And routine swimming involves continual random changes in direction and speed, often thought of as spontaneous activity (e.g., Smit 1965). Smit (1965) first suggested that spontaneous activity may be more costly than straight swimming. He observed large amounts of oxygen consumption in fish swimming spontaneously, and yet the fish covered relatively little distance, leading him to assume that energy was being wasted. Weatherly and Gill (1987) found that, according to oxygen consumption rates and corresponding

electromyogram (EMG) values in rainbow trout, spontaneous activity produced a metabolic rate almost 4 times as high as that measured for similar speeds during forced swimming. Webb (1991) demonstrated that fish expend more energy during routine swimming than during forced swimming of comparable speeds due to increases in drag by a factor of 3. Finally, the empirical analysis of Boisclair and Tang (1993), mentioned above, showed that the energetic costs of routine swimming were on average 9.4 times higher than those of forced swimming.

The differences between *Daphnia* and these undulatory swimmers become very obvious when one considers that, of the three types of swimming mentioned above for fish, the one that most closely resembles the modeled "optimal" trajectories of *Daphnia* is the very costly routine swimming. Routine swimming similarly compares to the three-dimensionally tracked trajectories of the real *Daphnia* (Uttieri 2004). It can be presumed that *Daphnia* could execute a forced swim, a directed swim, and a routine swim at similar speeds and all at a similar metabolic cost.

Why, then, do paddlefish swim in circles? Boisclair and Tang (1993) also showed that directed swimming was, on average, only 1.6 times more expensive than forced swimming, while routine swimming was 6.2 times more expensive than directed swimming, indicating that swimming in circles is highly efficient compared to spontaneous activity. This may be especially important for species like paddlefish, which are ram ventilators, and can only maintain adequate levels of oxygen through constant motion (Burggren & Bemis 1992).

In addition, circling may be a strong indicator for patchy food sources. If we extended the patch size in our destructive-foraging model to infinity, simulating uniform food sources continuously in all directions, the TADs for both the *Daphnia* and the paddlefish models will evolve to a delta function at zero (data not shown), and simulated foragers will swim directly away from the starting point for the entire trajectory. This result ensures for both sets of agents that there are no path-recrossing events, and for paddlefish, that there are no energy penalties for turning (a minimum amount of drag). But an unlimited patch of food does not exist in the wild. If a fish finds a favorable spot, swimming straight may not be the best strategy. For instance, swimming at only 10 cm/s, if our juvenile paddlefish headed on a straight trajectory, they would cover 60 m in only 10 min. Considering that aggregations of *Daphnia* are typically on the order of 1-10 m, a paddlefish may want to exploit the area by feeding in this aggregation for longer than just a couple of minutes. Circling may be the most efficient way to do this.

Although our paddlefish model evolved circling trajectories almost identical to those of the real fish, the underlying mechanisms are certainly different. In fact, the distributions themselves have differences, as seen when comparing the bimodal TAD of the real animal (figure 1*b*) with the single-mode distributions of the modeled paddlefish (figure 2, "Paddlefish-TAD" and "Paddlefish HiRes-TAD"). If angles are picked at random from the single-mode, non-zero-mean distributions evolved in the model, angles of similar sign would obviously often follow each other, resulting in circling. This is precisely what occurs in our model. However, if the modeled agents constructed trajectories from symmetric bimodal TADs, as are often seen in the measurements of the real paddlefish (figure 1*b*), random selection by agents surely would not result in circling, as positive and negative turning angles would alternate randomly. We show here that, obviously, the real fish do not select angles randomly. They must use a form of

"memory" to choose angles from only a single side of the bimodal distribution for extended periods of time, and even when they become distracted, they are able to resume this strategy quickly, as seen in figure 1*c*. In any case, it is remarkable that, despite the limited 'intellectual' capabilities of our model, the final result of the evolution is similar to that of the real animals. This shows that the physical constraints that act upon an animal (in this case, the Reynolds numbers) dictate to a large degree the final behavior of the animal, independent of the evolutionary pathway which leads to this behavior.

References

Alexander, R. (ed.) 1992 *Advances in Comparative and Environmental Physiology*, Vol. 11. New York: Springer-Verlag.

Batty, R. S., Blaxter, J. H. S. & Libby, D. A. 1986 Herring (Clupea harengus) filter-feeding in the dark. *Marine Biology* **91**, 371-375.

Blake, R. W. 2004 Fish functional design and swimming performance. *Journal of Fish Biology* **65**, 1193-1222.

Boisclair, D. & Tang, M. 1993 Empirical analysis of the influence of swimming pattern on the net energetic cost of swimming in fishes. *Journal of Fish Biology* **42**, 169-183.

Burggren, W. W. & Bemis, W. E. 1992 Metabolism and ram gill ventilation in juvenile paddlefish, Polyodon-Spathula (Chondrostei, Polyodontidae). *Physiological Zoology* **65**, 515-539.

Catton, K. B., Webster, D. R., Brown, J. & Yen, J. 2007 Quantitative analysis of tethered and free-swimming copepodid flow fields. *Journal of Experimental Biology* **210**, 299-310.

Dees, N. D., Bahar, S. & Moss, F. 2008 Stochastic resonance and the evolution of *Daphnia* foraging strategy. *Physical Biology* **5**, 044001.

Domenici, P., Claireaux, G. & McKenzie, D. J. 2007 Environmental constraints upon locomotion and predator-prey interactions in aquatic organisms: an introduction. *Philosophical Transactions of the Royal Society B* **362**, 1929-1936.

Folt, C., Schulze, P. C. & Baumgartner, K. 1993 Characterizing a zooplankton neighbourhood: small-scale patterns of association and abundance. *Freshwater Biology* **30**, 289-300.

Frith, H. R. & Blake, R. W. 1995 The mechanical power output and hydromechanical efficiency of Northern Pike (Esox lucius) fast-starts. *The Journal of Experimental Biology* **198**, 1863-1873.

Garcia, R., Moss, F., Nihongi, A., Strickler, J. R., Göller, S., Erdmann, U., Schimansky-Geier, L. & Sokolov, I. M. 2007 Optimal foraging by zooplankton within patches: the case of *Daphnia*, *Mathematical Biosciences.* **207**, 165-188. (DOI 10.1016/j.mbs.2006.11.014.)

Gould, S. J. 2002 *The Structure of Evolutionary Theory*, pp. 144-146, 1035-1037. Cambridge, MA: Harvard University Press.

Hunter, J. R. & Dorr, H. 1982 Thresholds for filter feeding in northern anchovy, Engraulis mordax. *California Cooperative Oceanic Fisheries Investigations (CalCOFI)* **23**, 198-204.

Kajikawa, Y. & Hackett, T. A. 2005 Entropy analysis of neuronal spike train synchrony. *Journal of Neuroscience Methods* **149**, 90-93.

Muir, B. S., Nelson, G. J. & Bridges, K. W. 1965 A method for measuring swimming speed in oxygen consumption studies on the Aholehole Kuhlia sandvicensis. *Transactions of the American Fisheries Society* **94**, 378-382.

Nelson, J. D. & Eckert, S. A. 2007 Foraging ecology of whale sharks (Rhincodon typus) within Bahía de Los Angeles, Baja California Norte, México. *Fisheries Research* **84**, 47-64.

Pennak, R. W. 1953 *Fresh-water invertebrates of the United States*. New York: Ronald Press Company.

Smit, H. 1965 Some experiments on the oxygen consumption of goldfish (Carassius Auratus L.) in relation to swimming speed. *Canadian Journal of Zoology* **43**, 623-633.

Uttieri, M., Mazzocchi, M. G., Nihongi, A., D'Alcalà, M. R., Strickler, J. R. & Zambianchi, E. 2004 Lagrangian description of zooplankton swimming trajectories. *Journal of Plankton Research* **26**, 99-105.

Videler, J. J., Stamhuis, E. J., Müller, U. K. & van Duren, L. A. 2002 The scaling and structure of aquatic animal wakes. *Integrative and Comparative Biology* **42**, 988-996.

Viswanathan, G. M., Buldyrev, S. V., Havlin, S., da Luz, M. G. E., Raposo, E. P. & Stanley, H. E. 1999 Optimizing the success of random searches. *Nature* **401**, 911-914.

Weatherley, A. H. & Gill, H. S. 1987 *The Biology of Fish Growth.* Orlando, FL: Academic Press.

Webb, P. W. 1991 Composition and mechanics of routine swimming of Rainbow Trout, Oncorhynchus mykiss. *Canadian Journal of Fisheries and Aquatic Sciences* **48**, 583-590.

Weihs, D. 1972 A hydrodynamical analysis of fish turning manoeuvres. *Proceedings of the Royal Society of London B* **182**, 59-72.

Weihs, D. 1973 The mechanism of rapid starting of slender fish. *Biorheology* **10**, 343-350.

BIBLIOGRAPHY

Benzi, R., Parisi, G., Sutera, A., Vulpiani, A., 1982. Stochastic resonance in climatic change. *Tellus* **34**:10-16.

Benzi, R., Sutera, A., Vulpiani, A., 1981. The mechanism of stochastic resonance. *Journal of Physics A* **14**:L453-L457.

Burkhardt, Jr., R. W., 1985. Darwin on animal behavior and evolution. pp 327-366. In: Kohn, D. (Ed.) *The Darwinian Heritage.* Princeton University Press, New Jersey.

Brown, R., 1828. A brief account of microscopical observations made in the months of June, July and August, 1827, on the particles contained in the pollen of plants; and on the general existence of active molecules in organic and inorganic bodies. *Philosophical Magazine* **4**:161-173.

Chatterjee, M., Robert, M. E., 2001. Noise enhances modulation sensitivity in cochlear implant listeners: stochastic resonance in a prosthetic sensory system? *Journal of the Association for Research in Otolaryngology* **2**:159-171.

Clark, W. R., Grunstein, M., 2000. *Are We Hardwired?* Oxford University Press, New York.

Clavero, M., Prenda, J., Delibes, M., 2003. Trophic diversity of the otter (*Lutra lutra* L.) in temperate and Mediterranean freshwater habitats. *Journal of Biogeography* **30**:761-769.

Dees, N. D., Bahar, S., Garcia, R., Moss, F., 2008a. Patch exploitation in two dimensions: from *Daphnia* to simulated foragers. *Journal of Theoretical Biology* **252**:69-76.

Dees, N. D., Bahar, S., Moss, F., 2008b. Stochastic resonance and the evolution of *Daphnia* foraging strategy. *Physical Biology* **5**:044001.

Dees, N.D., Hofmann, M., Bahar, S., 2009. Living with different Reynolds numbers: Physical constraints drive evolution of different foraging strategies in water fleas and paddlefish. *Submitted to Proceedings of the Royal Society of London B.*

Douglass, J. K., Wilkens L., Pantazelou, E., Moss, F., 1993. Noise enhancement of information transfer in crayfish mechanoreceptors by stochastic resonance. *Nature* **365**:337-340.

Folt, C. L., Burns, C. W., 1999. Biological drivers of zooplankton patchiness. *TREE* **14**:300-305.

Franks, P. J. S., Jaffe, J. S., 2001. Microscale distributions of phytoplankton: initial results from a two-dimensional imaging fluorometer, OSST. *Mar. Ecol. Prog. Ser.* **220**:59-72.

Garcia, R., Moss, F., Nihongi, A., Strickler, J.R., Göller, S., Erdmann, U., Schimansky-Geier, L., Sokolov, I.M., 2007. Optimal foraging by zooplankton within patches: The case of *Daphnia*. *Mathematical Biosciences* **207**:165-188.

Gammaitoni, L., Hänggi, P., Jung, P., Marchesoni, F., 1998. Stochastic resonance. *Reviews of Modern Physics* **70**:223-287.

Gloria-Soria, A., Azevedo, R. B. R., 2008. *npr-1* regulates foraging and dispersal strategies in *Caenorhabditis elegans*. *Current Biology* **18**:1694-1699.

Haeggqwist, L., Schimansky-Geier, L., Sokolov, I.M., Moss, F., 2008. Hopping on a zig-zag course. *The European Physical Journal Special Topics* **157**:33-42.

Hartgers, E. M., Heugens, E. H. W., Deneer, J. W., 1999. Effect of Lidane on the clearance rate of *Daphnia magna*. *Archives of Environmental Contamination and Toxicology* **36**:399-404.

Hoyt, D. F., Taylor, C. R., 1981. Gait and the energetics of locomotion in horses. *Nature* **292**:230-240.

Jaramillo, F., Wiesenfeld, K., 1998. Mechanoelectrical transduction assisted by Brownian motion: a role for noise in the auditory system. *Nature Neuroscience* **1**:384-388.

Kamil, A.C., Drebs, J.R., Pulliam, H.R. (Eds.), 1987. *Foraging Behavior*. Springer, Berlin.

Keiyu, A.Y., Yamazaki, H., Strickler, J.R., 1993. A new modeling approach for zooplankton behavior. *Deep-Sea Research II* **40**:171-184.

Komin, N., Erdmann, U., Schimansky-Geier, L., 2004. Random walk theory applied to *Daphnia* Motion. *Fluctuation and Noise Letters* **4**:L151-L159.

Lampert, W., 1989. The adaptive significance of diel vertical migration of zooplankton. *Functional Ecology* **3**:21-27.

Li, L., Nørrelykke, S. F., Cox, E. C., 2008. Persistent cell motion in the absence of external signals: a search strategy for eukaryotic cells. *PLoS ONE* **3**:e2093. doi:10.1371/journal.pone.0002093.

MacArthur, R.H., Pianka, E.R., 1966. On optimal use of a patchy environment. *The American Naturalist* **100**:603-609.

Moore, D. S., 2001. *The Dependent Gene.* Henry Holt and Company, New York.

Morse, R. P., Evans, E. F., 1996. Enhancement of vowel coding for cochlear implants by addition of noise. *Nature Medicine* **2**:928-932.

Moss, F., Chioutan, F., Klinke, R., 1996. Will there be noise in their ears? *Nature Medicine* **2**:860-862.

Moss, F., Ward, L. M., Sannita, W. G., 2004. Stochastic resonance and sensory information processing: a tutorial and review of application. *Clinical Neurophysiology* **115**:267-281.

Nicolis, C., 1982. Stochastic aspects of climatic transitions – response to a periodic forcing. *Tellus* **34**:1-9.

Nunez, P.L., Srinivasan, R., 2006. *Electric Fields of the Brain.* Oxford University Press, New York.

Pennak, R.W., 1953. *Fresh-Water Invertebrates of the United States.* Ronald Press Company, New York.

Pulliam, H.R., 1975. Diet optimization with nutrient constraints. *The American Naturalist* **109**:765-768.

Ringelberg, J., (Ed.), 1993. Diel vertical migration of zooplankton: Proceedings of an international symposium held at Lelystad, The Netherlands. *Arch Hydrobiol Beih Ergebn Limnol* **39**:1-222.

Russell, D., Wilkens, L., Moss, F. 1999. Use of behavioral stochastic resonance by paddlefish for feeding. *Nature* **402**:219-223.

Rechtschaffen, A., Bergmann, B.M., Everson, C.A., Kushida, C.A., Gilliland, M.A., 1989. Sleep Deprivation in the Rat: X. Integration and Discussion of the findings. *Sleep* **12**:68-87.

Schimansky-Geier, L., Erdmann, U., Komin, N., Advantages of hopping on a zig-zag course. *Physica A* **351**:51-59.

Schmidt-Nielsen, K., 1972. Energy cost of swimming, flying, and running. *Science* **177**:222-228.

Schmidt-Nielsen, K., 1997. *Animal Physiology.* Cambridge University Press, New York.

Shang, Y., Claridge-Chang, A., Sjulson, L., Pypaert, M., Miesenböck, G., 2007. Excitatory local circuits and their implications for olfactory processing in the fly antennal lobe. *Cell* **128**:601-612.

Stephens, D.W., Krebs, J.R., 1986. *Foraging Theory*. Princeton University Press, Princeton, NJ.

Uttieri, M., Mazzocchi, M.G., Nihongi, A., D'Alcalà, M.R., Strickler, J.R., 2004. Lagrangian description of zooplankton swimming trajectories. *Journal of Plankton Research* **26**:99-105.

van Gool, E., Ringelberg, J., 1996. Daphnids respond to algae-associated odours. *Journal of Plankton Research* **18**:197-202.

Videler, J. J., Stamhuis, E. J., Müller, U. K., van Duren, L. A., 2002. The scaling and structure of aquatic animal wakes. *Integrative and Comparative Biology* **42**:988-996.

Viswanathan, G.M., Buldyrev, S.V., Havlin, S., da Luz, M.G.E., Raposo, E.P., Stanley, H.E., 1999. Optimizing the success of random searches. *Nature* **401**:911-914.

Ward, T. J., Robinson, W. E., 2005. Evolution of cadmium resistance in *Daphnia magna*. *Environmental Toxicology and Chemistry* **24**:2341-2349.

Webb, P. W., 1991. Composition and mechanics of routine swimming of Rainbow Trout, *Oncorhynchus mykiss*. *Canadian Journal of Fisheries and Aquatic Sciences* **48**:583-590.

Weihs, D., 1972. A hydrodynamical analysis of fish turning manoeuvres. *Proceedings of the Royal Society of London B* **182**:59-72.

Wiesenfeld, K., Moss, F., 1995. Stochastic resonance and the benefits of noise: from ice ages to crayfish and SQUIDs. *Nature* **373**:33-36.

VITA

Nathan Daniel Dees was born in Vicksburg, Mississippi on August 23, 1980 to loving parents, Kenneth L. and Mary T. Dees. He attended Saint Aloysius High School in Vicksburg, and then graduated after one year at Loveland High School in Loveland, Ohio. He enrolled in the College of Engineering at the University of Cincinnati, and received a Bachelor of Science degree in Electrical Engineering in 2003. He then switched fields from engineering to physics, and received a Master's Degree in Physics from the University of Cincinnati in 2005. After completing his master's degree, Nathan moved to Saint Louis, Missouri, and enrolled at the University of Missouri – Saint Louis. At that time, he also became engaged to his wife, Robin Marie Dees, and they were married in Saint Louis in 2007. Nathan received his Ph.D. in Physics in the spring of 2009 from the cooperative Ph.D. program of the University of Missouri – Saint Louis and Missouri University of Science and Technology.